United States
Consumer Product Safety Commission

February, 2024

CPSC Staff Statement on: Defining and categorizing modeling approaches to support source characterization for indoor exposure assessment of consumer products

The U.S. Consumer Product Safety Commission (CPSC, or Commission) contracted with ICF International (Contract No. 61320622A0005, Order No. 61320623F2022) to complete a critical review of modeling approaches that can be used for indoor exposure assessment of consumer products.

This statement was prepared by the CPSC staff and the attached report was prepared by ICF International. The statement and report have not been reviewed or approved by, and may not necessarily represent the views of, the Commission.

There are a wide range of chemical substances used in consumer products. Similarly, there are many ways that these substances could emit or migrate from products over time. These processes can be quantified through empirical measurements, mathematical modeling, or both. Using both empirical measurements and mathematical modeling makes it possible to increase the throughput of exposure estimates and evaluate estimates based on available empirical information.

CPSC staff uniquely consider each exposure assessment for chemical substances used in consumer products. CPSC staff consider criteria such as soundness, applicability/representativeness, accessibility/reproducibility, variability and uncertainty, and evaluation status when selecting model(s). Each modeling choice is based on meeting the needs of the assessment.

CPSC staff lead a task group under ASTM D22.05 subcommittee on indoor air with the same name and scope as this report. The task group provided valuable insights as part of this effort. CPSC staff plan to continue to work with the task group to transfer much of this content into one or more ASTM guide(s), recognizing that there will be formatting and potentially some content-based differences as a result of the voluntary standards development process.

Defining and categorizing modeling approaches to support source characterization for indoor exposure assessment of consumer products

FINAL REPORT

Prepared for

U.S. Consumer Product Safety Commission (CPSC)

By

Zhishi Guo, Ph.D. and Heidi Hubbard, Ph.D.

ICF International

1902 Reston Metro Plaza, Reston, VA 20190

Under

CPSC Contract No. 61320622A0005

Order No. 61320623F2022

January 15, 2024

Table of Contents

1. Introduction 1
1.1. Purpose 1
1.2. Approach 1
1.3. Report organization 2
2. Categorization of modeling approaches 3
3. Mass transfer from solid articles/building materials to air: (I) Diffusion-based models 4
3.1. Symbols and abbreviations 4
3.2. Overview 5
3.3. Description of analytical solution models 8
3.4. Description of numeric approximation models 12
3.5. Description of dimensionless relationship models 16
3.6. Description of state-space models 19
3.7. Parameter estimation methods 23
3.8. Additional comments 25
3.9. Summary 26
4. Mass transfer from solid articles/building materials to air: (II) More mass transfer models and empirical models 28
4.1. Symbols and abbreviations 28
4.2. Overview 28
4.3. Model description 29
4.4. Summary 35
5. Mass transfer from liquid consumer products to air: (I) Models for liquid cleaners, air fresheners, and personal care products 36
5.1. Symbols and abbreviations 36
5.2. Overview 38
5.3. Model description 42
5.4. Additional comments 50
5.5. Summary 51
6. Mass transfer from liquid consumer products to air: (II) Models for emissions from interior coating materials and sealants 52
6.1. Symbols and abbreviations 52

6.2. Overview 53
6.3. Model description 54
6.4. Additional comments 61
6.5. Summary 62
7. Models for spray applications 63
7.1. Symbols and abbreviations 63
7.2. Overview 64
7.3. Model description 65
7.4. Additional comments 67
7.5. Summary 70
8. Models for emissions from indoor combustion sources 71
8.1. Symbols and abbreviations 71
8.2. Overview 72
8.3. Model description 73
8.4. Additional comments 79
8.5. Summary 80
9. Models for emissions from indoor appliances and devices 81
9.1. Symbols and abbreviations 81
9.2. Overview 82
9.3. Model description 82
9.4. Additional comments 88
9.5. Summary 89
10. Mass transfer from solid articles/building materials to suspended and settled particulate matter 90
10.1. Symbols and abbreviations 90
10.2. Overview 92
10.3. Model description 93
10.4. Additional comments 100
10.5. Summary 103
11. Models for leaching from solid consumer products to drinking water 105
11.1. Symbols and abbreviations 105
11.2. Overview 105
11.3. Model description 107
11.4. Summary 110

12. Models for non-dietary ingestion exposure to consumer products 112
12.1. Symbols and abbreviations 112
12.2. Overview 113
12.3. Model description 115
12.4. Additional comments 119
12.5. Summary 120
13. Models for dermal exposures associated with consumer products 121
13.1. Symbols and abbreviations 121
13.2. Overview 122
13.3. Model description 124
13.4. Additional comments 128
13.5. Summary 129
14. Crosswalk tables of consumer products with chemical substances and models 130
References 136

1. Introduction

1.1. Purpose

This report provides an overview of the mathematical models available for characterization of chemical substance emissions and migration in indoor environments associated with the use of consumer products. It serves as a general guide for those who enquire about the availability of mathematical models, their applicability and usefulness to consumer products, and their limitations.

Mathematical modeling is an essential part of exposure assessment and indoor environment quality research. Predictive models are frequently used to achieve various tasks, including:

- Predicting the emission of chemical substances from consumer products and the temporal and spatial variations of chemical substance concentrations in indoor environments,
- Predicting the potential human intake of chemical substances through inhalation, dermal, and nondietary routes,
- Predicting the migration of chemical substances from the source to indoor media such as interior surfaces and suspended particles, and settled dust,
- Identifying and prioritizing potentially hazardous consumer products,
- Using models as a tool to design test plans for field measurements and laboratory studies,
- Interpreting and generalizing experimental data, and
- Developing pollution control measures and risk management strategies.

A large number of models have been developed over the years. It is impractical and unnecessary to conduct a comprehensive review that covers all available models. Although the models described in this report represent only a portion of available models, it is our intention to present representative and practically useful models. For some models, we indicated their ambiguities and errors so that readers can use them with discretion.

1.2. Approach

We used Google Scholar as the main search engine to find papers and reports that might contain mathematical models relevant to consumer products because it covers multiple sources, including peer-reviewed journals, academic book chapters, conference papers, research reports, government reports, and "gray literature." In addition, PubMed, ScienceDirect, Medline, and Science.gov were used as supplemental search tools. Through screening the available titles and abstracts, we collected roughly 500 full papers and reports, from which representative and commonly used models were selected based on the following criteria:

- Models that can be applied to consumer products,
- Models that are suitable for exposure assessment,
- Model validity, and
- Usefulness to a broad range of users.

The following model types were given higher priority:

- Mass transfer models, whose parameters are well defined and can be independently determined or estimated,

- Empirical models whose key parameters can be related to the properties of the chemical substance, or the product matrix, or both.

The following model types were given lower priority:

- Statistical models whose parameters can only be determined using experimental data,
- Data reduction models for interpreting the emissions data (i.e., models in which the chemical concentration appears on the right-hand side of the equation).

It should be noted that, although a large number of models are available, not all of them are genuine predictive models suitable for use in exposure assessment. Overall, a significant knowledge gap still exists.

1.3. Report organization

This report consists of 14 sections.

Section 1 is the introduction.

Section 2 discusses categorization of existing modeling approaches.

Sections 3 through 13 present model descriptions.

Section 14 contains eight crosswalk tables of consumer product types with chemical substances of concern, including example models and references.

2. Categorization of modeling approaches

The models were categorized into 23 modeling approaches, including 22 identified by an ASTM workgroup. These approaches are discussed in Sections 3 through 13. A crosswalk of report sections with the 23 approaches is shown in TABLE 2.1.

TABLE 2.1 List of 23 modeling approaches and their corresponding sections in this report.

Modeling Approach	Exposure Route	Sections in Report
1. Mass transfer from surface of solid-hard article/building material to air	Inhalation	3 & 4
2. Mass transfer from surface of solid-soft-porous article/building material to air	Inhalation	3 & 4
3. Liquid/semi solid products applied to indoor surfaces	Inhalation	5 & 6
4. Liquids sprayed onto surfaces	Inhalation	5 & 6
5. Liquid/semi-solid products applied to solid indoor surfaces and longer-term emissions	Inhalation	5 & 6
6. Liquid/semi-solid where additional changes need to be considered	Inhalation	5 & 6
7. Liquids sprayed into the air	Inhalation	7
8. Spray-applied article/building material	Inhalation	7
9. Particle generation and resuspension of solid powder/granule applied to a surface	Inhalation	7
10. Combustion-based gas-powered appliances	Inhalation	8
11. Combustion of solid waxes and wicks to smoke	Inhalation	8
12. Combustion of solid fuels to smoke	Inhalation	8
13. Emission to air from electrical appliances and devices	Inhalation	9
14. Particle generation and resuspension of solid powder/granule applied to a surface	Migration	10
15. Leaching from solid consumer products to drinking water	Migration	11
16. Liquid that is ingested	Ingestion	12
17. Solid that is ingested (includes beads, powders, granules, gummies, etc.)	Ingestion	12
18. Migration from solid-hard frequent contact article mouthing	Ingestion	12
19. Migration from solid-soft/porous frequent contact article mouthing	Ingestion	12
20. Liquid/semi solid products applied to skin	Dermal	13
21. Migration from solid-hard frequent-contact article/building material to skin	Dermal	13
22. Migration from solid-soft, porous frequent-contact article/building material to skin	Dermal	13
23. Migration of solid/powder applied and absorbed into the skin	Dermal	13

3. Mass transfer from solid articles/building materials to air: (I) Diffusion-based models

3.1. Symbols and abbreviations

A = area of emission source (m^2),
Bi_m = Biot number for mass transfer and $Bi_m = h_a \delta / D_m$ (dimensionless),
C_a = concentration in air ($\mu g/m^3$),
C_{ai} = air concentration at the material-air interface ($\mu g/m^3$),
C_m = concentration in solid material ($\mu g/m^3$),
C_{m0} = initial concentration in the solid material (source) ($\mu g/m^3$),
C_s = concentration adsorbed on chamber surface ($\mu g/m^3$),
C_{sa} = air concentration at the chamber surface ($\mu g/m^3$),
C_{TSP} = concentration of total suspended particles in air ($\mu g/m^3$),
D_e = effective solid-phase diffusion coefficient for porous materials (m^2/s),
D_m = solid-phase diffusion coefficient (m^2/s),
E = emission factor ($mg/m^2/s$),
$\dot{E}$ = dimensionless emission factor,
f_m = fraction of contaminant mass emitted from the source,
Fo_m = Fourier number for mass transfer and $Fo_m = D_m\, t/\delta^2$ (dimensionless),
h_a = gas-phase mass transfer coefficient (m/s),
h_m = solid-phase mass transfer coefficient (m/s),
h_s = gas-phase mass transfer coefficient at chamber surfaces (m/s),
H_a = overall gas-phase mass transfer coefficient (m/s),
K_{ma} = material-air partition coefficient (dimensionless),
K_{oa} = octane-air partition coefficient (dimensionless),
K_{pa} = particle-air partition coefficient ($\mu g/m^3$),
K_{sa} = surface-air partition coefficient (m),
L = loading factor and $L = A/V$ (m^{-1}),
m = molecular weight (g/mol),
M = amount of contaminant emitted from the source (μg),
M_0 = initial amount of contaminant in the source and $M_0 = A\ \delta\ C_{m0}$ (μg),
N = ventilation rate (s^{-1}),
Q = ventilation flow rate (m^3/s),
R = emission rate (μg/h),
$\bar{R}$ = universal gas constant ($J\ K^{-1}\ mol^{-1}$),
t = time (s),
T = temperature (K),
V = room or chamber volume (m^3),
x = distance from the bottom of the solid material and $x = \delta$ at the exposed surface (m),
δ = thickness of the material (m),
θ = porosity (fraction),

ΔH_{ma} = enthalpy of the partitioning between material and air (J/mol),
ΔH_v = enthalpy of vaporization (J/mol).

Abbreviations

IAQ: indoor air quality,
PFAS: per- and polyfluoroalkyl substances,
QSAR: quantitative structure-activity relationship,
QPPR: quantitative property-property relationship,
SVOC: semi-volatile organic compound,
TVOC: total volatile organic compound,
VOC: volatile organic compound.

3.2. Overview

3.2.1. Theoretical considerations

Chemical substances, mainly volatile organic compounds (VOCs) and semi-volatile organic compounds (SVOCs), may be present in solid articles/products as either additives (e.g., plasticizers, flame retardants, light stabilizers, biocides, catalysts, colorants) or impurities generated during the manufacturing process (e.g., formaldehyde in engineered wood products and per- and polyfluoroalkyl substances (PFAS) in certain polymeric materials). These chemical substances can be emitted from the source to room air, affecting indoor air quality (IAQ). This emission process involves three mass transfer mechanisms (Figure 3.1):

- Diffusion in the solid phase,
- Solid-air equilibrium at the solid-air interface, and
- Diffusion through the boundary layer above the interface.

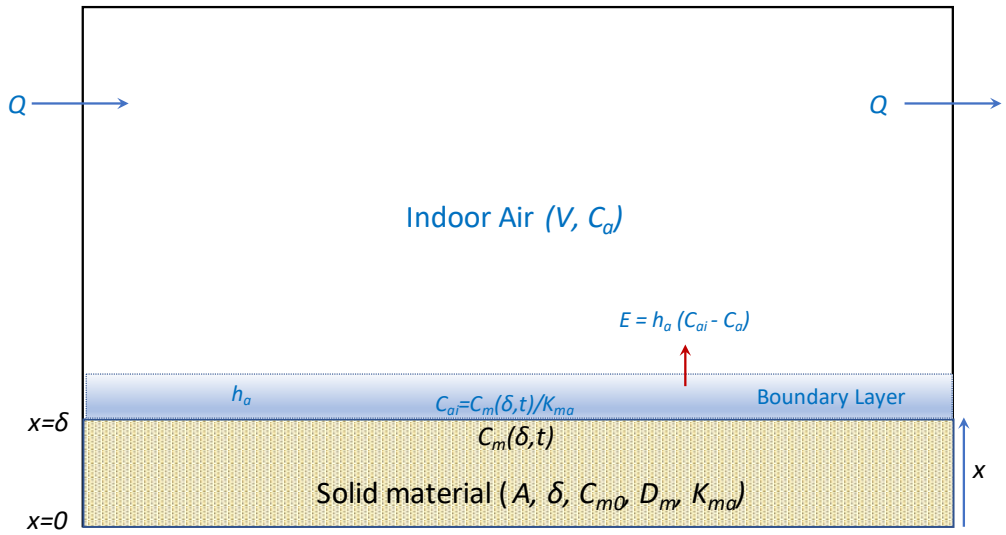

Figure 3.1 Schematic representation of mechanisms of chemical emissions from a solid material into air.

The source is described by five parameters: *A*, *δ*, C_{m0}, D_m, and K_{ma}. $C_m(\delta,t)$ is the solid-phase concentration at the exposed surface, C_{ai} is the equilibrium air concentration at the solid-air interface, and *E* is the emission factor.

The first transfer mechanism is diffusion in the solid phase. Migration of chemical substances from the interior to the exposed surface of the material is driven by a concentration gradient. This diffusion process is commonly represented by Fick's Second Law (Equation 3.1), in which $C_m(x,t)$ is the chemical concentration in the solid at depth *x* and time *t*. Note that, by convention, $x = 0$ is the bottom of the material, and $x = \delta$ is the exposed surface.

$$\frac{\partial C_m(x,t)}{\partial t} = D_m \frac{\partial^2 C_m(x,t)}{\partial x^2} \tag{3.1}$$

The second mass transfer mechanism is the equilibrium between the solid-phase concentration at the surface layer, $C_m(\delta,t)$, and the gas-phase concentration immediately surrounding the solid-air interface, C_{ai}. The equilibrium constant K_{ma} is known as the solid-air partition coefficient (Equation 3.2). All existing models assume that this interfacial equilibrium takes place instantaneously.

$$C_{ai} = \frac{C_m(\delta,t)}{K_{ma}} \tag{3.2}$$

The third mass transfer mechanism is for the diffusant in the gas phase at the interface to migrate from the solid-air interface to bulk air though a thin layer of air, known as the boundary layer (Figure 3.1). The net mass flux is proportional to the concentration difference between C_{ai} and C_a. The proportional constant h_a is called the gas-phase mass transfer coefficient (Equation 3.3).

$$E = h_a(C_{ai} - C_a) \tag{3.3}$$

The chemical concentration in indoor air, C_a, can then be determined using the mass balance equation for the room air (Equation 3.4), ignoring the contribution from ambient air.

$$V\frac{dC_a}{dt} = A\,E - QC_a \tag{3.4}$$

Equations 3.1 through 3.4 form a complete model that describes the effect of chemical substance emissions from a solid material on IAQ.

Although it is feasible to use this fundamental model directly for exposure assessment,[1, 2] it is undesirable for most users because solving the partial differential equation (Equation 3.1) requires proprietary computational software and user knowledge of numerical computation. Efforts have been made since the 1990s to develop simpler, easier-to-use models, resulting in four distinctive classes of models for chemical substance emissions from solid materials:

- Analytical solution models,
- Numeric approximation models,
- Dimensionless relationship models, and
- State-space models.

Descriptions of these model classes are given in Sections 3.3 through 3.6. Methods for estimating the key input parameters in those models are briefly discussed in Section 3.7.

Note that the mass flux between the solid material and indoor air may go in either direction. When the escaping tendency of the contaminant is greater in the gas phase than in the solid phase, the net flux is from the air to the solid. In such cases, the solid material becomes a sink for the airborne contaminant. When the escaping tendencies in the two phases are equal, there is no net mass flux across the interface. Also note that Equation 3.4 ignores the sink effect (i.e., the absorption and absorption of airborne chemical substances by interior surfaces).

3.2.2. VOCs versus SVOCs

One important factor in selecting models for chemical emissions from solid materials is the volatility of the target chemical. Some models are suitable for VOCs only and some are suitable for both VOCs and SVOCs.

According to ASTM D1356-20a, VOCs are organic chemicals with vapor pressures greater than 10^{-2} kPa (0.15 mm Hg) at 25°C while SVOCs covers a vapor pressure range from 10^{-2} to 10^{-8} kPa (0.15 to 1.5×10^{-7} mm Hg) at 25°C.[3] Because of their low volatilities, SVOCs tend to be adsorbed or absorbed by indoor media such as interior surfaces, suspended particles, and settled dust. This process is sometimes referred to as the sink effect. Although the mass transfer mechanisms described above are applicable to both chemical classes, the sink effect must be considered when modeling SVOC emissions.

3.2.3. Porous versus non-porous materials

Another factor to consider in modeling the chemical emissions from solid materials is the porosity of the material. A porous material contains voids. Because it contains less solid material than its non-porous counterpart, its partition coefficient (K_{ma}) is smaller while its diffusion coefficient (D_m) is greater than its non-porous counterpart. The models described in this section are applicable to both porous and non-porous materials so long as the partition and diffusion coefficients appropriate for either porous or non-porous materials are used. These parameters are influenced by both chemical and material properties. See Section 3.8.1 for more discussion on this topic.

3.2.4. List of models discussed

Twelve models are discussed below that cover all four model classes mentioned in Section 3.2.1. For the analytical solution model class, which contains over 20 models, three representative models with different levels of complexity are presented. TABLE 3.1 shows their model types and applicable chemicals.

TABLE 3.1 List of models for emissions from solid materials.

Model ID	Model Type	Applicable Chemical Classes	References
M1-A	Analytical solution	VOCs	Little et al., 1994[4]
M1-B	Analytical solution	VOCs	Deng & Kim, 2004[5]
M1-C	Analytical solution	VOCs	Zhang et al., 2022[6]
M1-D	Numeric solution	VOCs	Huang & Haghighat, 2002[7]
M1-E	Numeric solution	VOCs	Deng et al., 2010[8]
M1-F	Numeric solution	VOCs and SVOCs	Guo et al., 2020[9]
M1-G	Dimensionless relationship	VOCs	Yang et al., 1998[10]
M1-H	Dimensionless relationship	VOCs	Xu & Zhang, 2003[11]
M1-I	Dimensionless relationship	VOCs	Qian et al., 2007[12]
M1-J	State-space	VOCs and SVOCs	Yan et al., 2009[13]
M1-K	State-space	VOCs and SVOCs	Guo, 2013[14]
M1-L	State-space	VOCs and SVOCs	Huang et al., 2021[15]

3.3. Description of analytical solution models

3.3.1. General information

Given certain assumptions and a set of initial and boundary conditions, the fundamental model described in Section 3.2.1 above can be solved to yield analytical solutions for the concentration in room air (C_a) and the emission factor (E). Typical assumptions are as follows:

- The space is a single zone,
- The ventilation rate and room temperature are both constant,
- There is only one source in the room,
- The solid material is homogeneous,
- The chemical substance in the material is uniformly distributed initially,
- The adsorption and absorption by interior surfaces are negligible,
- The initial concentration in indoor air is zero, and

- The chemical substance concentration in ambient air can be ignored.

More than 20 analytical solution models have been developed.[16, 17] Depending on the derivation methods used and the assumptions made, these models look different but function in a similar manner. Each model contains three equations: one for chemical substance distribution in the solid as functions of depth and time, one for the concentration in indoor air, and one non-linear equation for an intermediate parameter known as the eigenvalue. Many models include a fourth equation for the emission factor.

Most of these models assume that the solid material is made of one homogeneous material, and that only one side of the material is exposed to indoor air. Models for other cases are also available, including:

- Single-layer material plus barrier (Little et al., 2002)[18]
- Double-layer material (Kumar et al, 2003) [19]
- Including interactions with airborne particles (Xu and Little, 2006)[20]
- Multiple-layer material with both sides exposed to air (Hu et a., 2007)[21]
- Multiple-layer material with both sides exposed to air plus chemical reactions in the solid (Wang and Zhang, 2011)[17]

Three representative analytical solution models with different complexities are described below (TABLE 3.2). They are all for single-layer materials with one side exposed to indoor air.

TABLE 3.2 Features of the three analytical solution models.

Model ID	M1-A	M1-B	M1-C
Considered solid-phase resistance	√	√	√
Considered gas-phase resistance	×	√	√
Considered surface adsorption	×	×	√
Key input parameters [A]	C_{m0}, K_{ma}, D_m	C_{m0}, K_{ma}, D_m, h_a	C_{m0}, K_{ma}, D_m, h_a, K_{sa}
Intended chemical substances	VOCs	VOCs	VOCs/SVOCs

[A] Other required input parameters include A, δ, V, and Q or N,

3.3.2. Model M1-A (Little et al., 1994) [4]

This is the first published model in its class. The model consists of three equations. Equation 3.5 calculates the chemical substance concentration in the solid material at any depth x and time t (C_m). Equation 3.6 calculates the chemical substance concentration in indoor air, C_a. Equation 3.7 is a non-linear equation with respect to intermediate parameter q_n, which is required by Equation 3.5.

$$C_m(x,t) = 2C_{m0}\sum_{n=1}^{\infty}\frac{\exp(-D_m q_n^2 t)\,(h-kq_n^2)\cos(q_n x)}{[\delta(h-kq_n^2)^2+q_n^2(\delta+k)+h]\cos(q_n\delta)} \tag{3.5}$$

$$C_a = \frac{C_m(\delta,t)}{K_{ma}} \tag{3.6}$$

$$q_n \tan(q_n \delta) = h - k q_n^2 \tag{3.7}$$

where

$$h = \frac{Q}{A\, D_m\, K_{ma}}$$

$$k = \frac{V}{A\, K_{ma}}$$

This model does not require the gas-phase mass transfer coefficient because it assumes that solid-phase diffusion is the rate-determining step.

3.3.3. Model M1-B (Deng and Kim, 2004) [5]

This model takes into consideration the mass transfer resistance in the gas-phase and, thus, requires gas-phase mass transfer coefficient h_a as an input parameter. Equations 3.8 through 3.10 correspond to Equations 3.5 through 3.7 in model M1-A.

$$C_m(x,t) = 2C_{m0} \sum_{n=1}^{\infty} \frac{(\alpha - q_n^2)}{A_n} \cos\left(\frac{x\, q_n}{\delta}\right) e^{-D_m\, \delta^{-2}\, q_n^2\, t} \tag{3.8}$$

$$C_a = 2C_{m0}\, \beta \sum_{n=1}^{\infty} \frac{q_n \sin q_n}{A_n}\, e^{-D_m\, \delta^{-2}\, q_n^2\, t} \tag{3.9}$$

$$q_n \tan q_n = \frac{\alpha - q_n^2}{K_{ma}\beta + (\alpha - q_n^2) K_{ma} Bi_m^{-1}} \tag{3.10}$$

where

$$A_n = [K_{ma}\beta + (\alpha - q_n^2) K_{ma} Bi_m^{-1} + 2] q_n^2 \cos q_n + q_n \sin q_n [K_{ma}\beta + (\alpha - 3q_n^2) K_{ma} Bi_m^{-1} + \alpha - q_n^2]$$

$$Bi_m = \frac{h_a\, \delta}{D_m}$$

$$\alpha = \frac{N\, \delta^2}{D_m}$$

$$\beta = L\, \delta$$

This model was later verified by Xiong et al. (2012), who also added an equation for cases when there is no ventilation air flow (i.e., Q = 0).[22]

3.3.4. Model M1-C (Zhang, et al., 2022) [6]

In addition to the three transfer mechanisms in the basic model, this model takes into consideration a fourth mechanism to account for adsorption by impermeable surfaces (e.g., the walls of a stainless-steel chamber). This addition allows SVOCs to be studied in the environmental chamber. The equation used for surface adsorption is given by Equation 3.11:

$$K_{sa}\ \frac{dC_{sa}}{dt} = \ h_s\ (C_a - \ C_{sa}) \tag{3.11}$$

The unit of the surface-air partition coefficient K_{sa} is in (m) and defined as $K_{sa} = C_a/C_{sa}$ at equilibrium. Thus, the chemical concentration absorbed on the surfaces is given by $C_s = K_s C_{sa}$ in (μg/m^2).

Like other analytical solution models, this model consists of three equations, one for air concentration, one for concentrations in the solid, and one non-linear equation for intermediate parameter q_n.

$$C_a = 2C_{m0}\beta \sum_{n=1}^{\infty} \frac{(q_n - \ B_s q_n^3\ )\sin q_n}{A_n}\ e^{-D_m\,\delta^{-2}\,q_n^2\,t} \tag{3.12}$$

$$C_m(x,t) = 2C_{m0} \sum_{n=1}^{\infty} \frac{A_u \cos\left(\frac{q_n\,x}{\delta}\right)}{A_n}\ e^{-D_m\,\delta^{-2}\,q_n^2\,t} \tag{3.13}$$

$$q_n tan\ q_n = \frac{A_u}{K_{ma}\beta(1 - B_s q_n^2) + K_{ma} B i_m^{-1} A_u} \tag{3.14}$$

where

$$A_n = \ q_n \sin q_n \{A_u + K_{ma}\beta\ (1 - 3B_s q_n^2) + K_{ma} B i_m^{-1}[\alpha - 3(1 + \alpha B_s + \xi) q_n^2 + 5B_s q_n^4]\}$$
$$+\ q_n^2 \cos q_n\ [K_{ma}\beta + (1 - B_s q_n^2) + K_{ma} B i_m^{-1} A_u + 2(1 - \alpha B_s + \xi) - 4B_s q_n^2]$$

$$A_u = \ \alpha - (1 + \alpha B_s + \xi) q_n^2 + B_s q_n^4$$

where $\alpha = N\delta^2/D_m$; $\beta = \delta A/V$; $\xi = K_{sa} A_s/V$; and $B_s = \frac{K_{sa}\,D_m}{\delta^2\ h_s}$.

While this model does improve upon models M1-A and M1-B by including consideration of one sink, it is still only suitable for interpreting chamber data, and not recommended for predicting SVOC distribution in real buildings because it does not handle absorption by porous surface materials such as gypsum board walls and vinyl flooring.

3.3.5. Calculations

For all the models in this class, it takes three steps to calculate the chemical substance concentration in indoor air as a function of time. Using model M1-B as an example, the necessary steps are:

- Gather input parameters V, A, Q, C_{m0}, K_{ma}, D_m, and h_a.
- Solve non-linear Equation 3.10 for n smallest positive roots ($q_1, q_2, \ldots q_n$), where n is a finite number. Depending on the convergence speed of the summation term in Equation 3.8, the value of n needed ranges from several dozen to several thousand. In most cases, however, n = 200 is sufficient.
- Substitute $q_1, q_2, \ldots q_n$ into Equation 3.9 to calculate the chemical substance concentration in air.

3.3.6. Advantages and disadvantages

The advantages of the analytical solution models include:

- They are true mass transfer models,
- All parameters are well defined and can be estimated independently,
- The model equations are clean and clear, as they are in forms that most readers are accustomed to,
- They can be used to estimate both short and long-term exposures, and
- They can be run quickly once the computer code is developed.

A major disadvantage of these models is their inflexibility. To use these models, the following conditions must be met:

- There is only one air zone,
- The ventilation air flow rate and indoor temperature are constant,
- There is only one emission source in the zone,
- Models in this class are suitable for VOCs only because none of them consider absorption by porous materials. Model M1-C allows only surface adsorption and cannot handle diffusive sinks, and
- The initial air concentration must be zero.

In addition, these analytical models can only be used alone. They cannot be easily incorporated into an IAQ simulation program.

As a minor glitch, model M1-A gives a run-time error when the time is zero. This problem can be avoided by substituting t = 0 with a small positive value, such as $t = 10^{-4}$ sec.

3.4. Description of numeric approximation models

3.4.1. General information

Numeric methods can provide numerical approximations to the solutions of differential equations. The numeric approximation models often work as well as the analytical solution models. To show how this class of models works, consider the simplest case, where there is a constant source R in a room with a volume V and an air exchange flow rate Q. The mass balance is given by Equation 3.15.

$$V\frac{dC_a}{dt} = R - QC_a \tag{3.15}$$

Given the initial concentration of C_a = 0 when t = 0, the analytical solution to Equation 3.15 is:

$$C_a = \frac{R}{Q}\,(1 - e^{-Nt}) \tag{3.16}$$

where $N = Q/V$ is the ventilation rate.

To obtain a numeric solution to Equation 3.15, consider time series $t_0 = 0$, $t_1 = \Delta t$, $t_2 = 2\Delta t$, … $t_i = i\,\Delta t$…, where Δt is a small increment of time. Then, Equation 3.15 can be approximated by replacing dC_a/dt with $\Delta C_a/\Delta t$:

$$V\frac{dC_a}{dt} \approx V\frac{\Delta C_a}{\Delta t} = V\frac{C_i - C_{i-1}}{\Delta t} = R - Q\frac{C_i + C_{i-1}}{2} \tag{3.17}$$

where

C_i and C_{i-1} are the air concentrations at time t_i and t_{i-1};

$\frac{C_i + C_{i-1}}{2}$ is the average concentration between t_{i-1} and t_i.

Rearranging Equation 3.17 yields Equation 3.18,

$$C_i = \frac{2\,R\,\Delta t + (2\,V - Q\,\Delta t)\,C_{i-1}}{2\,V + Q\,\Delta t} \tag{3.18}$$

This is the numeric approximation solution to Equation 3.15. Although it looks completely different from the analytical solution (Equation 3.16), the two models work equally well so long as Δt is sufficiently small (Figure 3.2).

Note that to calculate C_i, the concentration at the previous time step (C_{i-1}) is needed. Therefore, the concentrations at t_0, t_1, t_2… are calculated sequentially starting from the initial condition:

$C_0 = 0$ (this is the initial condition)

$$C_1 = \frac{2\,R\,\Delta t + (2\,V - Q\,\Delta t)\,C_0}{2\,V + Q\,\Delta t}$$

$$C_2 = \frac{2\,R\,\Delta t + (2\,V - Q\,\Delta t)\,C_1}{2\,V + Q\,\Delta t}$$

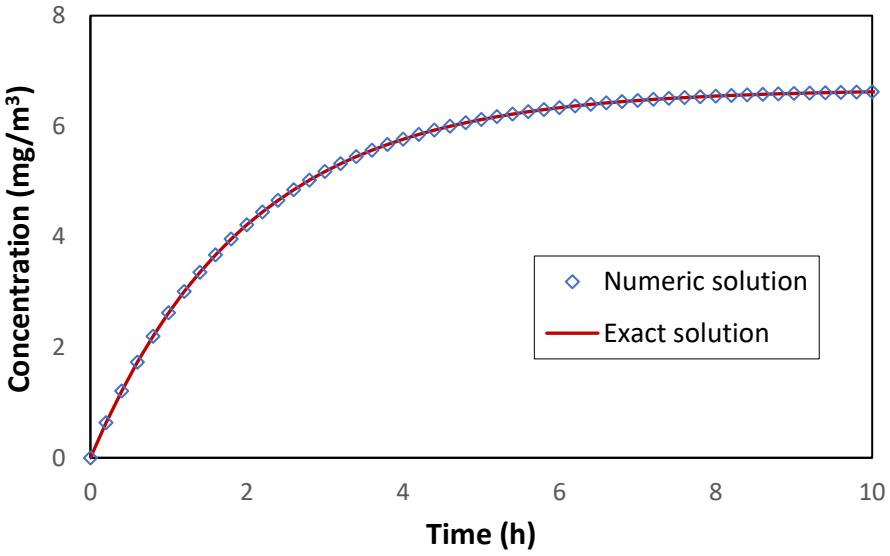

Figure 3.2 Comparison of the air concentrations predicted by the analytical and numeric solutions to Equation 3.15.

Input parameters: $V = 30\ m^3$, Q = 15 m³/h, and R = 100 mg/h.

The numeric approximation solution to the partial differential equation in the fundamental model (Equation 3.1) can be obtained similarly, and the most common method used is the finite-difference method.

Three models are discussed below. Their key features are shown in TABLE 3.3.

TABLE 3.3 Features of three numeric approximation models.

Model ID	Features	Intended Chemical substances
M1-D	One single-layer source	VOCs
M1-E	One multiple-layer source	VOCs
M1-F	Multiple single-layer sources	VOCs [A]

[A] May be applicable to SVOCs.

3.4.2. Model M1-D (Huang and Haghighat, 2002) [7]

The level of detail for this model is comparable to that of the analytical solution model M1-B, in which the gas-phase resistance is considered. The VOC concentration at the exposed material surface, $C_m(\delta,t)$, and the concentrations in room air, $C_a(t)$, are given by Equations 3.19 and 3.20.

$$\left[\frac{D_m}{\Delta x}+\frac{\Delta x}{\Delta t}+\frac{h_a}{K_{ma}}-\frac{L\,h_a^2\,\Delta t}{\alpha}\right]C_m(\delta,t)=\frac{D_m}{\Delta x}C_m(\delta-\Delta x,t)+\frac{\Delta x}{\Delta t}C_m(\delta,t-\Delta t)+\frac{h_a}{\alpha}C_a(t-\Delta t) \quad (3.19)$$

$$C_a(t)=\frac{L\,h_a\,\Delta t}{\alpha}C_m(\delta,t)+\frac{1}{\alpha}C_a(t-\Delta t) \quad (3.20)$$

where $\alpha = K_{ma}\,(N\,\Delta t + L\,h_a\,\Delta t + 1)$.

This model looks simpler than the analytical solution models, does not contain a non-linear equation, and requires only arithmetic operations. Theoretically, it can be implemented in a spreadsheet. However, the actual calculations are much more complex because it requires a large number of finite difference "grids" or "nodes."

The spacing and scaling of the finite-difference nodes is key to the accuracy of the model. The authors did not provide sufficient detail about how this model is implemented. For example, the proper value of Δx—the distance between two adjacent nodes—is needed for a given solid product with a certain area and thickness.

3.4.3. Model M1-E (Deng et al., 2010) [8]

This model is for VOC emissions from a multi-layer source. Each layer can have its own chemical substance content and partition and diffusion coefficients. The model description is abridged, and some details are missing. For example, it is unclear how mass transfer between two layers is handled and whether a solid-solid partition coefficient is used.

This is a rather complex model. There are equivalent analytical solution models such as the double-layer model proposed by Kumar et al, 2003).[19] The state-space models described below can also handle multi-layer sources.

3.4.4. Model M1-F (Guo et al., 2020) [9]

A key feature of this numeric approximation model is that it allows multiple diffusion sources to co-exist in a single-zone environment. The numeric solutions consist of three equations: one for VOC concentrations inside the solid material, one for the concentrations at the exposed surface of the solid material, and one for the concentrations in indoor air. These equations (Equations 9, 10, and 11 in the original manuscript) are too long to be listed in this document. Readers should consult the original paper for details.

Although this model was initially developed for VOC emissions, it may allow diffusive sinks in the room because diffusion-based sources and sinks work similarly. The only difference between a diffusive source and a diffusive sink is their initial concentrations in the solid material. This model works only in a single-zone environment, however.

Theoretically, this model may be applicable to SVOCs as well because diffusive sources and sinks share the same models. Further evaluation is needed, however.

3.4.5. Calculations

Numeric approximation models require only arithmetic operations. It is possible to implement those models in a spreadsheet. However, the calculations are rather tedious. In most cases, the calculations are performed by a computer program.

3.4.6. Advantages and disadvantages

The numeric models described above simplify the analytical solution models by eliminating non-linear equations. They usually work as well as analytical solution models and have the same limitations. For example, they work only for a single source in a single zone, with model M1-F being an exception.

3.5. Description of dimensionless relationship models

3.5.1. General information

In a dimensionless relationship model, the ordinary input parameters (such as room volume, ventilation rate, partition coefficient, and diffusion coefficient) are replaced with a set of dimensionless numbers, which are unitless physical quantities. The constant π—the circumference-to-diameter ratio of a circle—is perhaps the best-known dimensionless number. Regardless of the size of a circle, the value of π is always the same. Models based on dimensionless numbers have two major advantages:

- They reduce the number of parameters in the model, which makes sensitivity analysis easier. This approach does not reduce the number of input parameters, however.
- They improve the scalability of the model significantly. For instance, a dimensionless relationship model developed from micro chamber data can be readily applied to much larger spaces, such as large chambers and homes.

The most commonly used dimensionless numbers in emission models are the Fourier number for mass transfer, Fo_m, and Biot number for mass transfer, Bi_m, which are defined in Section 3.1.

3.5.2. Model M1-G (Yang et al., 1998) [10]

This model was developed to predict long-term (e.g., several months) VOC emissions from carpet backing. It uses a single dimensionless number, Fo_m. The amount of total VOC (TVOC) or VOC emitted from the source, $M(t)$, is given by Equation 3.21.

$$\frac{M(t)}{M_0} = 1 - \sum_{n=0}^{\infty} \left\{ \frac{2}{\left[\left(n+\frac{1}{2}\right)\pi\right]^2} \, exp\left[-\left(n+\frac{1}{2}\right)^2 \pi^2 \, Fo_m\right] \right\} \tag{3.21}$$

For a small time-interval between t_1 and t_2, the average emission factor can be calculated from Equation 3.22.

$$E = \frac{M(t_1) - M(t_2)}{A(t_2 - t_1)} \tag{3.22}$$

A steady-state mass balance equation is used to calculate the average air concentration (Equation 3.23):

$$C_a = \frac{E\,A}{N\,V} \tag{3.23}$$

According to the authors, the summation in Equation 3.21 converges rather quickly for long-term predictions and the first few terms are sufficient.

3.5.3. Model M1-H (Xu and Zhang, 2003) [11]

This model uses two dimensionless numbers: the Fourier number for mass transfer, Fo_m, and Biot number for mass transfer, Bi_m. The fraction of contaminant mass emitted at time t (f_m) is given by Equation 3.24. Unlike other dimensionless models in its class, this model requires solving a non-linear equation (Equation 3.25).

$$f_m = \frac{M(t)}{M_0} = \sum_{n=1}^{\infty} \frac{2\ sin^2 q_n}{q_n^2 + \ q_n \sin q_n \cos q_n} \left(1 - \ e^{q_n^2\, Fo_m}\right) \tag{3.24}$$

$$q_n \tan q_n = \frac{Bi_m}{K_{ma}} \tag{3.25}$$

The emission rate can then be calculated from $R = \frac{df_m}{dt}\ M_0 \ \approx \ \frac{\Delta f_m}{\Delta t}\ M_0$.

3.5.4. Model M1-I (Qian et al., 2007) [12]

This model correlates the normalized emission factor ($\dot{E}$) with four dimensionless numbers: dimensionless air exchange rate (α), dimensionless loading factor (β), Fourier number for mass transfer, Fo_m, and Biot number for mass transfer, Bi_m. This idea was first proposed by Deng and Kim (2004).[5] Qian et al. (2007) then implemented the idea and generated three correlations for different values of the Fourier number for mass transfer (Fo_m).

For $Fo_m \leq 0.01$ ($R^2 = 0.972$):

$$\dot{E} = 1.34\ \alpha^{8.4\times10^{-3}} (\beta K_{ma})^{-1.3\times10^{-4}} \left(\frac{Bi_m}{K_{ma}}\right)^{0.26} e^{-\frac{0.0059}{Fo_m + 0.0038}} \tag{3.26}$$

For $0.01 < Fo_m \leq 0.2$ ($R^2 = 0.986$):

$$\dot{E} = 0.469\ \alpha^{0.022} (\beta K_{ma})^{-0.021} \left(\frac{Bi_m}{K_{ma}}\right)^{0.021} {Fo_m}^{-0.48} \tag{3.27}$$

For $Fo_m > 0.2$ ($R^2 = 0.992$):

$$\dot{E} = 2.104\ \alpha^{-7.2'10^{-3}} (\beta K_{ma})^{8.5'10^{-3}} \left(\frac{Bi_m}{K_{ma}}\right)^{-7.0'10^{-3}} e^{-2.36\, Fo_m} \tag{3.28}$$

where

$\alpha = N\ \delta^2/D_m$ is the dimensionless air exchange rate, and

$\beta = A\,\delta/V$ is the dimensionless loading factor.

Once $\dot{E}$ is known, the emission factor I can be calculated from

$$E = \frac{D_m\, C_0\, \dot{E}}{\delta} \tag{3.29}$$

Then, the VOC concentrations in indoor air can be obtained by solving Equation 3.30 numerically. Note that the emission factor E is a function of time and, thus, should be given as an input data table.

$$V\,\frac{dC_a}{dt} = A\,E - Q\,C_a \tag{3.30}$$

This model works well for predicting short-term concentration but is unsatisfactory for long-term predictions (Figure 3.3). Adjustments are needed to make Equation 3.28 (for $Fo_m > 0.2$) more suitable for predicting long-term emissions.

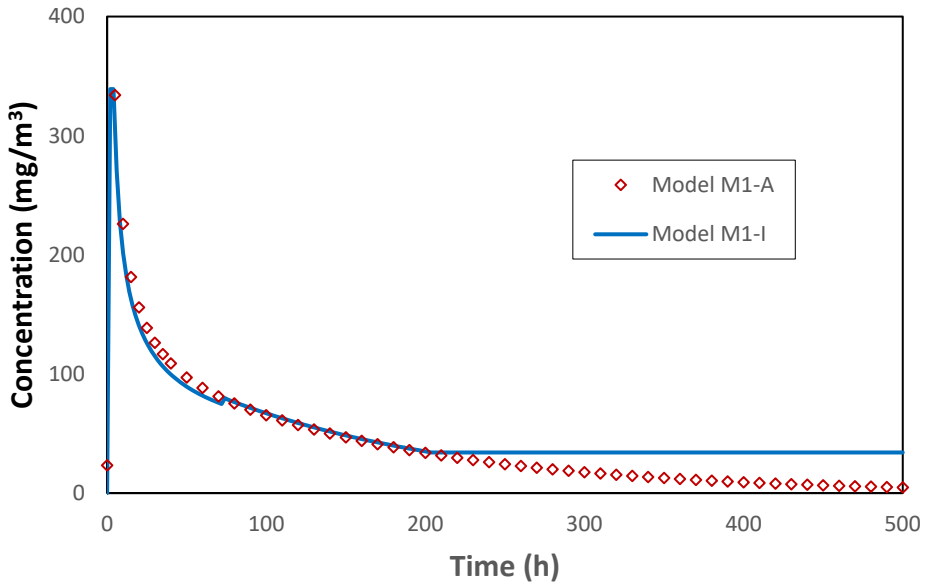

Figure 3.3 Comparison of hexanal concentrations emitted from a particle board predicted by analytical solution model M1-A and model M1-I.

Input parameters were: V = 50 m^3, Q = 50 m^3/h, A = 10 m^2, δ = 0.01 m, C_{m0} = 1.15 × 10^7 µg/m^3, K_{ma} = 3289, D_m = 2.75 × 10^{-7} m^2/h, and h_a = 1 m/h. Values for C_{m0}, K_{ma}, and D_m were from Ref. [5].

3.5.5. Calculations

Calculation the emission factor with model M1-G is straightforward, whereas model M1-H requires solving a non-linear equation (see Section 3.3.5). With model M1-I, it takes the following three steps to calculate the emission factor E, and an additional step to calculate the VOC concentrations in room air:

- Calculate the dimensionless numbers α, β, Bi_m, and Fo_m,
- Select the applicable equation from Equations 3.26, 3.27, and 3.28 based on the value of the Fourier number (Fo_m) and then calculate the dimensionless emission factor $\dot{E}$,
- Use Equation 3.29 to calculate the emission factor E, and
- Use Equation 3.30 to calculate the air concentrations.

3.5.6. Advantages and disadvantages

Dimensionless relationship models usually have fewer parameters, and the calculation is much simpler than the analytical solution models. On the other hand, these models are less accurate than the analytical solution models because the regression process introduces additional uncertainty.

Model M1-I is accurate in predicting short-term emissions but has two disadvantages: (1) The model consists of three correlations. The user must calculate the Fourier number Fo_m at each time step to ensure that the correct equation is selected. (2) The transition from one correlation to another is not smooth, as shown in Figure 3.3.

3.6. Description of state-space models

3.6.1. General information

The state-space method is a spatial discretization technique that, among many applications, can be used to provide approximate solutions to partial differential equations. Modeling emissions from solid materials is done by dividing the solid material into a finite number (n) of layers or slices, resembling a quire of printer paper. It is assumed that, if the slice is thin enough, the chemical substance inside each slice is uniformly distributed all the time. Thus, the mass transfer between two adjacent slices can be represented by the compartment model in the form of ordinary differential equations, which are more suitable for computation.

Three state-space models are described below.

3.6.2. Model M1-J (Yan et al., 2009) [13]

This is the first state-space model developed for VOC emissions from solid materials. It uses the conventional method to divide the source into n layers or slices with the same thickness. If the thickness of the source is δ, the thickness of each slice is $\Delta\delta = \delta/n$ (Figure 3.4).

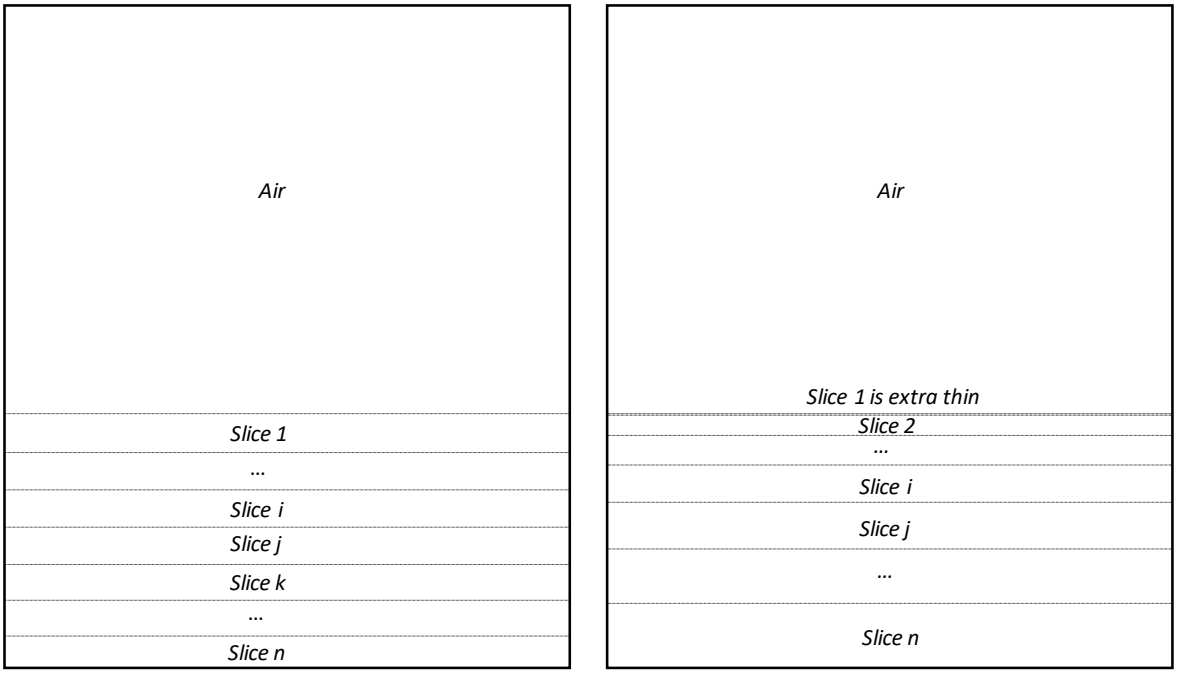

Figure 3.4 Even discretization used in model M 1-J (left) and uneven discretization in model M1-K (right).

If *i*, *j*, and *k* are three adjacent slices, the mass transfer rate from slice *j* to slice *i*, R_{ji}, and from slice *k* to slice *j*, R_{kj}, are given by Equations 3.31 and 3.32,

$$R_{ji} = A\, h_m\left(C_{mj} - C_{mi}\right) \tag{3.31}$$

$$R_{kj} = A\, h_m\left(C_{mk} - C_{mj}\right) \tag{3.32}$$

where $h_m = D_m/\Delta\delta$ is the solid-phase mass transfer coefficient in each slice.

Thus, the mass balance equation for slice *j* is given by Equation 3.33,

$$V_j \frac{dC_{mj}}{dt} = R_{ki} - R_{ji} \tag{3.33}$$

where $V_j = A\,\Delta\delta$ is the volume of slice *j*.

The transfer rate from the top slice (slice 1) to air, R_{ma}, is similar to Equations 3.2 and 3.3 in the basic model,

$$R_{ma} = A\, h_a\left(\frac{C_{m1}}{K_{ma}} - C_a\right) \tag{3.34}$$

and the mass balance for indoor air is given by Equation 3.35,

$$V\frac{dC_a}{dt} = R_{ma} - Q\,C_a \tag{3.35}$$

With the source divided into *n* slices, the number of ordinary differential equations needed to represent the source is *n*. While the accuracy of the model increases with the value of *n*, too many slices result in computation complexity. The authors suggest that a reasonable number of *n* be estimated from Equation 3.36.

$$n = \frac{30\,\delta}{0.00159}\sqrt{\frac{D_m}{7.65\times 10^{-11}}} \tag{3.36}$$

where the solid-phase diffusion coefficient D_m is in m^2/s. For example, if δ = 0.01 m and $D_m = 1\times 10^{-12}$ m^2/s, 22 slices are needed.

3.6.3. Model M1-K (Guo, 2013) [16]

This model made two major modifications to model M1-J described above. First, the slices are in different thicknesses. The exposed top slice is ultrathin, and the thickness of other slices increases with the depth (Figure 3.4). This uneven discretization helps reduce the number of slices needed and improve the performance by ensuring there are more slices near the exposed surface, where the concentration gradient is the steepest.

Another key modification is the use of the two-resistance theory [23] to represent the mass transfer between the solid and gas phases, as described below.

Mass transfer between two adjacent slices, *i* and *j*:

$$R_{ij} = A\,h_{mij}\left(C_{mi} - C_{mj}\right) \tag{3.37}$$

where

$h_{mij} = \frac{2\,D_m}{\delta_i+\delta_j}$ is the solid-phase mass transfer coefficient between slices *i* and *j*;

$\Delta\delta_i$ and $\Delta\delta_j$ are the thicknesses of slices *i* and *j*; and

$(\Delta\delta_i + \Delta\delta_j)/2$ is the average travel distance between slices *i* and *j*.

Mass transfer between the top slice (slice 1) and air:

$$R_{1a} = A\,H_a\left(\frac{C_{m1}}{K_{ma}} - C_a\right) \tag{3.38}$$

where

H_a = overall gas-phase mass transfer coefficient defined by Equation 3.39,

C_{m1} = chemical substance concentration in the top slice.

$$\frac{1}{H_a} = \frac{1}{K_{ma}\, h_{m1}} + \frac{1}{h_a} \tag{3.39}$$

where h_{m1} = the solid-phase mass transfer coefficient in in the exposed slice and determined by the solid-phase diffusion coefficient, D_m, and the thickness of the top slice, $\Delta\delta_1$:

$$h_{m1} = \frac{2\, D_m}{\Delta\delta_1} \tag{3.40}$$

As shown in Figure 3.5, this state-space model compares favorably with an analytical solution model.

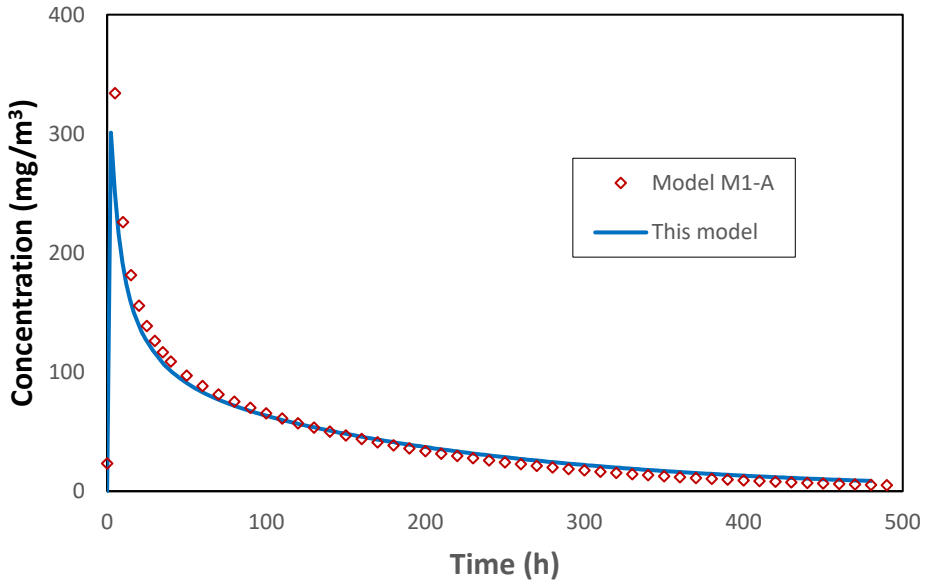

Figure 3.5 Comparison of hexanal concentrations emitted from a particle board predicted by analytical solution model M1-A and model M1-K.

Input parameters were: V = 50 m^3, Q = 50 m^3/h, A = 10 m^2, δ = 0.01 m, C_{m0} = 1.15 × 10^7 µg/m^3, K_{ma} = 3289, D_m = 2.75 × 10^{-7} m^2/h, and h_a = 1 m/h. Values for C_{m0}, K_{ma}, and D_m were from Ref. [5].

3.6.4. Model M1-L (Huang et al., 2021) [15]

This model uses an uneven discretization method to divide the solid phase, similar to that used by model M1-K. Unlike model M1-K, which uses the two-film theory for interfacial transfer, this model uses Equation 3.41, in which the air concentration C_a includes chemical substances absorbed by the total suspended particles. The other difference is that this model treats the boundary conditions by the finite difference approximation.

$$V\frac{dC_a}{dt} = \mathrm{A}\, h_a\left(\frac{C_{m1}}{K_{ma}} - \frac{C_a}{1+K_{pa}C_{TSP}}\right) - QC_a \quad (3.41)$$

where C_{m1} is the concentration in the top layer of the material.

According to the authors, the performance of this model is comparable to that of model M1-K.

3.6.5. Calculations

State-space models consist of a large number of ordinary differential equations. For the simplest case, where there is a single source in a room and the source is divided into 10 slices, 11 equations are needed, 10 for the solid-phase transfer and 1 for room air. Thus, these models are solved numerically with a computer program.

3.6.6. Advantages and disadvantages

The state-space models are much more flexible than those of the other three classes and suitable for both VOCs and SVOCs. They can be used in either a single zone or multiple zones, they allow multiple sources and diffusive sinks, they can handle multi-layer sources, they work in scenarios where suspended and settles particles are present [14, 15], and they can handle temperature and ventilation rate changes during the simulation [24].

State-space models are computationally intensive. For most users, these models are useful only if they are incorporated into IAQ simulation software, which handles the calculations. At present, model M1-K is implemented in two IAQ simulation programs: i-SVOC [25] and IECCU [24].

3.7. Parameter estimation methods

The key parameters for modeling chemical emissions from solid materials are the initial concentration in the solid material (C_{m0}), the solid-air partition coefficient (K_{ma}), the solid-phase diffusion coefficient (D_m), and gas-phase mass transfer coefficient (h_a). Select methods for estimating these parameters are discussed below.

3.7.1. Using experimentally determined C_{m0}, K_{ma}, and D_m

The initial concentration of the chemical in the solid material, C_{m0}, is usually determined experimentally. In the absence of measured data, information from the product formulation can be used.

Limited data on experimentally determined K_{ma} are available in the literature. Huang and Jolliet (2018) compiled 991 data points for 179 chemicals in 22 consolidated material types. More recent data are reported among many journal papers and are not yet compiled and analyzed.

Similarly, limited data on experimentally determined D_m are available. Huang et al. (2017) compiled 1103 data points for 158 chemicals in 32 consolidated material types.[26]

3.7.2. QPPR models for estimating soils-air partition coefficient (K_{ma})

Huang and Jolliet (2018) developed two quantitative property-property relationship (QPPR) models based on 991 measured K_{ma} values for 179 chemicals in 22 consolidated material types. Equation 3.42 is material-type-specific whereas Equation 3.43 is not. [27]

$$log_{10}\, K_{ma} = -0.38 + 0.63\, log_{10}\, K_{oa} + 0.96 \frac{\Delta H_{ma}}{2.303\, \bar{R}} \left(\frac{1}{T} - \frac{1}{298.15}\right) + b \quad (n = 991,\ R^2 = 0.934) \quad (3.42)$$

$$log_{10}\, K_{ma} = -0.37 + 0.75\, log_{10}\, K_{oa} + 3.29 \frac{\Delta H_{ma}}{2.303\, \bar{R}} \left(\frac{1}{T} - \frac{1}{298.15}\right) \quad (n = 991,\ R^2 = 0.80) \quad (3.43)$$

where

K_{oa} is the octanal-air partition coefficient and can be found from physical/chemical property estimation programs such as EPI Suite™ [28] and ChemSpider (www.chemspider.com).

b is the material-specific coefficient, which can be found in a look-up table in the original paper.

ΔH_{ma} is the enthalpy of the partitioning between material and air and can be calculated from Equation 3.44.

$$\Delta H_{ma} = 1.37\, \Delta H_v - 14.0 \quad (3.44)$$

where the enthalpy of evaporation (ΔH_v) can be found in chemical structure databases such as ChemSpider.

Note that if the material type falls into the 22 consolidated types in the look-up table, Equation 3.42 is preferred over 3.43 because the latter has greater uncertainties.

3.7.3. QPPR models for estimating solid-phase diffusion coefficient (D_m)

Two commonly used QPPR models are discussed below.

The Huang et al. method [26] was based on 1103 measured diffusion coefficients for 158 chemicals in 32 consolidated material types (Equation 3.44).

$$log_{10}\, D_m - \frac{\tau - 3486}{T} = 6.39 - 2.49\, log_{10}\, m + b \quad (n = 1103,\ R^2 = 0.932) \quad (3.44)$$

Material-specific parameters τ and b can be found in a look-up table for the 22 material types.

The Begley et al. method [29] is an empirical model for estimating the upper-bound of solid-phase diffusion coefficient in polymers (Equation 3.45).

$$D_m = 10^4\, exp\left(A_p - 0.1351 m^{\frac{2}{3}} + 0.003\, m - \frac{10454}{T}\right) \quad (3.45)$$

where

D_m is in (m^2/s),

$A_p = A'_p - \tau/T$, where A'_p and τ are empirical coefficients. Their values for several polymers are given in the original paper.

3.7.4. Uncertainties in estimating partition and diffusion coefficients K_{ma} and D_m

A major source of uncertainty in predicting emissions from solid materials is from the input parameters, especially the solid-air partition coefficient (K_{ma}) and solid-phase diffusion coefficient (D_m). These two parameters are difficult to measure due to two factors. First, in developing experimental methods, most researchers inexplicitly assume that K_{ma} and D_m are independent of each other and, therefore, can be measured simultaneously. This assumption is not justifiable. It is well known that, within each chemical class, K_{ma} increases and D_m decreases as the carbon number increases. For example, Wang et al. (2018) show that solid-air partition coefficient is associated with the liquid molar volume of the target VOCs.[30] Solid-phase diffusion coefficient is inversely associated with molecular weight, molar volume or LeBas volume of the target compounds.[26, 31, 32] There are even empirical models for estimating K_{ma} from D_m.[33] The mutual dependence of these parameters makes it difficult to determine both parameters in a single experiment. Thus, it is preferrable to determine K_{ma} and D_m separately.

Another source of uncertainty is from the classification of material types. When numerous solid consumer products and articles are classified into a limited number of categories, such as the 22 categories used by Huang and Jolliet (2019) [27], the physical properties among the products within each material type—such as chemical composition, density, and lipophilicity—may vary significantly.

3.8. Additional comments

3.8.1. Models for porous solid materials

Several analytical solution models have been developed specifically for porous materials. [34-36] By including porosity as an additional input parameter, these models help inform the relationship between the diffusion and partition coefficients for porous and neat materials. For the purpose of exposure assessment, however, the distinction between porous and neat materials is useful but not absolutely necessary because the two can be treated as different types of materials. Many reported diffusion and partition coefficients in the literature are for porous materials. Experimentally determined “effective” diffusion and partition coefficients for porous materials can be used directly to predict emissions without further adjustments.

According to Liu et al. (2022), [37] the effective diffusion coefficient for a porous material, D_e, is defined by Equation 3.46,

$$D_e = \theta\, D_m\, K_{ma} \tag{3.46}$$

Three parameters are required to calculate the effective diffusion coefficient. This definition also implies that 100% of the gas pockets, or cells, in the material are interconnected, forming air channels. In the real world, however, few solid materials meet this criterion. For example, polyurethane foam (PUF)

materials on the market are divided into two groups: closed-cell and open-cell foams. The gas pockets in closed-cell foam are almost entirely enclosed by walls. Since they are closed, they do not interconnect with other cells. Closed-cell foam is considered semi-impermeable. A foam is classified as an open-cell foam if 50% or more cells are open. In other words, open-cell foams are considered semi-permeable. Thus, in most cases, Equation 3.46 tends to overestimate the effective diffusion coefficient for porous materials.

3.8.2. A special issue in modeling formaldehyde emissions from engineered wood products

The formaldehyde content in an engineered wood product may come from two sources: (1) free formaldehyde that existed as an unwanted byproduct during the manufacturing process, and (2) secondary formaldehyde generated from the hydrolysis reaction of the binding resin under daily use conditions.[38] The reaction rate is affected by the resin type, moisture content in the wood, and temperature. Most models described in this section do not consider the second source and, thus, may underestimate the emission rates. The analytical solution model developed by Wang and Zhang (2011) [17] includes the generation of secondary chemical substances in the solid phase but no details are provided on how the generation rate should be represented in the model.

3.9. Summary

Four classes of models are available for predicting VOC and SVOC emissions from solid materials:

- Analytical solution models,
- Numeric approximation models,
- Dimensionless relationship models, and
- State-space models.

The first three classes are suitable mainly for VOC emissions.

The analytical models require solving a non-linear equation, which is usually done with a computer program. Once the code is written and checked, these models run quickly and can be used to estimate both short and long-term exposures. Among the over 20 models in this class, model M1-B is the one most frequently cited. This model was later verified by Xiong et al., who also added an equation for cases with no ventilation air flow (i.e., $Q = 0$).[22]

The performance of numeric solution models is similar to that of analytical models. While these models require only basic arithmetic operations, the calculations are rather tedious.

Dimensionless number relationship models simplify the equations but do not reduce the number of input parameters. Because of the reduced number of parameters, these models are most convenient for sensitivity analysis. Their performance is usually inferior to the corresponding analytical models because the regression process introduces additional uncertainty.

State-space models are more flexible than other types of models:

- They are suitable for both VOCs and SVOCs,
- They allow multiple sources and multiple diffusion sinks to exist in either single or multi-zone environments,
- They can handle multi-layer sources and sinks,

- They can include airborne and settled particles, and
- They can handle temperature and ventilation rate changes.

State-space models are computationally intensive. For most users, they are more useful only after being incorporated in IAQ simulation programs, which take over the calculations and allow the user to focus on resolving IAQ problems.

Model M1-K has been used to investigate emissions of organophosphorus flame retardants (OPFRs) from polyurethane foam and flame retardant [39] and OPFR sorption by building materials and consumer products [40].

A general guide on selecting models for emissions from solid materials is shown in TABLE 3.4.

TABLE 3.4 Suggestions on selecting models for emissions from solid materials.

Chemical Class	Conditions	Models	Notes
VOCs	Single zone	M1-A	Included in simulation tool IAQX.[41]
VOCs	Single zone	M1-B	Performs better than M1-A; requires coding
VOCs	Multi zone	M1-K	Included in simulation tool IECCU.[24]
SVOCs	Single zone	M1-K	Included in simulation tools IECCU and iSVOC.[24, 42]
SVOCs	Multi zone	M1-K	Included in simulation tool IECCU.[24]

4. Mass transfer from solid articles/building materials to air: (II) More mass transfer models and empirical models

4.1. Symbols and abbreviations

A = exposed area of emission source (m^2),
C_a = concentration in air ($\mu g/m^3$),
C_m = concentration in solid material ($\mu g/m^3$),
C_{m0} = initial concentration in the source ($\mu g/m^3$),
C_{TSP} = concentration of total suspended particles in air ($\mu g/m^3$),
C_v = saturation concentration in air converted from the vapor pressure of the chemical ($\mu g/m^3$)
D_m = solid-phase diffusion coefficient (m^2/s),
E = emission factor ($mg/m^2/s$),
E_N = normalized emission factor ($\mu g/m^2/s$),
E_{Nx} = normalized emission factor for congener x ($\mu g/m^2/s$),
E_{Nref} = normalized emission factor for the reference congener ($\mu g/m^2/s$),
f_{em} = fraction of chemical substance mass emitted from the source,
h_a = gas-phase mass transfer coefficient (m/s),
K_{ma} = material-air partition coefficient (dimensionless),
K_{pa} = particle-air partition coefficient ($m^3/\mu g$),
M = amount of chemical substance emitted from the source the source (μg),
M_0 = initial amount of chemical substance in the source and $M_0 = A\ \delta\ C_{m0}$ (μg),
P_x = vapor pressure for congener x (mm Hg),
P_{ref} = vapor pressure for the reference congener (mm Hg),
Q = ventilation flow rate (m^3/s),
R = emission rate ($\mu g/s$),
t = time (s),
V = room or chamber volume (m^3),
y_0 = gas-phase concentration at solid-air interface ($\mu g/m^3$),
δ = thickness of the material (m).

Abbreviations

IAQ: indoor air quality,
PCB: polychlorinated biphenyl,
SVOC: semi-volatile organic compound,
TCEP: tris(2-chloroethyl) phosphate,
TSP: total suspended particles,
VOC: volatile organic compound.

4.2. Overview

The models described in this section include four relatively simple mass transfer models for volatile organic compound (VOC) and semi-volatile organic compound (SVOC) emissions from solid

articles/products, one model for sublimation, and one model for polychlorinated biphenyl (PCB) emissions from aged caulking materials, as shown in TABLE 4.1.

TABLE 4.1 List of mass transfer and empirical models for solid materials discussed in this section.

Model ID	Model Type	Intended Chemicals
M2-A	Simplified mass transfer model for solid materials	SVOCs
M2-B	Simplified mass transfer model for solid materials	SVOCs
M2-C	Simplified mass transfer model for solid materials	VOCs
M2-D	Simplified mass transfer model for solid materials	VOCs
M2-E	Mass transfer model for sublimation	VOCs
M2-F	Empirical model for PCB emissions from aged caulking materials	PCBs

4.3. Model description

4.3.1. Model M2-A (Xu and Little, 2006; Little et al., 2012) [20, 43]

This is a simplified mass transfer model for SVOC emissions from solid materials. The key assumptions are:

- The amount of SVOC emitted from the source is negligible as compared with the SVOC mass in the solid material and, thus, the SVOC concentration in the solid material can be treated as a constant.
- The SVOC concentration in the solid phase at the exposed surface is approximately the same as the average concentration obtained from bulk analysis (Equation 4.1).

$$C_m(\delta, t) \approx C_{mo} \tag{4.1}$$

Let $y_0 = \frac{C_{m0}}{K_{ma}}$ be the gas-phase concentration at the solid-air interface. Then, the original equations for emission factor (see Equations 3.2 and 3.3 in Section 3.2.1) can be simplified to Equation 4.2:

$$E = h_a\left(\frac{C_m(\delta, t)}{K_{ma}} - C_a\right) \approx h_a\left(\frac{C_{m0}}{K_{ma}} - C_a\right) = h_a(y_0 - C_a) \tag{4.2}$$

Equation 4.3 below is the mass balance equation for indoor air. The steady-state air concentration C_a can be obtained from Equation 4.4. Both equations ignore the sink effect.

$$V\frac{dC_a}{dt} = A\,h_a(y_0 - C_a) - Q\,C_a \tag{4.3}$$

$$C_a = \frac{A\,h_a\,y_0}{Q + A\,h_a} \tag{4.4}$$

Parameter y_0 is usually obtained from laboratory testing but can also be estimated from $y_0 = C_{m0}/K_{ma}$.

This simple model is much more flexible and is easier to use than the analytical and numerical solutions models described in Section 3.3. This model can be used in multi-zone, multi-source, and multi-sink models. The simplicity of this model makes it suitable for high-throughput product screening. It has also been used to develop other indoor mass transfer models such as transfer from sources to settled dust by direct contact.

Caution should be exercised when using this model for long-term exposure assessment without experimental data because it can overestimate the air concentrations (Figure 4.1). Unless y_0 is determined experimentally, it may also overestimate SVOC emissions from aged products/articles, in which a concentration gradient forms near the exposed surface (Figure 4.2).

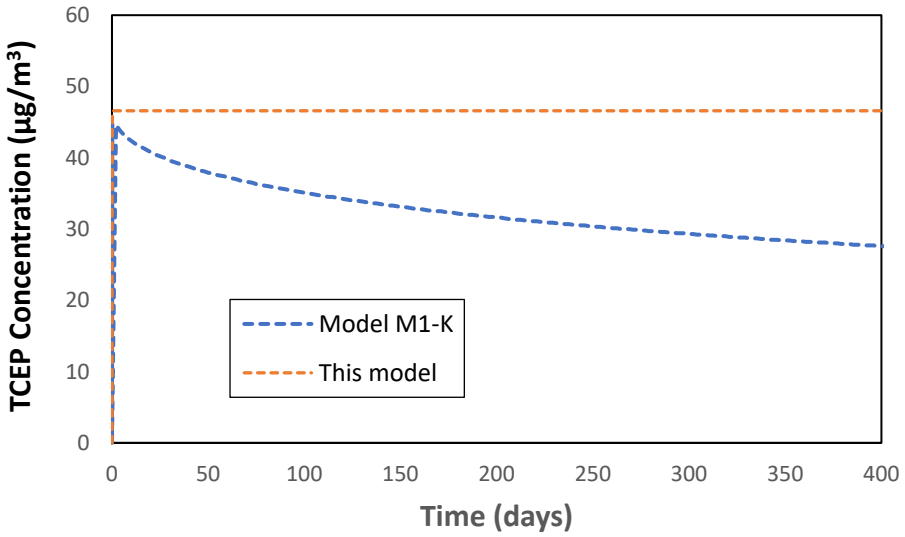

Figure 4.1 Comparison of predicted concentrations for flame retardant tris(2-chloroethyl) phosphate (TCEP) emissions from a polyurethane foam.

Input parameters: V = 30 m^3, Q = 15 m^3/h, A = 10 m^2, δ = 0.004 m, C_0 = 9.04 × 10^8 µg/m^3, K_{ma} = 7.76 × 10^6 (dimensionless), and D_m = 2.01 × 10^{-10} m^2/h. Values for δ, C_0, K_{ma}, and D_m are from Liang et al. (2018). [44]

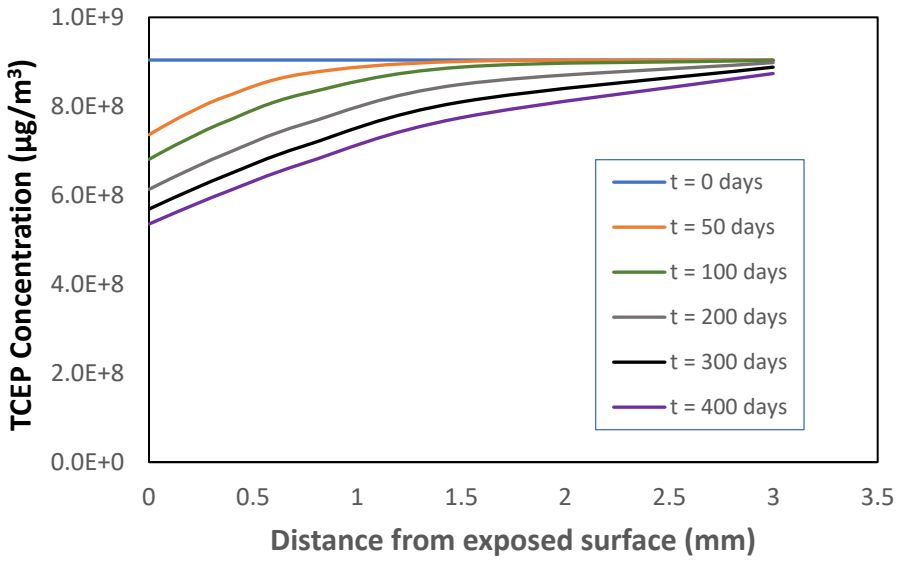

Figure 4.2 Predicted concentration gradient for flame retardant TCEP in a polyurethane foam as a function of time.

The data were generated by the indoor air quality simulation program i-SVOC.[25] Input parameters were the same as in Figure 4.1.

4.3.2. Model M2-B (Huang et al., 2021) [15]

Known as the K-limited model, this is a simplified model for SVOC emissions from solid materials. The model was simplified by assuming that the gas-phase mass transfer resistance ($1/h_a$) is dominant in the overall resistance and that the concentration gradient in the solid phase is negligible.

By accounting for adsorption by the total suspended particles (TSP), the emission rate can be calculated from Equation 4.5. The chemical substance concentrations in the solid material and air are calculated from Equations 4.6 and 4.7, respectively.

$$R = A\, h_a \left(\frac{C_m}{K_{ma}} - \frac{C_a}{1 + K_{pa}\, C_{TSP}} \right) \tag{4.5}$$

$$\frac{dC_m}{dt} = -R/V_m \tag{4.6}$$

$$V \frac{dC_a}{dt} = R - Q\, C_a \tag{4.7}$$

Without considering the particle-phase concentration, the performance of this model is almost identical to that of model M2-A (Figure 4.3).

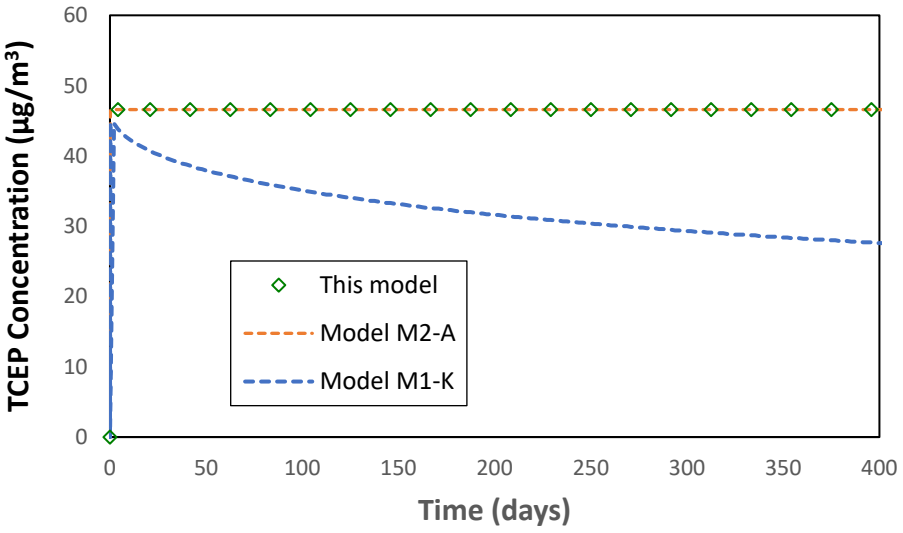

Figure 4.3 Comparison of predicted concentrations for TCEP emissions from a polyurethane foam with three models.

Input parameters were the same as those in Figure 4.1.

4.3.3. Model M2-C (Huang and Jolliet, 2016) [45]

Known as the D-limited model, this model assumes that, for VOCs, the emission rate is mainly limited by diffusion in the solid-phase and that the air concentration is at quasi-steady-state between the emissions and the loss to ventilation. Equation 4.8 calculates the mass fraction emitted at any time *t*. Then, the air concentration can be calculated from Equation 4.9.

$$f_{em} = \frac{M(t)}{M_0} = \alpha_1\left(1 - e^{-\beta_1^2 D_m t}\right) + (1 - \alpha_1)\left(1 - e^{-\beta_2^2 D_m t}\right) \quad (4.8)$$

$$C_a(t) = \frac{df_{em}}{dt}\frac{M_0}{Q} \quad (4.9)$$

The empirical coefficients α_1, β_1, and β_2 in Equation 4.8 are given in a table in the original paper. There are three sets of coefficients and the method to determine which set of values to use is somewhat awkward. The authors provided an example to help readers navigate through the selection process. Comparisons between this model and models M1-A and M1-K are shown in Figure 4.4. All the input parameters are from the original paper except $C_{m0} = 1 \times 10^9$ µm/m^3.

There appears to be a typographical error in the manuscript. The exponent in the denominator of Equation 19 is 433. According to the example the authors provided, the correct value should be 4.33.

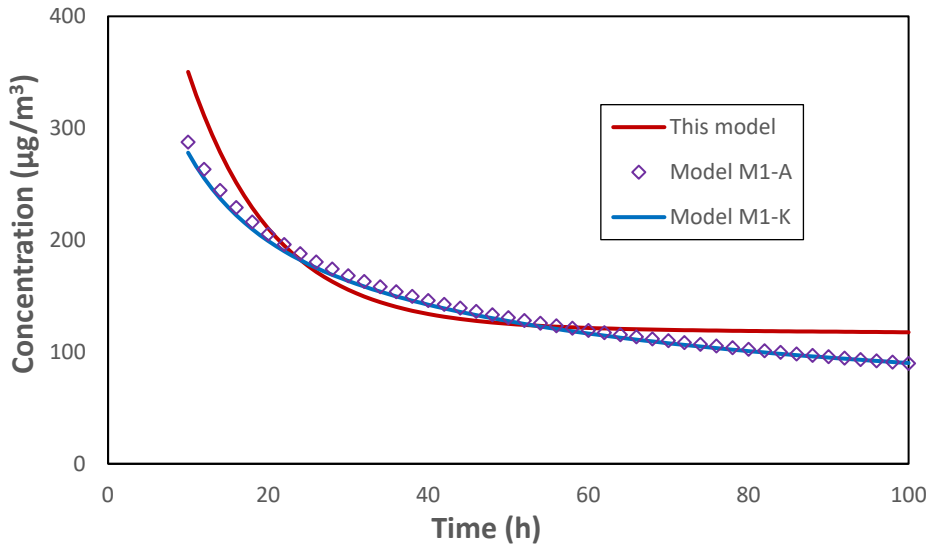

Figure 4.4 Short term (10–100 days) *n*-pentadecane concentrations predicted by three models.

4.3.4. Model M2-D (Christiansson et al., 1993) [46]

This is a simplified diffusion model initially developed for VOC emissions from polyvinyl chloride (PVC) flooring. Like model M2-C described above, this model assumes that the VOC emissions are controlled by solid-phase diffusion. The model consists of two equations. Equation 4.10 is for the first 50% emittable mass and Equation 4.11 is for the remaining 50% emittable mass.

$$E = 2\,\frac{C_{m0}\,D_m}{\delta}\exp\left(-\frac{D_m\,\pi}{4\,\delta^2}\,t\right) \tag{4.10}$$

$$E = C_{m0}\left(\frac{D_m}{\pi\,t}\right)^{0.5} \tag{4.11}$$

In this model, the source is represented by four parameters: A, δ, C_{m0}, and D_m, and the calculation is simple. The steady-state concentration can be determined from $C_a = A\,E/Q$. As a trade-off, this model is less accurate, especially during the first phase (Equation 4.10), as shown in Figure 4.5.

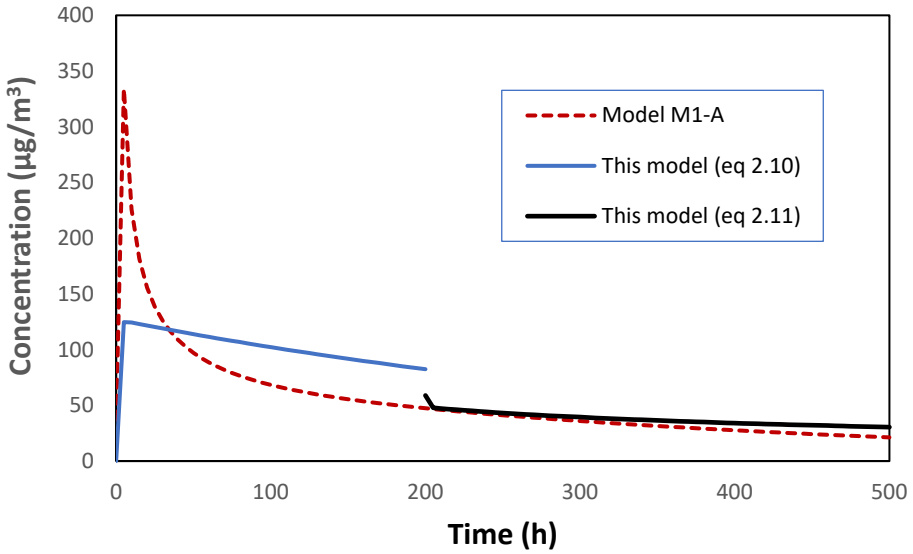

Figure 4.5 Comparison of model M2-D (Equation 4.8) with model M1-A for hexanal emissions from a particle board.

Input parameters were: V = 50 m^3, Q = 50 m^3/h, A = 10 m^2, δ = 0.0159 m, C_{m0} = 1.15 × 10^7 µg/m^3, K_{ma} = 3289, and D_m = 2.75 × 10^{-7} m^2/h. Values for δ, C_{m0}, K_{ma}, and D_m were from Ref. [5]. The second phase emissions started after 55% of hexanal mass was emitted. Earlier emission rate data from Equation 4.11 were unusable.

4.3.5. Model M2-E (Chang and Krebs, 1992) [47]

This model is for VOC sublimation from evaporative solids, such as mothballs, which are made of either *p*-dichlorobenzene or naphthalene. C_v in Equation 4.12 is the saturation concentration in air converted from the vapor pressure of the chemical substance at a given temperature.

$$R = A\, h_a\, (C_v - C_a) \tag{4.12}$$

This model can also be used to measure the gas-phase mass transfer coefficient and characterize environmental chambers.

4.3.6. Model M2-F (Liu et al., 2015) [48]

PCBs are legacy hazardous chemicals consisting of 209 congeners. Although the production of PCBs was banned in the U.S. in 1987, emissions from aged PCB-containing building materials such as caulking, sealants, and paints remain an indoor air quality (IAQ) problem even today. Results from chamber testing show that the emission rates of individual congeners are mainly controlled by their concentration in the material, their volatilities, and temperature. The emission factor can be predicted using an empirical model (Equation 4.13).

$$\ln E_N = 14.02 + 0.976 \ln P_x \quad (R^2 = 0.885) \tag{4.13}$$

where E_N is the normalized emission factor and defined as the emission factor if the congener content in the caulking material is 1000 µg/g. Once the normal emission factor is calculated from Equation 4.13, the emission factor for a given congener can be calculated from Equation 4.14.

$$E = \frac{C_m}{1000} E_N \tag{4.14}$$

Equation 4.13 can also be used to estimate the normalized emission factor for a PCB congener (E_{Nx}) from that of a reference congener (E_{Nref}) with Equation 4.15.

$$E_{Nx} = E_{Nref} \left(\frac{P_x}{P_{ref}} \right)^{0.976} \tag{4.15}$$

4.4. Summary

The simplified mass transfer models—M2-A through M2-D—are easier to use than the models described in Section 3 at the cost of greater predictive errors. Model M2-A is widely used as a high-throughput, screening-level tool but may overestimate long-term exposures for aged articles unless experimentally determined y_0 data are available.

5. Mass transfer from liquid consumer products to air: (I) Models for liquid cleaners, air fresheners, and personal care products

5.1. Symbols and abbreviations

A = area of application of liquid film (m^2),
A_0 = initial area of liquid film (m^2),
A_{tot} = total area of liquid film at the end of application phase (m^2),
A_s = skin area with a liquid personal care product applied to (m^2),
A_t = liquid area at time t (m^2),
C_a = concentration in air (μg/m^3 or mg/m^3 or kg/m^3),
C_L = concentration of substance in product (mg/m^3 or kg/m^3),
C_{L0} = initial concentration of substance in liquid product (mg/m^3 or kg/m^3),
C_m = concentration of chemical substance in the liquid absorbed by the solid material (μg/m^3),
C_{in} = concentration in inlet air (μg/m^3),
C_{out} = concentration in ambient air (μg/m^3),
C_r = concentration of other components in the liquid product (g/kg or kg/m^3),
C_{s0} = initial concentration in skin lipids (μg/m^3),
C_{sw} = saturation concentration of water vapor converted from vapor pressure (kg/m^3),
C_w = concentration of water vapor converted from vapor pressure (kg/m^3),
$C_{w\text{-}in}$ = concentration of water vapor in ambient air (kg/m^3),
d_w = density of water (g/mol),
D_m = solid-phase diffusion coefficient (m^2/s),
D_s = diffusion coefficient in skin lipids (m^2/s),
E = emission factor (kg/m^2/h),
f_{dl} = dilution factor (unitless),
f_w = weight fraction of chemical substance in liquid product (unitless),
f_w' = adjusted weight fraction of chemical substance in liquid product due to dilution (unitless),
h_a = gas-phase mass transfer coefficient (m/s or m/h),
h_L = liquid-phase mass transfer coefficient (m/h),
h_w = gas-phase mass transfer coefficient for water evaporation (m/h),
H_a = overall gas-phase mass transfer coefficient (m/h),
H_L = overall liquid-phase mass transfer coefficient (m/h),
H_s = Henry's law solubility constant (Henry solubility for short)
H_s^{cc} = dimensionless Henry's law solubility constant (dimensionless Henry solubility for short),
H_v = Henry's law volatility constant (Henry volatility for short),
H_v^{cc} = dimensionless Henry's law volatility constant (dimensionless Henry solubility for short),
k = first-order decay rate constant (min^{-1}),
K_{aw} = air-water partition coefficient, $K_{aw} = H_v^{cc}$ (dimensionless),
K_{oa} = octanol-air partition coefficient (dimensionless),
K_{ma} = material-air partition coefficient (dimensionless),
K_{OL} = overall liquid phase mass transfer coefficient (m/h),

K_{sa} = skin-air partition coefficient (dimensionless),
m = molecular weight (g/mol),
m_i = molecular weight of component I in a solvent mixture (g/mol),
m_r = average molecular weight of other components in the liquid product (g/mol),
M_0 = mass of chemical substance applied (mg/m^2),
N = air exchange rate (s^{-1} or h^{-1}),
P = vapor pressure (Pa or inches Hg),
P_{eq} = partial pressure of chemical substance (Pa),
P_{air} = partial pressure of chemical substance in air (Pa),
Q = air exchange flow rate (m^3/h),
r_w = water evaporation rate (kg/s),
R = emission rate (mg/min),
$\bar{R}$ = universal gas constant (m^3 Pa K^{-1} mol^{-1}),
R_i = emission rate of the i^{th} incremental area (mg/min),
R_w = emission rate of water vapor (kg/h),
R_s = emission rate of chemical substance (kg/h),
t = time (h),
t_{app} = time of application (h),
T = temperature (K),
u = air velocity (ft/min),
V = room volume (m^3),
W_0 = liquid mass applied on surface (kg),
W_a = mass of chemical substance in room air (kg),
W_c = mass of chemical substance in concentrated liquid product (kg),
W_{app} = chemical substance mass applied on surface (kg),
W_{dl} = mass of dilution liquid (usually water) (kg),
W_i = mass of component I in a solvent mixture (g),
W_L = liquid mass remaining on surface (kg),
W_{tot} = total mass of liquid product applied on surface (kg),
x = distance from the bottom of the solid material (m),
x_i = mole fraction for component i in a solvent mixture, (unitless),
δ_L = wet film thickness (m),
δ_s = thickness of skin lipids (m).

Abbreviations

IUPAC: International Union of Pure and Applied Chemistry,
SI: International system (of units),
VOC: volatile organic compound,
WPEM: Wall Paint Exposure Model.

5.2. Overview

When selecting a model for chemical substance emissions from liquid products, three factors should be considered:

- Composition of the liquid (e.g., aqueous solution, single-component organic solvent, and multi-component solvent mixture),
- Use scenario (e.g., bulk liquid stored in an open container or as a thin film applied to indoor surfaces), and
- Permeability of the surface. For impermeable surfaces, only wet-stage emissions should be considered. For permeable surfaces, however, both wet and dry-stage emissions should be considered.

This section covers models for liquid surface cleaners, liquid or gel air fresheners, and personal care products. Emissions from indoor coating materials, which are pigmented liquids before application and solids after curing, are discussed in Section 6.

5.2.1. Mass transfer mechanisms for aqueous solutions

Most surface cleaners on the market are water-based. The mechanisms for chemical emissions from water-based products are commonly described by the two-film resistance theory or two-film theory. [49, 50] Mass transfer resistance is the inverse of the mass transfer coefficient. For chemical molecules to migrate from a liquid into room air, they must overcome two mass transfer resistances, one in the liquid phase ($1/h_L$) and the other in the gas phase ($1/h_a$), as shown in Figure 5.1.

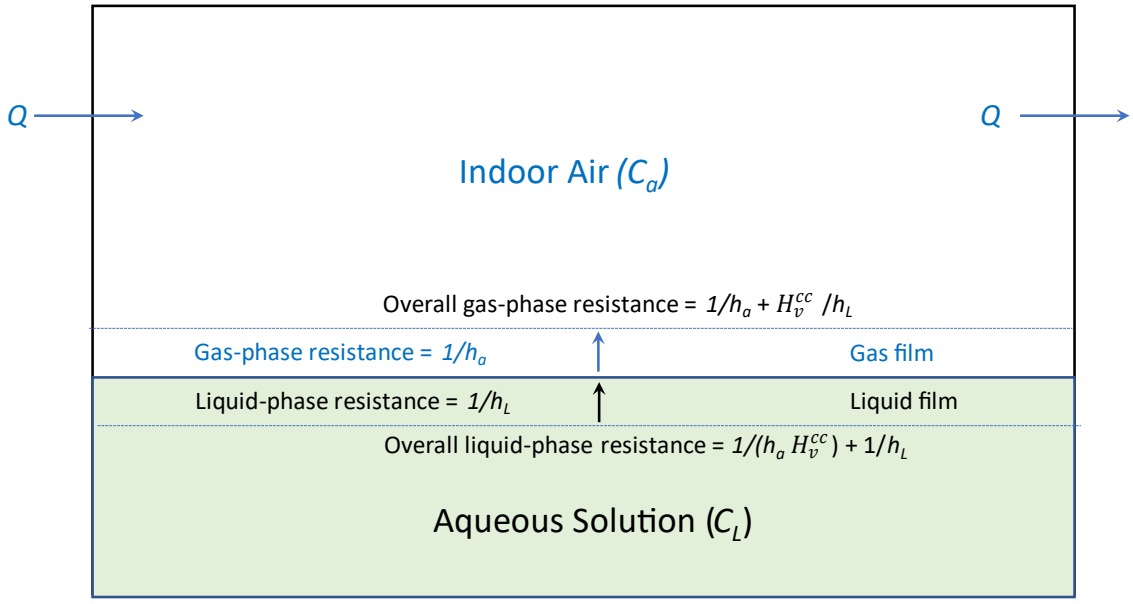

Figure 5.1 Illustration of the two-film resistance theory. *Hv* is Henry's law volatility constant.

The overall mass transfer resistance cannot be calculated by simply adding these two resistance values because they apply to two different phases. Rather, the overall resistance is expressed as either the

overall liquid-phase resistance ($1/H_L$) or overall gas-phase resistance ($1/H_a$), where H_L and H_a represent the overall liquid-phase mass transfer coefficient and the overall gas-phase mass transfer coefficient, as determined by Equations 5.1 and 5.2, respectively.

$$\frac{1}{H_L} = \frac{1}{h_L} + \frac{1}{h_a H_v^{cc}} \tag{5.1}$$

$$\frac{1}{H_a} = \frac{H_v^{cc}}{h_L} + \frac{1}{h_a} \tag{5.2}$$

Thus, calculating the overall mass transfer coefficients (H_L or H_a) requires three parameters: the phase mass transfer coefficients (h_L and h_a) and Henry's law constant (H_v^{cc}).

Then, the emission factor can be calculated from either Equation 5.3 or 5.4.

$$E = H_L \left(C_L - \frac{C_a}{H_v^{cc}}\right) \tag{5.3}$$

$$E = H_a \left(C_L H_v^{cc} - C_a\right) \tag{5.4}$$

Readers should pay close attention to the units used for Henry's law constants. Because of the wide variety of applications for Henry's law historically, Henry's law constants are expressed in many units. To avoid confusion, the International Union of Pure and Applied Chemistry (IUPAC) recommended in 2021 that two umbrella terms be used: Henry's law solubility constant and Henry's law volatility constant.[51] The distinction between the two depends on whether the gas phase is in the denominator or numerator (TABLE 5.1).

TABLE 5.1 IUPAC recommended terms, symbols, and definitions for Henry's law constants.

Recommended Term	Recommended Short Term	Recommended Symbol	Definition [A]
Henry's law solubility constant	Henry solubility	H_s	$H_s = Q_l/Q_g$
Henry's law volatility constant	Henry volatility	H_v	$H_v = Q_g/Q_l$

[A] Q_l and Q_g are the abundances of the solute in the liquid and gas phases, respectively.

Note that there are four variants under each umbrella term, depending on the units used.[51] Details are shown in Table 5.2.

TABLE 5.2 Classification of Henry's law constants: definitions, symbols, and SI units.

Umbrella Term	Numerator	Denominator	Symbol	Units
Henry solubility	amount concentration	pressure	H_s^{cp}	mol m^{-3} Pa^{-1}
	amount fraction	pressure	H_s^{xp}	Pa^{-1}
	molality	pressure	H_s^{bp}	mol kg^{-1} Pa^{-1}
	amount concentration (l)	amount concentration (g)	H_s^{cc}	dimensionless
Henry volatility	pressure	amount concentration	H_v^{pc}	Pa m^3 mol^{-1}
	pressure	amount fraction	H_v^{px}	Pa
	pressure	mass fraction	H_v^{pw}	Pa
	amount concentration (g)	amount concentration (l)	H_v^{cc}	dimensionless

In mass transfer studies, dimensionless Henry's constants are more convenient. The dimensionless Henry solubility (H_s^{cc}) and volatility (H_v^{cc}) are defined by Equations 5.5 and 5.6, respectively, under equilibrium conditions.

$$H_s^{cc} = \lim_{C_l \to 0} \frac{C_L}{C_a} \tag{5.5}$$

$$H_v^{cc} = \lim_{C_l \to 0} \frac{C_a}{C_L} \tag{5.6}$$

In the emission models described below, both H_s^{cc} and H_v^{cc} are used. H_v^{cc} is also known as the air-water partition coefficient (K_{aw}).

Some popular QSAR models predict Henry's law constant in (atm m^3 mol^{-1}), which is Henry volatility H_v^{pc} but not in SI units. To convert the value in (atm m^3 mol^{-1}) to dimensionless Henry volatility (H_v^{cc}), divide the value by the universal gas constant (8.20575×10^{-5} atm-m^3/mol-K) and temperature (K). At 25°C, the conversion factor is 1 (atm m^3 mol^{-1}) = 40.9 H_v^{cc} (dimensionless).

5.2.2. Mass transfer mechanisms for pure organic solvents

Emissions from pure liquids have been thoroughly studied in chemical engineering. The models are rather complex and may not be suitable for indoor environments, which have limited ventilation, and the sources are rather small. Simpler models are used in indoor air quality simulations such as Equation 5.7 [52, 53] or, equivalently, Equation 5.8.

$$E = h_a \left(\frac{m_l}{\bar{R}\, T} P - C_a \right) \tag{5.7}$$

$$E = h_a \left(C_v - C_a \right) \tag{5.8}$$

where C_v is the saturation concentration converted from the vapor pressure of the chemical at a given temperature. In Equation 5.7, the universal gas constant $\bar{R}$ is in (m^3 Pa K^{-1} mol^{-1}) and the vapor pressure *P* is in (Pa).

5.2.3. Mass transfer mechanisms for organic solvent mixture

Volatile chemical emissions from a solvent mixture can be described by Raoult's law (Equation 5.9) and the emission factor is calculated from Equation 5.10.

$$P_i = x_i P_{eq} \tag{5.9}$$

$$E = h_a (C_{vi} - C_a) \tag{5.10}$$

where

$C_{vi} = x_i \frac{m}{R T} P$ is the saturation concentration for component *i* in the mixture converted from partial pressure and x_i is the mole fraction of component *i* in the mixture with *n* components, obtained from Equation 5.11.

$$x_i = \frac{\frac{w_i}{m_i}}{\sum_{j=1}^{n} \frac{w_j}{m_j}} \tag{5.11}$$

where *w/m* is the mole number in the liquid mixture.

5.2.4. List of models discussed

Nine models for chemical substance emissions from surface cleaners, personal care products, and air fresheners are discussed below. They cover all three liquid types and several use scenarios (TABLE 5.3).

TABLE 5.3 List of models for chemical substance emissions from liquid products discussed in this section.

Model ID	Liquid Type	Product Use Scenario	Emission Stages Considered	
			Wet stage	Dry stage
M3-A	Pure solvent	Cleaner for pools or open containers	√	N/A
M3-B	Pure solvent	Cleaner applied on porous surfaces or personal care product on skin	√	√
M3-C	Non-specific [A]	Cleaner applied on hard surfaces	√	×
M3-D	Solvent mixture	Cleaner applied on hard surfaces	√	×
M3-E	Solvent mixture	Liquid/gel air fresheners	√	×
M3-F	Water-based	Cleaner pool or open container	√	×
M3-G	Water-based	Cleaner applied on hard surfaces	√	×
M3-H	Water-based	Simplified version of model M3-G	√	×
M3-I	Non-specific	Personal care product applied on skin	√	√

[A] This is an empirical model applicable to both water and solvent-based surface cleaners.

5.3. Model description

5.3.1. Model M3-A (Braun and Caplan, 1989) [54]

This model was based on experimental data collected from a wind tunnel. The general form of the equation is given by Equation 5.12. For a certain air velocity range, Equation 5.12 can be simplified to Equation 5.13.

$$E = a\, m^b\, P^c\, u^d \tag{5.12}$$

$$E = a\, m^b\, P^c \tag{5.13}$$

where

E is the emission factor in (lb/h/ft^2). The conversion factor is: 1 (lb/h/ft^2) = 4.882 (kg/h/m^2).

P is vapor pressure at a given temperature in (inches Hg), and

u is the air velocity in (ft/min).

The empirical constants—*a*, *b*, *c*, and *d*—in these two equations were experimentally determined. Their values are presented in two tables in the original report. The values measured at the low velocity range (0.5 m/s) are most suitable for indoor environments. In this velocity range, the values of the coefficients in Equation 5.13 for all liquid chemicals tested excluding water and low vapor pressure alcohols are: $a = 0.0069$, $b = 1.08$, and $c = 0.98$ with $R^2 = 0.934$.

Values for six solvent classes—alcohols, ketones, aliphatics, aromatics, water, and low vapor pressure alcohols—are also reported.

Once the emission factor is known, the steady-state air concentration can be calculated from Equation 5.14 and the time-varying concentration from Equation 5.15. The difference between the two equations is that Equation 5.14 considers the "fill-up" stage early on.

$$C_a = \frac{A\,E}{Q} \tag{5.14}$$

$$C_a = \frac{A\,E}{Q}\,(1 - e^{-N\,t}) \tag{5.15}$$

This model tends to overestimate the air concentration at low ventilation rates because it does not consider the "back pressure" effect, which means that the evaporation rate decreases when the partial pressure of the vapor in air increases. This effect becomes significant when the ventilation rate is low. Equations 5.14 and 5.15 do not work in a static chamber (i.e., $Q = 0$).

It is important to emphasize that several models have been used to predict the emission rates for pure solvents. Braun and Caplan (1989) [54] compared model M3-A with six other models and found that the

models differed significantly. More evaluation is needed to select models that are most suitable for indoor environments, where air movements are not unidirectional and air speeds are low.

5.3.2. Model M2-B (Wei et al., 2022) [55]

This differential equation model accounts for both wet and dry-stage emissions from cleaning liquids applied to permeable surfaces or personal care products applied to skin. The penetration of the liquid through permeable surfaces is described by Fick's second law (Equation 5.16). The wet and dry-stage emissions are described by Equations 5.17 and 5.18, respectively. Note that symbol *V* is missing in Equation 5.17 in the original paper.

$$\frac{\partial C_m(x,t)}{\partial t} = D_m \frac{\partial^2 C_m(x,t)}{\partial x^2} \tag{5.16}$$

$$V\frac{dC_a}{dt} = Q(C_{out} - C_a) + h_a\, A\left(\frac{C_L}{K_{oa}} - C_a\right) \tag{5.17}$$

$$V\frac{dC_a}{dt} = Q(C_{out} - C_a) + h_a\, A\left(\frac{C_m}{K_{ma}} - C_a\right) \tag{5.18}$$

While this is the only model in TABLE 5.3 that addresses both wet and dry stage emissions, the model description in the original paper is incomplete and needs clarification.

First, it is unclear how to determine the time when the wet-stage emission stops, and the dry-stage emission starts. It appears that an additional equation is needed to track the amount of liquid remaining on the surface.

Second, mass transfer from the liquid film to the porous material usually requires a liquid-phase mass transfer coefficient, which cannot be found in either the model equations or the list of input parameters.

The authors did not mention the types of liquids the model applies to. Judging from Equation 5.17, in which the octanol-air partition coefficient is used as the liquid-air partition coefficient, one can safely assume that this model is for single-component solvents only. However, the surface cleaner used to generate the chamber data was a water-based all-purpose cleaner containing 4% acetic acid.[56]

5.3.3. Model M3-C (Arnold et al., 2020) [56]

This empirical model is for cleaning large surface areas such as floors. It is a combination of the first-order decay model (Equation 5.19) and area discretization (Figure 5.2).

$$E = M_0\, k\, e^{-kt} \tag{5.19}$$

Area 1 $t_{start} = 0$ $t_{end} = \Delta t$	**Area 2** $t_{start} = \Delta t$ $t_{end} = 2\Delta t$	**Area 3** $t_{start} = 2\Delta t$ $t_{end} = 3\Delta t$	…	…
…	…	…	…	…
…	…	**Area i** $t_{start} = (i-1)\Delta t$ $t_{end} = i\Delta t$	…	…
…	…	…	…	…
…	…	…	…	**Area n** $t_{start} = (n-1)\Delta t$ $t_{end} = n\Delta t$

Figure 5.2 Illustration of area discretization. The floor is equally divided into *n* incremental areas. Each area is treated as a point source.

If the total area to be cleaned is A and is divided into n incremental areas, the area of each incremental area is $\Delta A = A/n$. If the time needed to clean the entire area is t_{app}, the time needed to clean each incremental area *is* $\Delta t = t_{app}/n$. Furthermore, if each incremental area is treated as a point source, the emission start time for the i^{th} area is $t_i = (t_{start} + t_{end})/2 = (i-0.5)\Delta t$. Then, the emission rate for the i^{th} area, R_i, is calculated from Equation 5.20.

$$R_i = 0 \ \ (\text{for t} < t_i)$$
$$R_i = \ \Delta A \ M_0 \ k \ e^{-k(t-t_i)} \ \ (\text{for t} \ \geq \ t_i \ ) \tag{5.20}$$

The total emission rate is the sum of all incremental areas (Equation 5.21)

$$R = \sum_{i=1}^{n} R_i \tag{5.21}$$

Figure 5.3 shows examples of the predicted emission rate profiles.

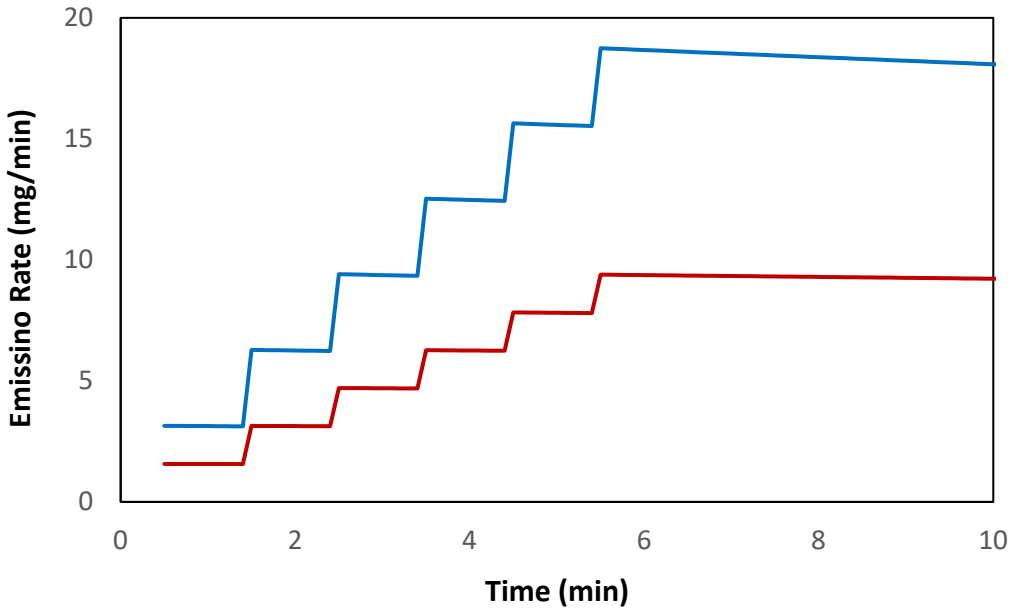

Figure 5.3 Time-varying emission rate generated by model M3-C.
Input parameters were from Ref. [56] with k = 0.004 and 0.008 min^{-1}.

Given that this is an empirical model, it is applicable to all liquid types. A major obstacle in using this model is the difficulty in estimating the first-order decay rate constant k in Equation 5.20. The experimental data show that k varies greatly depending on the liquid type and physical-chemical properties of the chemical substance (e.g., volatility and solubility).

This is one of the approaches to application-phase simulation. More discussion on this matter is provided in Section 5.4.3.

5.3.4. Model M3-D (Delmaar et al., 2017)) [52]

The online simulation tool *ConsExpo Web* contains a model for chemical emissions from liquids applied to hard surfaces. Although the document did not mention the types of liquids this model applies to, the equations suggest it is for either pure solvents or solvent mixtures.

$$\frac{dW_a}{dt} = h_a A \frac{m}{R\,T}\left(P_{eq} - P_{air}\right) - N\,V\,C_a \tag{5.22}$$

$$\frac{dW_L}{dt} = -h_a A \frac{m}{\bar{R}T}\left(P_{eq} - P_{air}\right) + \frac{W_0}{t_{app}} f_w \tag{5.23}$$

where the partial pressure of the target chemical, P_{eq}, is obtained from Equation 5.24.

$$P_{eq} = \frac{C_L}{C_L + C_r \frac{m}{m_r}} P \tag{5.24}$$

These equations cannot be used "as is" because of the following issues:

- P_{air} in Equations 5.22 and 5.23 is a variable. Although it is related to C_a, the units are different,
- The last term in Equation 5.23 is effective only during the application phase (i.e., $t < t_{app}$),
- The source area A is a variable during product application,

Equations 5.25 and 5.26 below fix these problems and are easier to read and understand.

$$\frac{dW_a}{dt} = h_a A \left(C_{eq} - C_a\right) - Q\, C_a \tag{5.25}$$

$$\frac{dW_L}{dt} = -h_a A \left(C_{eq} - C_a\right) + W_{app} \tag{5.26}$$

where

$A = \frac{t}{t_{app}} A_0$ if $t < t_{app}$; otherwise, $A = A_{tot}$

$C_{eq} = \frac{m}{R\,T} P_{eq}$

$W_{app} = \frac{W_{tot}}{t_{app}} f_w$ if $t < t_{app}$; otherwise, $W_{app} = 0$.

Pay attention to the units. C_{eq} will be in (g/m^3) if the molecular weight is in (g/mol).

5.3.5. Model M3-E (Yoo et al., 2022) [53]

This model is for chemical emissions from liquid or gel-type air fresheners. The equations are similar to those in model M3-D with modifications. Like model M3-D, this model is based on Raoult's law and consists of three differential equations: one for the concentration of the target chemical in air (Equation 5.27), one for the concentration in the liquid phase, and the third for other components in the liquid phase.

$$\frac{dC_a}{dt} = h_a A \frac{m}{V\ \bar{R}\,T}\left(x\, P_{eq} - \frac{R\,T}{m} C_a\right) - N\, C_a \tag{5.27}$$

where x is the molar fraction of the target chemical in the liquid and is given by Equation 5.28,

$$x = \frac{C_L}{C_L + C_r \frac{m}{m_r}} \tag{5.28}$$

5.3.6. Model M3-F (Guo and Roache, 2003) [57]

This model is for chemical emissions (acids, alkalis, or VOCs) from an aqueous solution pool, or a water-based product stored in an open container. If the chemical concentration in the liquid, C_L, remains constant, Equation 5.29 alone is sufficient to calculate the chemical concentration in the air.

$$V \frac{dC_a}{dt} = A\, H_L \left(C_L - \frac{C_a}{H_v^{cc}} \right) - Q C_a \tag{5.29}$$

If the chemical evaporates rapidly and the source is limited (e.g., liquid pool or a shallow container), the concentration in the liquid phase will decline over time. On the other hand, water evaporation will reduce the volume of the liquid and, thus, concentrate the chemical. These factors are handled by Equations 5.30 through 5.32.

For liquid phase mass balance,

$$\frac{dW_L}{dt} = -A\, H_L \left(C_L - \frac{C_a}{H_v^{cc}} \right) \tag{5.30}$$

where C_L is treated as a variable (Equation 5.31),

$$C_L = \frac{W_L}{V_L - \frac{r_w\, t}{d_w}} \tag{5.31}$$

where the water evaporation rate r_w is determined by Equation 5.32,

$$r_w = A\, h_w\, (C_{sw} - C_w) \tag{5.32}$$

5.3.7. Model M3-G (Guo et al., 2008) [58]

Initially developed for small-scale spills of aqueous solutions, this model can be used to predict the emissions of volatile chemicals from water-based surface cleaners applied onto impermeable surfaces. A key assumption made is that the area of the wet film decreases over time while the thickness remains unchanged. The model consists of four ordinary differential equations: Equation 5.33 is for the liquid mass remaining on the surface, Equation 5.34 is for the water vapor concentration in indoor air, Equation 5.35 is for the solute concentration in the liquid, and Equation 5.36 is for the solute concentration in indoor air.

$$\frac{dW}{dt} = -R_w - R_s \tag{5.33}$$

$$\frac{dC_w}{dt} = -R_w + Q\left(C_{w\_in} - C_w\right) \tag{5.34}$$

$$V_L \frac{dC_L}{dt} = -R_s \tag{5.35}$$

$$V \frac{dC_a}{dt} = R_s - Q\ C_a \tag{5.36}$$

where R_w is the rate of water evaporation from the liquid film, from Equation 5.37.

R_s is the emission rate of the solute, from Equation 5.38.

$$R_w = A_t\ h_w\ (C_{sw} - C_w) \tag{5.37}$$

$$R_s = A_t\ K_{OL}\ \left(C_L - \frac{C_a}{H_v^{cc}}\right) \tag{5.38}$$

Note that the area of the wet film is a variable and can be calculated from Equation 5.39.

$$A_t = A_0 \frac{W_L}{W_0} \tag{5.39}$$

5.3.8. Model M3-H (Guo et al., 2008) [58]

This is a simplified version of model M3-G for emissions from water-based cleaners applied to impermeable surfaces. If $C_L \gg \frac{C_a}{H_v^{cc}}$ in Equation 5.38, the emission factor can be represented by the first-order decay model (Equation 5.40). The mass balance for indoor air is given by (Equation 5.41).

$$R_s = \frac{A_0\ K_{OL}\ C_{L0}}{V\ (q - N)} e^{-q\ t} \tag{5.40}$$

$$V \frac{dC_a}{dt} = R_s - QC_a \tag{5.41}$$

Given $C_a = 0$ when $t = 0$, the exact solution for the air concentration is given by Equation 5.42.

$$C_a = \frac{A_0\, K_{OL}\, C_{L0}}{V\,(q - N)}\,(e^{-N\,t} - e^{-q\,t}) \tag{5.42}$$

where q is calculated from Equation 5.44,

$$q = \frac{A_0\, h_w\,(1 - r_h)}{W_0} + \frac{K_{OL}}{\delta_L} \tag{5.43}$$

The valid range for the assumption of $C_L \gg \frac{C_a}{H_v^{cc}}$ was discussed by Guo et al. (2008). Under "typical" use conditions, if the dimensionless Henry's volatility is greater than 0.001, $\frac{C_a}{H_v^{cc}}$ will be smaller than 11% of C_L.[58]

5.3.9. Model M3-I (Yang et al., 2018) [59]

This model is for VOC emissions from personal care products applied to human skin. It is a mass transfer model based on Fick's second law and is similar to the diffusion models described in Section 3. The authors presented three models: one is the full analytical solution, one is a simplified version of the full analytical solution, and the last one allows for multiple emitters in the room. The first two models allow more than one person in the room to be emitters so long as all persons have the same initial concentration in the skin (C_{s0}). The third model allows different people to have different initial concentrations in the skin. All three models require solving a non-linear equation. The third model also requires numeric integration to calculate the concentration in room air. The model described below is the simplified version. Equation 5.44 is the concentration in room air and Equation 5.45 is the non-linear equation.

$$C_a = C_{in} + \sum_{n=1}^{\infty} \frac{2\,\beta\, C_{s0}}{(\alpha - q_n^2)\left(1 + \frac{K_{sa}}{Bi_m} + q_n^2\, K_{sa}^2/Bi_m^2\right)}\, exp\,(-D_s\, \delta_s^2\, q_n^2\, t) \tag{5.44}$$

$$q_n\, tan\, q_n = \frac{\mathrm{Bi_m}}{\mathrm{K_{sa}}} \tag{5.45}$$

where

$$\alpha = \frac{Q\, \delta_s^2}{D_s\, V}$$

$$\beta = \frac{A_s\, \delta_s}{V}$$

$$Bi_m = \frac{h_a \, \delta_s}{D_s}$$

This model was initially developed for modeling emissions of cyclic volatile methyl siloxanes in personal care products applied on skin. The authors assume that, after the product is applied on skin, the siloxanes permeate into the skin lipids with a thickness of 1 µm, and that the emissions are from skin lipids.

5.4. Additional comments

5.4.1. Dilution of concentrated products

Some cleaner products, especially water-based products, are sold as "concentrates." They should be used according to the recommended dilution factor (f_{dl}), which is calculated from Equation 5.46. Consequently, the weight fraction of the target chemical (f_w) should be adjusted with Equation 5.47.

$$f_{dl} = \frac{W_{dl} + W_c}{W_c} \tag{5.46}$$

$$f_w' = \frac{f_w}{f_{dl}} \tag{5.47}$$

5.4.2. Effect of surfactant on chemical emissions from liquid products

Most water-based cleaners contain surfactants, which function to lower the surface tension of the liquid and increase the solubility of the solutes, especially non-polar organic compounds. According to the definition of Henry's law constants (see Section 5.2.1), increased solubility means a larger Henry's law solubility constant and a smaller Henry's law volatility constant. In other words, in the presence of a surfactant, the actual Henry's law constants for liquid cleaners are likely smaller than those reported in the literature for a neat chemical. This effect has not been quantitatively studied. Without this knowledge, models tend to overestimate the peak emissions.

This problem can be resolved with two approaches. The first approach is using experimentally determined Henry's law constants for cleaner mixtures instead of the literature values and the second is developing quantitative relationships for the effects of surfactants in mixtures on Henry's law constant.

5.4.3. Application-phase simulation

When a liquid product is applied to large surfaces, such as interior walls and flooring, the source area increases over time before the application ends. During this period, known as the application phase, the emission rate calculation must treat the area as a variable. There are three approaches to this problem, as described below.

<u>Analytical solutions</u>

Evans (1996) developed analytical solutions for emissions during application phase for two types of sources: constant and first-order decay.[60] The methods were implemented in EPA's Wall Paint

Exposure Model (WPEM)[61] This is the most accurate method for application-phase simulation. The drawbacks are (1) The solutions are available only for constant and first-order decay sources, and (2) The air exchange rate must remain constant throughout the application phase.

Numerical solutions

Zeh et al. (1994) developed a numerical solution for VOC emissions during application phase.[62] It is implemented in EPA's IAQX program.[41] The User's Guide includes mathematical proof of the Zeh et al. method. This method is more flexible than the analytical solution method for first-order decay sources.

Area discretization

This is the method used in model M3-C.

5.5. Summary

The transfer mechanisms for chemical substance emissions from water-based products are different from those for organic solvent-based products. When selecting a model, users should check the model's applicability carefully.

When a cleaning product is applied to porous surfaces, a portion of the liquid is absorbed by the surface material. After the liquid dries, the treated surface material acts like a diffusion source, causing long-term, low-level emissions, known as dry-stage emissions. Attempts to model dry-stage emissions from surface cleaners have been largely unsuccessful. A major difficulty is determining the fraction of the liquid that is absorbed by the surface material, which is highly dependent on the properties of the solid material, such as porosity and lipophilicity.

The effects of surfactant in liquid products on the emission rate are well understood qualitatively but not quantitatively. Existing models tend to overestimate the peak emission rate without taking this factor into consideration. This factor may not affect the total emissions, however.

Suggestions on model selection for liquid and semi-liquid products are provided in Table 5.4.

TABLE 5.4 Suggestions on selecting models for emissions from liquid cleaners and air fresheners.

Liquid Product	Chemical Class	Conditions	Models
Pure solvents	VOCs	In container	M3-A, M3-D
Solvent mixture	Volatile components	Applied to hard surfaces	M3-D
Water-based cleaners	Volatile components	Applied to hard surfaces	M3-C, M3-G, M3-H
Gel-type air fresheners	VOCs	Product assembly	M3-E [A]
Personal care products	VOCs	Applied to human skin	M3-I

[A] This model needs minor adjustment. See Section 5.3.5.

6. Mass transfer from liquid consumer products to air: (II) Models for emissions from interior coating materials and sealants

6.1. Symbols and abbreviations

A = area of the source (m^2),
A_p = area of painted surface (m^2),
Bi_m = Biot number for mass transfer, $Bi_m = h_m \delta/D_m$ (dimensionless)
C_a = concentration in air (µg/m^3 or mg/m^3),
C_L = concentration in liquid phase (mg/m^3),
C_{p0} = initial concentration in paint (mg/m^3),
C_s = concentration in solid phase (mg/m^3),
C_v = gas-phase VOC concentration at air-paint interface (mg/m^3),
C_{v0} = vapor pressure of chemical of interest in concentration unit (mg/m^3),
d = density of paint product (g/m^3),
D_L = diffusion coefficient in liquid phase (m^2/s),
D_p = diffusion coefficient in wet paint (m^2/h),
D_s = diffusion coefficient in solid phase (m^2/s),
E = emission factor (mg m^{-2} h^{-1}),
E_0 = initial emission factor (mg m^{-2} h^{-1}),
E_c = area-specific emission rate (mg/m^{-2}/s),
E_1 = emission factor for wet-stage emissions (mg m^{-2} h^{-1}),
E_2 = emission factor for dry-stage emissions (mg m^{-2} h^{-1}),
f_D = diffusion constant ($h^{1/2}$),
Fo_m = Fourier number for mass transfer, $Fo_m = D_m t/\delta^2$ (dimensionless),
h_a = gas-phase mass transfer coefficient (m/h or m/s),
h_{ai} = gas-phase mass transfer coefficient for paint component i (m/h or m/s),
k = first-order decay rate constant (h^{-1}),
k_1 = first-order decay rate constant for wet-stage emissions (h^{-1}),
k_2 = first-order decay rate constant for dry-stage emissions (h^{-1}),
K_{ma} = material-air partition coefficient (dimensionless),
L = loading factor and $L = A_p/V$ (m^{-1}),
m = molecular weight (g/mol),
m = molecular weight of component i (g/mol),$\bar{m}$ = average molecular weight for TVOC in paint (g/mol),
M_0 = mass of chemical substance applied to unit area of the source (mg/m^2),
M_{01} = initial mass of chemical substance applied available for wet stage emissions (mg/m^2),
M_{02} = initial mass of chemical substance applied available for dry stage emissions (mg/m^2),
M_i = mass of chemical substance i remaining in unit area of the source (mg/m^2),
M_1 = mass of chemical substance available for wet-stage emissions (mg/m^2),
M_2 = mass of chemical substance available for dry-stage emissions (mg/m^2),
M_T = mass of TVOC remaining in unit area of the source (mg/m^2),
M_{T0} = mass of TVOC applied to unit area of the source (mg/m^2),

N = ventilation rate (s^{-1} or h^{-1}),
N_n = normalized ventilation rate (dimensionless),
p_w = partial pressure of water vapor (Pa),
P = vapor pressure (torr),
P_0 = total vapor pressure for TVOC in paint (torr),
P_i = partial pressure for component i in the paint (torr),
P_s = permeation coefficient of cured sealant (mol/m/s/Pa),
Q = ventilation flow rate (m^3/h),
R = emission rate (mg/h),
R_N = normalized emission rate (mg/h),
t = time (h),
v_m = volume of 1 mole gas at 1 atm and 23°C (m^3),
V = room or chamber volume (m^3),
V_L = volume of liquid (m^3),
y_0 = total TVOC content in paint (mg/g),
y_i = content of VOC_i in paint (mg/g),
z = depth of cured sealant (m),
δ = thickness of the material (m),
δ_p = wet film thickness of paint (m).

Abbreviations

MEKO: methylethyl ketone oxime,
TMPD-MIB: 2,2,4-trimethyl-1,3-pentanediol monoisobutyrate,
TVOC: total volatile organic compound,
U.S. EPA: United States Environmental Protection Agency,
VOC: volatile organic compound,
WPEM: Wall Paint Exposure Model.

6.2. Overview

Many types of paints and coatings used in indoor environments that are applied as liquids but subsequently harden or cure can be divided into two broad groups, organic solvent-based and water-based. Different models are needed to predict the volatile organic compound (VOC) emissions from these two paint types. Another issue to be considered is the absorption of chemical substances—mainly organic solvents—by permeable substrates, which causes continued emissions long after the paint is cured. Predicting dry-stage emissions has proven difficult because the amount of solvent absorbed is highly dependent on the properties of the substrate, such as porosity and lipophilicity. Seven models are discussed below (TABLE 6.1).

TABLE 6.1 List of paint models discussed.

Model ID	Material Type	Intended Chemicals	Emission Stages	
			Wet stage	Dry stage
M4-A	Petroleum solvent-based coatings	TVOC, VOCs	√	×
M4-B	Petroleum solvent-based coatings	TVOC, VOCs	√	×
M4-C	Non-specific	TVOC	√	√
M4-D	Water-based coatings	VOCs	√	×
M4-E	Water-based coatings	VOCs	√	√
M4-F	Water-based coatings	VOCs	√	√
M4-G	Solvent or water-based coatings	TVOC, VOCs	√	√
M4-H	Sealants	VOCs	√	√

6.3. Model description

6.3.1. Model M4-A (Guo et al., 1999) [63]

This model is for total volatile organic compound (TVOC) and VOC emissions from petroleum solvent-based indoor coating materials. All parameters can be calculated from the product formulation. The first-order decay model is used to describe the emission factor as a function of time (Equation 6.1). [64]

$$E = E_0\, e^{-kt} = M_0 k e^{-kt} \tag{6.1}$$

For a single zone, the air concentration is given by Equation 6.2:

$$C_a = \frac{A\, E_0}{V\,(N-k)}\left(e^{-kt} - e^{-Nt}\right) \tag{6.2}$$

The two key parameters in Equation 6.1, E_0 and k, are calculated from Equations 6.3 and 6.4 for TVOC and Equations 6.5 and 6.6 for an individual VOC (component i).

$$E_0 = 1.32\, h_a P_0\, \frac{\bar{m}}{v_m} \tag{6.3}$$

$$k = \frac{E_0}{\delta\, d\, y_0} \tag{6.4}$$

$$E_0 = 1.32\, h_{ai} P_i\, \frac{m_i}{v_m}\, \frac{y_i}{y_0} \tag{6.5}$$

$$k = \frac{E_{0i}}{\delta\, d\, y_i} \tag{6.6}$$

The total pressure P_0 for TVOC and partial pressure P_i are estimated from Equations 6.7 and 6.8, respectively.

$$P_0 = \frac{\sum_{i=1}^{n} P_i \frac{y_i}{m_i}}{\sum_{i=1}^{n} \frac{y_i}{m_i}} \tag{6.7}$$

$$P_i = \frac{P_i \frac{y_i}{m_i}}{\sum_{i=1}^{n} \frac{y_i}{m_i}} \tag{6.8}$$

where P_i is the vapor pressure of component *i* (mmHg), y_i is the content of component *i* in the product (mg/g), and m_i is the molecular weight of component *i* (g/mol). An example of how to calculate these two parameters is given in the original paper.

6.3.2. Model M4-B (Guo et al., 1999) [63]

This model was developed based on the VB [65] and VBX [66] models for VOC emissions from petroleum-based coatings. A major difference between this model and model M4-A is that this model takes into consideration the effect of organic vapor in room air on the emissions. As a trade-off, the calculation is more complex and requires solving two ordinary differential equations.

For TVOC,

$$E = h_a \left(1.32\, P_0 \frac{\bar{m}}{v_m} \frac{M_T}{M_{T0}} - C_a\right) \tag{6.9}$$

$$\frac{dC_a}{dt} = \frac{A\,E}{V} - N\,C_a \tag{6.10}$$

$$\frac{dM_T}{dt} = -E \tag{6.11}$$

The initial conditions are $C_a = 0$, and $M_T = M_{T0}$ when t = 0, where M_{T0} is the total amount of TVOC applied (g/m^2).

For individual VOCs,

$$E_i = h_{ai} \left(1.32\, P_i \frac{\bar{m}}{v_m} \frac{M_i}{M_T} - C_a\right) \tag{6.12}$$

$$\frac{dC_a}{dt} = \frac{A\,E_i}{V} - N\,C_a \tag{6.13}$$

$$\frac{dM_i}{dt} = -E_i \tag{6.14}$$

The initial conditions are $C_a = 0$, and $M_i = M_{i0}$ when t = 0, where M_{i0} is the amount of component *i* applied (g/m^2).

The method for estimating the total vapor pressure for TVOC, P_0, is given by Equation 6.7.

6.3.3. Model M4-C (Zhang et al, 2020) [67]

This model is for TVOC emissions from interior coating materials. The developers did not mention specifically the types of paint this model applies to. In the experimental section, the authors indicated that they tested two paints, interior wall paint and wood paint.

This model was developed based on Fick's second law and assumed that the chemical substance concentration at the paint surface decreases over time through exponential decay. The concentration in room air is given by Equation 6.15.

$$C_a = a_1 e^{-b_1 t} - (a_1 + c_1)\, e^{-b_2 t} + c_1 \tag{6.15}$$

where

$$a_1 = \frac{L\, h_a\, C_\infty}{K_{ma}\,(L\, h_a + N)}$$

b_1 = B, where B is an empirical parameter for the decay rate of the chemical substance in the paint. The reported B values were 0.0025 for the interior wall paint and 0.0052 for the wood paint.

$b_2 = L\, h_a + N$. Note that the expression in the original paper, $b_2 = -(L\, h_a + N)$, does not work.

$$c_1 = \frac{A\, L\, h_a}{K_{ma}\,(L\, h_a + N - B)}$$

This is essentially a first-order decay model for the source with a rather small decay rate constant B, which is determined experimentally. The model yields a smooth curve over a long period of time (Figure 6.1).

Clarifications are needed for the definitions of C_∞ and K_{ma}. The former appears to be the initial concentration of the chemical substance in the paint. It is unclear whether K_{ma} is the liquid-air or solid-air partition coefficient.

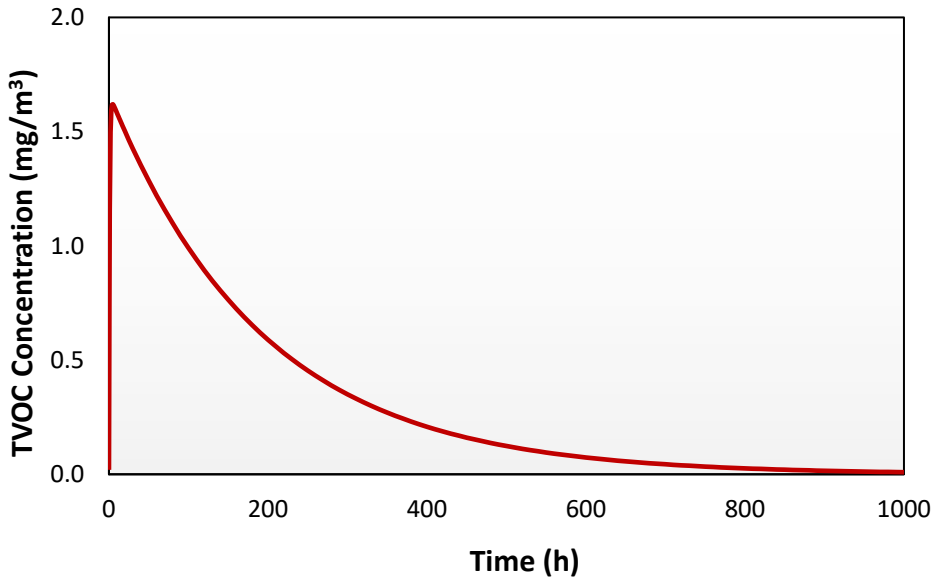

Figure 6.1 TVOC concentration predicted by model M4-D.

Input parameters were A = 1.0 m^2, L = 0.2 m^2/m^3, h_a = 1 m/h, N = 1 h^{-1}, C_∞ = 1 × 10^6 mg/m^3, K_{ma} = 1 × 10^5 (dimensionless). The decay rate constant B = 0.0052 is for interior wall paint from the original paper.

6.3.4. Model M4-D (Chang et al, 2011) [68]

Developed by using the dimensionless number relationship approach, this model is for VOC emissions from water-based paint. The normalized emission (R_N) is defined by Equation 6.16 and calculated from Equation 6.17.

$$R_N = \frac{R}{D_p\ \delta\ C_{p0}} \tag{6.16}$$

$$R_N = 6.581 \times 10^4\ \times\ N_n^{0.12}\ \times\ Bi_m^{0.32}\ \times e^{-Fo_m} \tag{6.17}$$

where the three dimensionless numbers are defined as follows:

$N_n = \frac{N\ \delta^2}{D_p}$ is the normalized air exchange rate,

$Fo_m = D_p\ t/\delta^2$ is the Fourier number for mass transfer, and

$Bi_m = h_m\ \delta/D_p$ is the Biot number for mass transfer.

Clarifications are needed on how to convert the emission rate to the emission factor. The area of the source is not included in any of the dimensionless numbers either explicitly or inexplicitly. Equation 6.17 may have been the result for a fixed area of A_p = 0.15 m^2, which is the area that the authors used to generate the emission data in their wind tunnel. If so, the emission rate obtained from the model should be converted to emission factor E by using Equation 6.18.

$$E = \frac{R}{A_p} = \frac{R}{0.15} \tag{6.18}$$

6.3.5. Model M4-E (Wilkes et al., 1996) [69]

Developed by Wilkes et al. and implemented in The United States Environmental Protection Agency (U.S. EPA)'s Wall Paint Exposure Model (WPEM) [61], this model predicts both wet and dry-stage VOC emissions from latex paint with the double exponential model (Equations 6.19 and 6.20 are equivalent).

$$E = E_1 e^{-k_1 t} + E_2 e^{-k_2 t} \tag{6.19}$$

$$E = M_{01} k_1 e^{-k_1 t} + M_{02} k_2 e^{-k_2 t} \tag{6.20}$$

where $M_1 + M_2 = M_0$ is the total emittable amount of VOC applied (mg/m^2). M_1 is the portion for wet-stage emissions and M_2 is for dry-stage emissions. The first-order decay rate constants, k_1 and k_2, in (h^{-1}) are estimated from Equations 6.21 and 6.22.

$$k_1 = 233.25\, P \tag{6.21}$$

$$k_2 = 5.84 \times 10^{-5}\, m \tag{6.22}$$

According to the user's guide for the WPEM model, Equation 6.21 overestimates k_1 while k_2 estimated from Equation 6.22 agrees with the experimental data reasonably well.

Another important issue in modeling emissions from latex paint is the relationship between the amount of VOC applied and the amount of VOC emitted. U.S. EPA's WPEM model assumes that 25% of the total available mass (determined based on the bulk analysis of the paint) is ultimately released. Of this 25% of total emissions, 10% is assumed to be released as described by the first (fast) exponential, and the remaining 90% is assumed to be released as described by the second (slow) exponential. The reliability of these default values depends on both the substrate to which the paint is applied and the paint formulation itself and may require further expert judgment in application of this model. See Section 6.4 for more discussion on this issue.

Limited data are available for the amounts of VOC available for the wet and dry-stage emission.

6.3.6. Model M4-F (Sparks et al., 1998)[70]

This is a semi-empirical model for VOC emissions from latex paint. The wet and dry-stage emissions are represented by Equations 6.23 and 6.24, respectively. The adjustment factor in Equation 8.24 $\left(1 - \frac{M_v}{M_{v0}}\right)^2$ makes the transition from wet to dry emissions.

$$E_1 = h_a \left(C_{v0} \frac{M_1}{M_{01}} - C_a \right) \tag{6.23}$$

$$E_2 = \left(1 - \frac{M_1}{M_{01}}\right)^2 \frac{f_D\, M_2}{\sqrt{t}} \tag{6.24}$$

The model consists of three differential equations for the air concentration (Equation 6.25), mass of chemical remaining for wet-stage emissions (Equation 6.26), and mass of chemical remaining for dry-stage emissions (Equation 6.27).

$$V \frac{dC_a}{dt} = A\,(E_1 + E_2) - Q\,C_a \tag{6.25}$$

$$\frac{dM_v}{dt} = -E_1 \tag{6.26}$$

$$\frac{dM_D}{dt} = -E_2 \tag{6.27}$$

Parameter f_D is a diffusion constant defined by Equation 6.28.[23]

$$f_D = \frac{0.632\sqrt{D_m}}{\delta} \tag{6.28}$$

An example of the predicted concentration profile is shown in Figure 6.2.

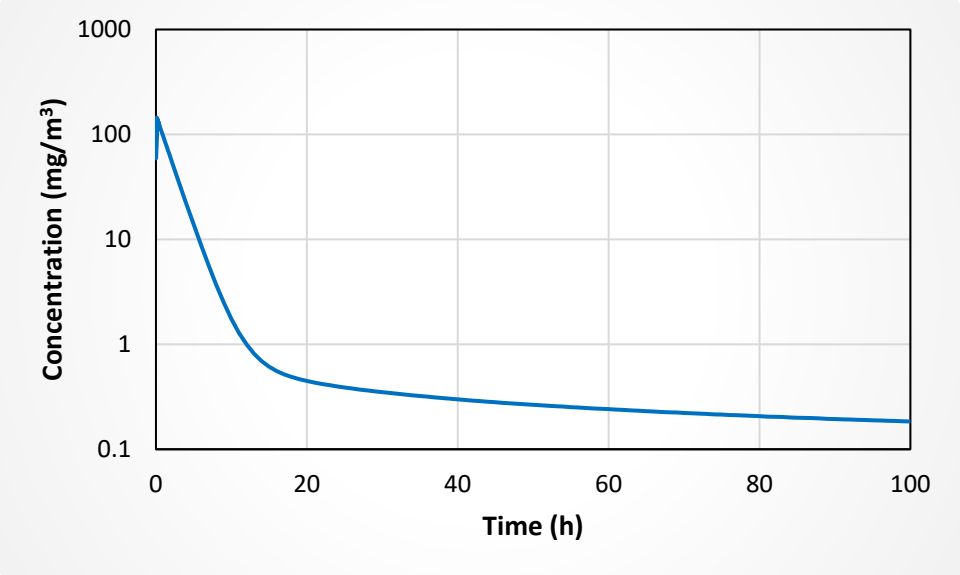

Figure 6.2 Predicted concentration profile for TVOC emissions from a latex paint.

Input parameters were V = 0.053 m^3, N = 0.5 h^{-1}, A = 0.02 m^2, C_{v0} = 2 × 10^4 mg/m^3, M_{01} = 404 mg/m^2. M_{02} = 1465 mg/m^2, f_D = 1.73 × 10^{-3} $h^{1/2}$, ha = 1 m/h. Values of V, N, C_v, M_{01}, M_{02}, and f_D were from Ref. [71].

Caution: The original paper of this model was retracted for a non-technical reason (misuse of a tradename). Model equations can be found in Corsi et al. (2009).[72] Reader discretion is advised.

6.3.7. Model M4-G (Zhou et al., 2020) [73]

This mass transfer model describes VOC emissions from indoor coating materials in three stages: wet, semi-dry, and dry stages. This is a rather complex paint model that requires solving partial differential equations. Interested readers should consult the original paper for details.

This model uses Equation 6.29 to calculate the emission factor. It works reasonably well for organic solvent-based paint but may work poorly for water-based paint. In the latter case, after paint application, water evaporates first, followed by organic solvents. Thus, C_v increases over time early on as the solvents become concentrated due to water evaporation.

$$E = h_a (C_v - C_a) \tag{6.29}$$

6.3.8. Model M4-H (He et al., 2019) [74]

This is a diffusion model for VOC emissions from silicone sealants during the curing process, in which the thickness of the cured layer increases and the uncured layer decreases over time. The moisture-driven curing reaction takes place at the curing interface (Figure 6.3).

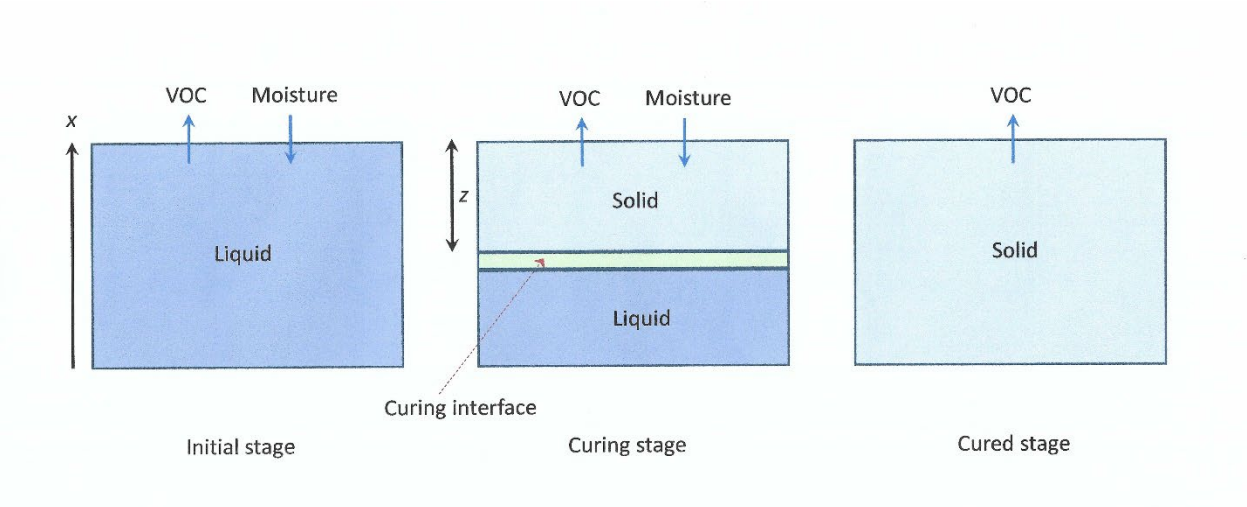

Figure 6.3 Graphical illustration of the curing process for a silicone sealant.

The sealant is applied as a liquid. The moisture-driven curing starts at the exposed surface. The thickness of the solidified layer (z) increases over time until the entire sealant becomes solid. The curing reaction takes place at the solid-liquid interface.

The VOC diffusion in the solid and liquid phases is represented by Fick's second law (Equations 6.30 and 6.31).

$$\frac{\partial C_s}{\partial x} = D_s \frac{\partial^2 C_s}{\partial x^2} \tag{6.30}$$

$$\frac{\partial C_L}{\partial x} = D_L \frac{\partial^2 C_L}{\partial x^2} \tag{6.31}$$

It is assumed that $C_L = C_s$ at the solid-liquid interface and that Equation 6.32 applies.

$$\frac{\partial C_L}{\partial x} = D_s \frac{\partial^2 C_s}{\partial x^2} - E_c \tag{6.32}$$

where E_c is the area-specific VOC generation rate due to the curing reaction and is determined by Equation 6.33. The specific chemical that the authors modeled was methylethyl ketone oxime (MEKO), which is a product of the curing reaction.

$$E_c = \frac{2\, m\, P_s\, p_w}{z} \tag{6.33}$$

where z is the thickness of the cured layer (see Figure 6.3), which increases overtime. Equation 6.3.3 gives the generation rate in (g/m^2/s) if the molecular weight is in (g/mol).

For the VOCs that are not generated by the curing reaction (e.g., solvents), $E_c = 0$.

The mass transfer at the solid-air interface is determined by Equation 6.34.

$$\frac{\partial C_s}{\partial x} = -h_a \left(\frac{C_s}{K_{ma}} - C_a\right) \tag{6.34}$$

The authors reported experimentally determined D_s, D_L, and K_{ma} for a silicone sealant.

This mass transfer model requires a computer program to run. Equations 6.30 through 6.34 are solved numerically with the state-space method (see Section 3.6) by dividing the sealant layer into 60 slices. No further details are provided regarding the numerical computation.

6.4. Additional comments

Results from laboratory testing show that, when water-based paint is applied to a porous material, such as a gypsum board, only a small portion of the VOCs—mainly oxygenated solvents such as glycols—are emitted as wet-stage emissions. A large portion of the solvents is trapped in the substrate. Predicting the VOC masses available for wet and dry-stage emissions is difficult. Furthermore, chamber tests have shown significant discrepancy between the amount of solvent emitted into the air and the amount applied. One factor that may be responsible for the low recovery in chamber tests is the strong adsorption by chamber walls.[75] Several studies showed that the recovery of 2,2,4-trimethyl-1,3-pentanediol monoisobutyrate (TMPD-MIB), an oxygenated organic solvent, during two-week tests ranged from 27% to 60%, and that the recovery over a 64-week period ranged from 50% to 90%.[72]

U.S. EPA's WPEM model assumes that 25% of the total available mass (determined based on bulk analysis of the paint) is ultimately released into the air. This estimate appears too low. It is inconceivable to assume the organic solvents will remain in the porous substrate forever.

The portions of organic solvents available for wet and dry emissions are also difficult to determine because they are highly dependent on the properties of the substrate. U.S. EPA's paint model WPEM assumes that, of the 25% of total emissions, 10% is released as described by the first ("fast") exponential, and the remaining 90% is released as described by the second ("slow") exponential in the model.

6.5. Summary

Models M4-A and M4-B predict the wet-stage emissions from oil-based paint reasonably well. It is our current understanding that, in most cases, the solvent mass available for dry-stage emissions represents only a small portion of the solvent mass applied to the surface.

A major error source in predicting solvent emissions from water-based paint is from the estimation of the emittable masses for wet and dry-stage emissions (M_{01} and M_{02}) when the paint is applied to porous materials, such as gypsum boards. It is inconceivable to assume that a large portion of the solvent will remain in the substrate forever. Once M_{01} and M_{02} are determined, either model M4-E or M4-F can be used.

Suggestions on model selection for emissions from indoor coating materials are shown in Table 6.2.

TABLE 6.2 Suggestions on selecting models for emissions from indoor coating materials.

Paint Type	Chemical Class	Models	Notes
Solvent based	Alkanes and aromatic hydrocarbons	M4-A, M4-B	Included in EPA's WPEM model.[61]
Water-based	Glycols	M4-E	Included in EPA's WPEM model.[61]

7. Models for spray applications

7.1. Symbols and abbreviations

A = total aerosol concentration (kg/m^3),
$A_{0,I,j}$ = initial aerosol concentration for the i^{th} pulse release and size bin j (kg/m^3),
$A_{I,j}$ = aerosol concentration for the i^{th} pulse release and size bin j (kg/m^3),
C_a = concentration in indoor air (kg/m^3),
C_{in} = concentration in inlet air (kg/m^3),
C_{sat} = saturation concentration (kg/m^3),
C_v = concentration of vapor in air (kg/m^3),
f_w = weight fraction of substance in spray product,
g = gravitational constant and g = 9.81 m/s^2,
m = molecular weight (kg/mol),
N = ventilation rate (s^{-1}),
N_r = number of pulse releases,
N_δ = number of aerosol size bins,
P = vapor pressure (Pa),
Q = air flow rate (m^3/s),
$P(\delta)$ = probability density of aerosol particles of diameter δ,
R = emission rate (kg/s),
$\bar{R}$ = gas constant (m^3 Pa K^{-1} mol^{-1}),
R_{A_evap} = rate of solvent evaporation from aerosol (kg/s),
R_{A_settle} = rate of aerosol settlement (kg/s),
R_{A_vent} = rate of aerosol carried out of room by ventilation (kg/s),
$R_{airborne}$ = rate of particle generation for all sizes (kg/s),
$R_{airborne}(\delta)$ = rate of particle generation for size δ (kg/s),
R_{F_evap} = rate of solvent evaporation from aerosol (kg/s),
$R_{release}$ = release rate for aerosol particles with all sizes (kg/s),
$R_{settle}(\delta)$ = rate of particle settlement for size δ (kg/s),
R_{spray} = release rate for product (kg/s),
R_{vent} = rate of particle loss to ventilation for size δ (kg/s),
R_{w_evap} = rate of solvent evaporation from treated wall (kg/s),
S = floor area (m^2),
S_c = Cunningham slip correction factor (dimensionless),
t = elapsed time (s),
t_r = duration of constant aerosol release (s),
T = temperature (K),
V = room volume (m^3),
v_s = settling velocity (m/s),
$v_s(\delta)$ = settling velocity for aerosols of diameter δ (m/s),
W_0 = amount of product released from spray device (kg),
$W_a(\delta)$ = amount of aerosols in air with diameter δ (kg),

δ = aerosol diameter (m),
Δt = time interval between two consecutive pulse release (s),
ρ = density of particle (kg/m^3),
η = viscosity of air (N s/m^2).

Abbreviations

CEM: Consumer Exposure Model,
EGRET: Generic Exposure Scenario Risk and Exposure Tool,
ESIG: European Solvents Industry Group,
SHEDS-HT: Stochastic Human Exposure and Dose Simulation-High Throughput,
U.S. EPA: United States Environmental Protection Agency.

7.2. Overview

Spraying is a convenient way to uniformly distribute a product in room air or on surfaces. There is a wide variety of consumer products that can be applied as aerosols, including air fresheners, surface cleaners, insecticides, cosmetics, and paints. The aerosolized products may lead to increased inhalation and dermal exposure to the components of the product.

When selecting models to estimate exposure due to spray activities, two factors must be considered. The first factor to consider is the type of contaminant. Some spray models were developed for the evaporation of volatile components, such as volatile solvents and propellants, and they predict inhalation exposure to vapors. Other spray models were created for low-volatility and non-volatile components, and they predict inhalation exposure to suspended particulate matter. The second factor to consider is the targeted area of the spray. Many spray products, such as spray paints and insecticides, are for application to surfaces. Spray cosmetics are applied to skin. These activities create two sources: emissions from the "overspray" and emissions from the treated surfaces. These sources may need to be modeled separately. Overspray is defined as the liquid droplets that do not reach the targeted surface and consequently disperse into the air.

More than 20 spray models are available. Many of them were initially developed for occupational exposures and some of them can be used for consumers. Several models were developed specifically for consumer exposures. Four relatively simple spray models are discussed below (TABLE 7.1). Four more spray models and tools for consumer exposures are briefly discussed in Section 7.4.1.

TABLE 7.1 List of spray models discussed.

Model ID	Applicable Chemical Substances	Use Scenario
M5-A	Evaporation of volatile components	Pulse release into air
M5-B	Evaporation of volatile components	Continuous release into air
M5-C	Aerosols of non-volatile components and powders	Continuous release
M5-D	Aerosols, vapor, and treated surface	Continuous release on to surfaces

7.3. Model description

7.3.1. Model M5-A (RIVM, 2017) [76]

This model is for instant (pulse) release of a liquid into air. It is assumed that, upon release, the volatile chemical evaporates instantly, that the vapor is distributed in the room air homogeneously, and that the only loss is due to ventilation (Equation 7.1).

$$C_a = \frac{W_0 \, f_w}{V} \, e^{-N \, t} \tag{7.1}$$

ConsExpo Web uses this model for exposure to both instant releases of vapor and solid spray. There is an upper limit for the maximum concentration in air, which is the saturation concentration calculated from the vapor pressure of the chemical substance (Equation 7.2).

$$C_{sat} = \frac{m \, P}{\bar{R} \, T} \tag{7.2}$$

7.3.2. Model M5-B (RIVM, 2017) [76]

This model is for the release of a volatile liquid into room air at a constant rate over a period, t_r. It consists of two equations: Equation 7.3 calculates the air concentration during the constant release period and Equation 7.4 applies after the release stops. It is assumed that the chemical evaporates instantly, and the decay of the air concentration is due solely to ventilation.

$$C_a = \frac{W_0 \, f_w}{V \, N \, t_r} \, (1 - \, e^{-N \, t}) \qquad \text{for } t \leq t_r \tag{7.3}$$

$$C_a = \frac{W_0 \, f_w}{V \, N \, t_r} \, (1 - \, e^{-N \, t_r}) \, e^{-N \, (t \, - \, t_r)} \qquad \text{for } t > \, t_r \tag{7.4}$$

This model is listed as a model for exposure to vapors in Ref. [76]. It is applicable to spray release of volatile components.

7.3.3. Model M5-C (Delmaar and Bremme, 2009; RIVM, 2017) [76, 77]

Implemented in *ConsExpo Web*, this model is for non-volatile components released from spray activities. Once sprayed, the non-volatile components are suspended in room air as polydisperse aerosols. In this model, the particles are divided into a few size bins and each size bin has its own generation and settlement rates.

This model assumes that the suspended particles contain only non-volatiles. TABLE 7.2 lists all the mass transfer mechanisms involved.

TABLE 7.2 Rate expressions used by spray model M5-C.

Transfer Mechanism	Rate Expression
Release rate for aerosol particles with all sizes	$R_{release} = R_{spray}\, f_w$
Rate of released non-volatile components that become airborne	$R_{airborne} = R_{release}\, f_{airborne}$
Rate of aerosol particle generation for size bin δ [A]	$R_{airborne}(\delta) = R_{airborne}\, P(\delta)\, d\delta$
Rate of gravitational settlement onto floor for aerosol particles of diameter δ [B]	$R_{settle}(\delta) = C_a(\delta)\, S\, v_s(\delta)$
Rate of particle loss due to ventilation	$R_{vent} = C_a(\delta)\, V\, N$

[A] *P(δ)* is the probability density of aerosol particles of diameter *δ*, and *dδ* is the width of the size bin. *ConsExpo Web* allows either normal or lognormal distribution.

[B] Settling velocity v_s for particles of size *δ* is calculated from $v_s(\delta) = \frac{g\,\rho\,\delta^2}{18\,\eta}\, S_c$, where S_C is set to 1.

The model consists of three equations: Equation 7.5 is for the change in particle mass for size bin *δ* during the spraying period, Equation 7.6 is for the change in particle mass for size bin δ after the spraying period, and Equation 7.7 is for the total particle concentration for all particle sizes. To calculate respirable or inhalable particles, the summation term in Equation 7.7 should include size bins that are smaller than or equal to the cut-off size.

$$\frac{dW_a(\delta)}{dt} = -R_{vent} - R_{settle} + R_{airborne} \tag{7.5}$$

$$\frac{dW_a(\delta)}{dt} = -R_{vent} - R_{settle} \tag{7.6}$$

$$C_a = \frac{\sum_{i=1}^{n} W_a(\delta_i)}{V} \tag{7.7}$$

where *n* is the number of size bins.

This model assumes that, after the droplets are released from the nuzzle, the volatile components evaporate almost instantaneously and that the dry aerosols mix with room air quickly. These assumptions are oversimplified in most cases. This problem can be eased by using a two-zone model, known as the near field-far filed model. See Section 7.4.2 for model details.

Model M5-C can be used for powder spray so long as the size distribution of the powder is known.

7.3.4. Model M5-D (Tischer and Meyer, 2022) [78]

Named *SprayEva*, this is a comprehensive spray model that considers aerosol generation, evaporation from liquid aerosols, and emissions from spray-treated surfaces. The model does not require an assumption that volatile components in the formulation evaporate quickly to work for not-so-volatile components. The continuous release of a multi-component liquid from spray operation is discretized by a number of sequential pulse releases. This mathematical treatment allows the aerosols released at different times to have different chemical compositions and particle sizes due to evaporation. The other discretized variable is the area the aerosol product is sprayed on. The treated surface is divided into a

number of equal-sized incremental areas so that the liquid films formed at different times have different compositions due to solvent evaporation.

For the i^{th} pulse release, the aerosol concentration of particle size j increases by $C_{I,j}$. The change of aerosol concentration in the room after one pulse release is given by Equation 7.8.

$$V \frac{dA_{i,j}}{dt} = -R_{A_{vent},j} - R_{A_{settle},j} - R_{A_{evap},j} \tag{7.8}$$

The initial condition for Equation 7.8 is $A_{i,j} = A_{0,I,j}$ when t = (i-1) Δt.

For N_r pulse releases and N_δ size bins, the total aerosol concentration in room air is given by Equation 7.9.

$$A = \sum_{i=1}^{N_\delta} \sum_{j=1}^{N_r} A_{i,j} \tag{7.9}$$

The change in vapor concentration for a component in the formulation after the i^{th} pulse release is given by Equation 7.10.

$$V \frac{dC_v}{dt} = R_{A\_evap} + R_{w\_evap} + R_{F\_evap} + Q\,(C_{in} - C_v) \tag{7.10}$$

This is a rather complex model. Readers are referred to the original paper for details on calculating the transfer rates in Equations 7.8 and 7.10.

This model includes an impaction module that calculates the overspray as a fraction of the total mass released from the spray nuzzle.

The rate of evaporation from spray-treated walls and floors (settled droplets) is based on Raoult's law. It is more suitable for organic solvent mixtures than for water-based products such as latex spray paint because, in the latter case, water evaporates first, followed by organic solvents.

Clarifications are needed on the following issues: (1) how the changing aerosol sizes are handled—the model defines the initial diameters of the droplets but it is unclear whether the ever-changing size distribution is tracked during the integration process; and (2) how the imperfect mixing of aerosols in the room is handled.

7.4. Additional comments

7.4.1. Additional spray models

Among the over 20 available spray models, several were developed or are suitable for consumer exposure assessment. In addition to the models described above, the models and tools listed in TABLE 7.3 are consumer-exposure oriented and with different levels of complexity and features. We did

not fully evaluate these models because the technical details are either unavailable (such as *ConsExpo Nano*) or partially missing (such as *SprayExpo*).

TABLE 7.3 Additional spray models and tools for consumer exposure assessment.

Model/Tool Name	Refs.	Features	Application Type
CEM[A]	[79]	Simple deterministic models for inhalation exposure	Stand-alone Windows app
EGRET[B]	[80]	Simple deterministic models for inhalation and dermal exposure	MS Excel file
ConsExpo Nano[C]	[81]	Deterministic and probabilistic models for exposure to nanomaterials in consumer spray products	Web-based
SprayExpo[D]	[82, 83]	Complex deterministic models for inhalation and dermal exposure	MS Excel file

[A] U.S. EPA's Consumer Exposure Model (CEM) 2.1.
[B] Generic Exposure Scenario Risk and Exposure Tool (EGRET) developed by the European Solvents Industry Group (ESIG).
[C] Developed by the Dutch National Institute for Public Health and the Environment. This on-line tool lacks a detailed technical document.
[D] *SprayExpo* 2.3 developed by the Federal Institute for Occupational Safety and Health, Germany.

Nanoparticles, due to their smaller particle size and unique physical-chemical properties require special consideration when applying spray-models. CPSC staff partnered with NIST to develop two spray-modeling applications. Both models provide short-term estimates of elevated air concentrations. One model is referred to as the single-size particle tool, is based on CONTAM, and includes capabilities common in aerosol exposure tools. The second model is referred to as the size-resolved tool and explores how properties of nanoparticles impact fate and transport. The technical details for these models are well documented in NIST's technical note.[84]

7.4.2. Using near/far-field model for spray activities

The well-mixing assumption may not be valid for some spray operations. One approach to ease this problem is to combine the spray model, such as model M5-C, with a two-zone model [85], in which the "operator" experiences higher exposure than the "bystander" (Figure 7.1).

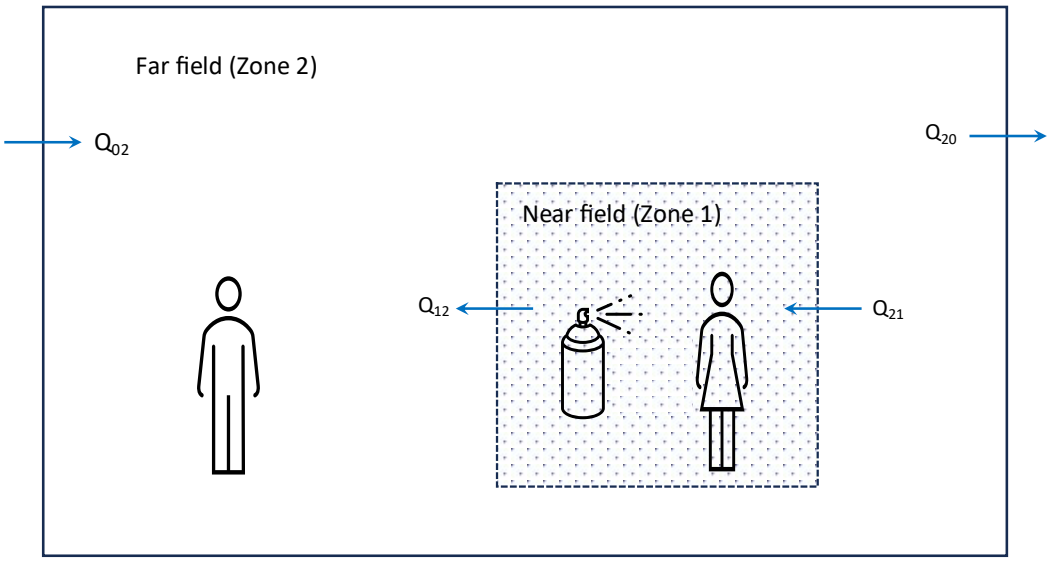

Figure 7.1 Illustration of spray activities in a near field/far-field setting, where Q_{ij} is the air flow from zone *i* to zone *j*.

The generic mass balance equations for the two zones are given by Equations 7.11 and 7.12. The added input parameters are the volume of the near field zone (V_1), and the interzonal air flows Q_{12} and Q_{21}. The values of these parameters are determined by the case to be modeled. Some existing simulation tools provide default values for these parameters.

$$V_1 \frac{dC_1}{dt} = R - (Q_{12} - Q_{21})\, C_1 \tag{7.11}$$

$$V_2 \frac{dC_2}{dt} = (Q_{12} - Q_{21})\, C_1 - Q_{20}\, C_2 \tag{7.12}$$

The volume of the near field zone (V_1) varies by model and case. According to Huang et al. (2017), *ConsExpo* uses 0.0625 m^3, the Stochastic Human Exposure and Dose Simulation-High Throughput (SHEDS-HT) model uses 0.0425–0.0825 m^3 with a mean value of 0.0625 m^3. The United States Environmental Protection Agency (U.S. EPA)'s Consumer Exposure Model (CEM) uses 1 m^3.[79] Some occupational models define the near field as "within approximately 1 m of the breathing zone."[86]

For more information about near and far-field modeling, see Refs [87] and [88].

7.4.3. Overspray during spray painting

According to Jayjock (2012) [89], overspray during spray painting takes 1 to 6% of the total amount of aerosols released from the spray nozzle.

7.4.4. Data needs

Household spray products include a large variety of products for different applications. To use the spray models, basic information about the products and use scenarios are needed, including:

- Composition of the spray product,
- Typical amount of liquids released from spray event,
- Typical duration of each spray event,
- Overspray as a fraction of the total amount released, and
- Particle size distribution, including nanoparticles and ultrafine particles.

The relevant data are spread among many publications, databases, guidance documents, and indoor exposure simulation tools. Compilation and analysis of existing information would help reduce the uncertainty in modeling spray activities.

7.5. Summary

Many mass transfer processes are involved in spray applications. Existing spray models reflect the balance between validity, simplicity, and usefulness. Models M5-A and M5-B are for evaporation of volatile components in spray formulations and consider exposure to vapors only. Model M5-C is for exposure to aerosols formed from non-volatile components. These models assume that the solvents evaporate rapidly after being released from the spray nuzzle, and that the room air is well mixed. These assumptions do not always hold true. The combination of a spray model with a near/far-field model may help reduce the uncertainties in the modeled vapor and aerosol concentrations.

Model M5-D is more complex than the above-mentioned models. It handles vapors, aerosols, and spray-treated surfaces. The combination of spray models with models that estimate longer term emissions of liquids from surfaces (Section 5 and Section 6) may also be warranted depending on the consumer product and timeframe of interest.

8. Models for emissions from indoor combustion sources

8.1. Symbols and abbreviations

A = indoor surface area (m^2),
C_0 = concentration in kitchen air from preceding time interval (mg/m^3),
C_a = concentration in room air (g/m^3, mg/m^3, or $\mu g/m^3$),
C_b = background concentration (mg/m^3),
C_{CO2} = measured CO_2 contaminant concentration in room air (mol CO_2/mol air),
C_{gi} = measured concentration of gas contaminant *i* in room air (mol *i*/mol air or ppb),
C_k = concentration in kitchen air (mg/m^3),
C_p = measured particle concentration in room air (#/cm^3 air),
C_{out} = concentration in outdoor air (mg/m^3),
E_{CO2} = fuel normalized CO_2 generation rate due to natural gas combustion (mol/MJ),
E_D = energy density of the fuel (MJ/kg),
E_{DC} = total daily cooking energy required (MJ),
E_F = fuel-based emission factor for contaminant (mg/kg fuel),
E_{gi} = fuel normalized emission factor for gas contaminant I (g/MJ or (ng/J),
E_p = fuel normalized emission factor for particulate matter (#/MJ or #/J),
F = fuel consumption rate (J/h),
f = fraction of emissions that enters the kitchen,
f_{hood} = capture efficiency of the range hood (fraction),
G = contaminant generation rate ($\mu g/m^3$/min) for particles and (ppm/min) for gasses,
G_B = candle burn rate (g/h),
G_{CO2} = carbon dioxide generation rate (g/h),
G_n = fuel normalized contaminant generation rate (g/J),
k = contaminant removal rate constant other than ventilation (h^{-1}),
k_2 = second-order reaction rate constant (ppb^{-1} min^{-1}),
k_d = deposition rate (hr^{-1}),
m = molecular weight (g/mol),
m_{CO2} = molecular weight of CO_2 (g/mol),
m_{fuel} = molecular weight of candle fuel (g/mol),
m_i = molecular weight of gas contaminant *i* (g/mol),
N = air exchange rate (h^{-1} or min^{-1}),
P = stove power (MJ/min),
P_n = penetration factor (fraction),
Q = air flow rate in room (m^3/h),
Q_{hood} = range hood air flow rate (m^3/h),
r_{NO2} = uptake efficiency for NO_2 deposition on interior surfaces (fraction),
R = emission rate (µg/min or g/h),
R_c = rate of contaminant emission from burning candle (ppb/min),
R_{in} = rate of contaminant infiltration from ambient air (ppb/min),
R_s = rate of contaminant deposition on interior surfaces (ppb/min),

R_{vent} = rate of contaminant removal from room due to ventilation (ppb/min),
R_x = rate of gas-phase chemical reaction (ppb/min),
S = source strength (μg/h),
t = time (min),
t_c = cooking duration (min),
$\bar{v}$ = average deposition velocity (m/min),
v_0 = molar volume of gas, v_0 = 22.4 L at 0 ^oC and 1 atm,
V = room volume (m^3),
V_T = volume of unvented tent (m^3),
η = stove's thermal efficiency (fraction).

Abbreviations

CO_2: carbon dioxide,
CO: carbon monoxide,
HCHO: formaldehyde,
HONO: nitrous acid,
HOMES: Household Multiple Emission Sources,
LPG: liquefied petroleum gas,
NO_2: nitrogen dioxide,
NO_x: nitrogen oxides,
PM: particulate matter,
SO_2: sulfur dioxide,
WHO: World Health Organization.

8.2. Overview

Even though emissions from indoor combustion sources have been a topic of active research for decades and a huge data pool has been accumulated, relevant models are scarce. Most existing models rely on experimental data as input. True predictive models are almost nonexistent. One of the difficulties in predicting the formation of combustion by-products—such as carbon monoxide (CO), carbon dioxide (CO_2), nitrogen oxides (NO_x), sulfur dioxide (SO_2), aldehydes, aromatic compounds, and particulate matter (PM)—is that the contaminant generation depends on combustion conditions even with the same combustion appliance and the same fuel. Eight models are discussed below (TABLE 8.1).

TABLE 8.1 List of models for emissions from combustion sources discussed in this section.

Model ID	Appliance/product Type	Contaminants modeled
M6-A	Non-specific indoor combustion sources	CO, NO_2, and PM
M6-B	Cooking stoves	CO and PM
M6-C	Cooking stoves	CO and PM
M6-D	Unvented kerosene heaters	CO, NO, SO_2, and PM
M6-E	Cooking with gas burners	NO_2 and PM
M6-F	Cooking with gas burners	CO, NO_2, and PM
M6-G	Candles	NO_x, NO, NO_2, HONO, HCHO, CO, and PM
M6-H	Candles	CO_2
M6-I	Incense	Organic carbon

8.3. Model description

8.3.1. Model M6-A (Traynor et al., 1989) [90]

This is a generic model for calculating indoor concentrations of combustion products. The mass balance equation for indoor air is given by Equation 8.1.

$$\frac{dC_a}{dt} = p_n\, N\, C_{out} + \frac{S}{V} - (N + k)\, C_a \tag{8.1}$$

If the source strength S is constant and the initial conditions are $C_a = C_a(0)$ when $t = 0$, the exact solution to Equation 8.1 is given by Equation 8.2 and the steady-state concentration by Equation 8.3.

$$C_a(t) = \frac{p_n\, N\, C_{out} + S/V}{N + k}\left[1 - e^{-(N+k)t}\right] + C_a(0)\, e^{-(N+k)t} \tag{8.2}$$

$$C_a = \frac{p_n\, N\, C_{out} + S/V}{N + k} \tag{8.3}$$

This model relies on experimental source strength S. Also note that, if the combustion source is vented, source strength S is the fugitive emission rate.

8.3.2. Model M6-B (WHO, undated) [91]

This is also a data-based generic model for predicting the concentrations of airborne contaminants in kitchen from cooking stoves. It is incorporated in the Household Multiple Emission Sources (HOMES) model developed by the World Health Organization (WHO). The indoor concentration is predicted by Equation 8.4.

$$C_a(t) = \frac{\sum_{i=1}^{n} R_i\, f_i}{N\, V}\,(1 - e^{-N\,t}) + C_0\, e^{-N\,t} + C_b \tag{8.4}$$

where *n* is the number of indoor combustion sources.

A minor change to Equation 8.4 is recommended. Parameter C_0 in Equation 8.4 is defined as the concentration from the preceding time interval, which is interpreted as the concentration in the kitchen resulting from the previous cooking event. If so, Equation 8.5 is more accurate because the background concentration C_b is counted twice in Equation 8.4.

$$C_a(t) = \frac{\sum_{i=1}^{n} R_i f_i}{N V} (1 - e^{-N t}) + (C_0 - C_b) e^{-N t} + C_b \quad (8.5)$$

The key input parameters regarding the sources are the emission rate (*R*) and the fraction of the emissions that enter the kitchen (*f*). These values are usually obtained from databases. Multiple databases are available. WHO has its own database, which contains typical air exchange rates, cooking time, kitchen volumes, and emission rates for carbon oxide and PM.[92]

This model ignores the particle loss due to deposition on interior surfaces.

8.3.3. Model M6-C (Johnson et al., 2011) [93]

This model (Equation 8.6) is similar to model M6-B except that the emission rate is estimated with an empirical formula (Equation 8.7).

$$C_k(t) = \frac{R f}{N V} (1 - e^{-N t}) + C_0 e^{-N t} \quad (8.6)$$

$$R = \frac{E_f}{E_D} P \quad (8.7)$$

Parameter C_0 in Equation 8.6 is defined as the "concentration from the preceding time unit," which is ambiguous. If the ambient concentration is ignored, C_0 is the initial concentration in the kitchen. Otherwise, Equation 8.5 applies.

The duration of each cooking event is calculated from Equation 8.8 by assuming that there are three cooking events a day and that the events consume the same amount of energy.

$$t_c = \frac{E_{DC}}{3 P \eta} \quad (8.8)$$

8.3.4. Model M6-D (Zhou et al., 2000) [94]

This is an empirical model for particulate and gas contaminant emissions from unvented kerosene heaters. The model was based on the emissions testing results in a 106-m^3 army tent for three types of heaters and three types of fuel. Two empirical models were used. Equation 8.9 is for PM and CO and Equation 8.10 is for NO and SO_2.

$$G = a + b\,t\,e^{-c\,t} \tag{8.9}$$

$$G = a\left(1 - e^{-b\,t}\right) \tag{8.10}$$

Coefficients *a*, *b*, and *c* in Equations 8.9 and 8.10 are given in a table in Ref. [94]. In addition, the average generation factors (µg/KJ) based on fuel consumption are also given.

Note that the generation rate *G* is in (µg/m^3/min) for PM and in (ppm/min) for gas contaminants. These values cannot be used "as is" because they are associated with the volume of the tent (V_T = 106 m^3) where the heaters were tested. To convert the generation rates to emission rates in (µg/min), use Equation 8.11 for PM and Equation 8.12 for gas contaminants.

$$R\ (\mu g/min) = V_T\ G \tag{8.11}$$

$$R\ (\mu g/min) = \frac{10^3\ m\ V_T}{v_0} G \tag{8.12}$$

where *m* is in (g/mol), V_T is in (m^3), and v_0 is in liters.

Typical concentration profiles for NO, SO_2, CO, and PM are shown in Figure 8.1.

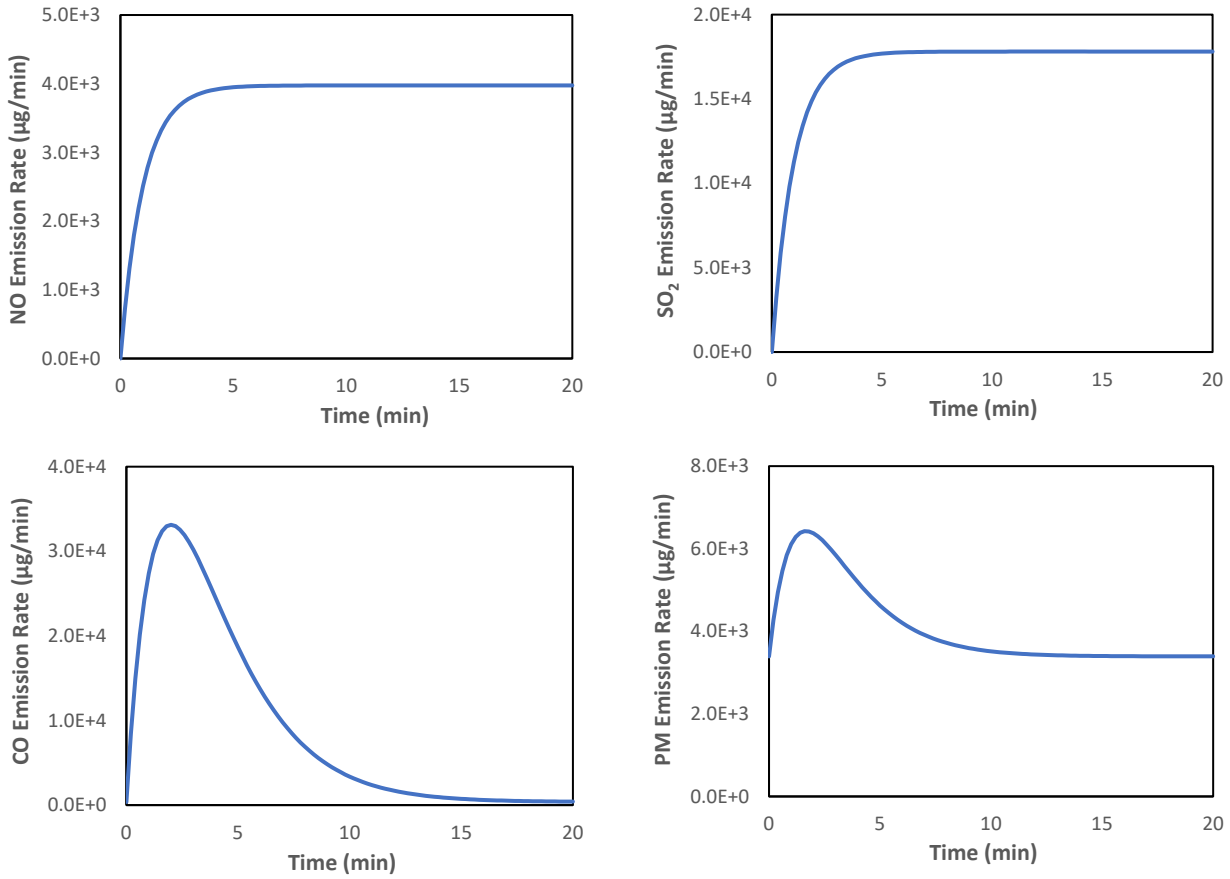

Figure 8.1 Examples of predicted emission rates for NO, SO_2, CO, and PM from unvented space heaters.

Input parameters were from Ref. [94]: Equation 8.10 for NO and SO_2; Equation 8.9 for CO and PM.

8.3.5. Model M6-E (Chan et al., 2020) [95]

Chan et al. used mass balance Equation 8.13 to determine the indoor concentrations of NO_2 and fine particulate matter ($PM_{2.5}$) resulting from natural gas-fueled cooking appliances and cooking activities.[95]

$$V\,\frac{dC_a}{dt} = P_n\,(Q + Q_{hood})\,C_{out} + (1 - f_{hood})\,R - (Q + Q_{hood} + V\,k_d)\,C \qquad (8.13)$$

where Q_{hood} is the range hood airflow rate (m^3/h) and f_{hood} is the capture efficiency of the range hood (fraction).

The emission rates for NO_2 and $PM_{2.5}$ are estimated from literature values. Note that NO_2 and $PM_{2.5}$ are from different sources. NO_2 is from combustion of natural gas while $PM_{2.5}$ is from cooking activities. Therefore, the emission rates are estimated differently.

The emission rate R (g/h) for NO_2 is estimated by multiplying the fuel consumption rate F (J/h) by the fuel normalized NO_2 generation rate G_n (g/J), as shown in Equation 8.14.

$$R = F \times G_n \quad (8.14)$$

The authors used F = 7 kBTU/hour for a single burner as the average fuel consumption rate. The fuel normalized NO_2 generation rate, G_n, ranges from 7 to 22 ng/J. The conversion factors for these values are as follows:

- 1 BTU = 1055 J,
- 1 (ng/J) = 10^{-9} (g/J).

For example, if two burners are operating and the fuel-normalized NO_2 generation rate is 10 (ng/J), then $F = 7 \times 1000 \times 2 \times 1055 = 1.48 \times 10^7$ (J/h); $G_n = 10 \times 10^{-9} = 1 \times 10^{-8}$ (g/J); $R = F \times G_n = 1.48 \times 10^7$ (J/h) × 1×10^{-8} (g/J) = 0.148 (g/h).

The generation rates for $PM_{2.5}$ during cooking events are from literature, as summarized by Chan et al. (2020). The authors used the following values in their simulations:

- Breakfast (bacon, eggs, and hash browns): 100 mg over 19 min,
- Lunch (stir-fry of chicken and vegetables): 50 mg over 17 min,
- Dinner (pasta Bolognese): 50 mg over 20 min.

This model can be used in two ways: (1) predicting the indoor NO_2 and $PM_{2.5}$ concentrations if the emission rate is known, and (2) calculating the minimum capture efficiency of the range hood that is needed to achieve a certain indoor air quality goal.

8.3.6. Model M6-F (Singer et al., 2017) [96]

This is another measurement-based model for predicting contaminant emissions from natural gas cooking burners. The contaminants measured included nitrogen oxides, carbon monoxide, nanoparticles with diameters of 6 nm or larger, and $PM_{2.5}$.

The fuel-normalized emission factors for gaseous contaminants in (ng/J) are calculated based on the measured contaminant concentration ratio to CO_2 and measured CO_2 generation rate (E_{CO2}) (Equation 8.15).

$$E_{gi} = \frac{C_{gi}}{C_{CO2}} E_{CO2}\, m_i \quad (8.15)$$

where C_{gi} and C_{CO2} are in (mol/mol air), and E_{CO2} is in (mol/MJ).

Note that the emission factor calculated from Equation 8.15 bears the unit of (g/MJ), which can be converted to a common unit (ng/J) by multiplying E_p by 1000.

For particles, Equation 8.16 is used.

$$E_p = \frac{C_p\, v_0}{C_{CO2}}\, E_{CO2} \tag{8.16}$$

where C_p is in (#/cm^3 air) and v_0 is in (cm^3/mol).

The fuel-normalized emission factor from Equation 8.16 is in (#/MJ), which can be converted to (#/J) by dividing E_p by 10^6. Note that the conversion factor in Equation 3 in the original paper is incorrect.

The fuel-normalized CO_2 generation rate used by the authors was G_{CO2} = 1.1 mol/MJ.

8.3.7. Model M6-G (Klosterköther et al., 2021) [97]

This model is for gaseous contaminants and particle emissions from burning candles. The general mass balance equation for gaseous contaminants is given by Equation 8.17.

$$\frac{dC_{gi}}{dt} = R_{in} + R_c - R_{vent} \pm R_x - R_s \tag{8.17}$$

where the reaction rate R_x is positive if the contaminant is a reaction product and negative for a reagent.

The concentration unit in Equation 8.17 is (ppb). The authors presented the experimentally determined emission factors, R_c, for three types of candles, assuming a wax burning rate of 3 g/h, and compared the results with literature values. The contaminants included NO_x, NO, nitrogen dioxide (NO_2), nitrous acid (HONO), formaldehyde (HCHO), and CO, as well as the particle mass and particle count.

A second-order reaction was used to describe the oxidation of NO to form NO_2 (Equation 8.18).

$$R_x = k_2\, [NO]\, [O_3] \tag{8.18}$$

where

k_2 is the second-order rate constant and k_2 = 2.36 × 10^{-2} (ppb^{-1} min^{-1}) at 293 K is from literature,

[NO] and [O_3] are concentrations of NO and O_3 in (ppm).

The deposition rate for NO_2 was calculated from Equation 8.19.

$$R_s = \frac{1}{4}\frac{A}{V}\, \bar{v}\, r_{NO2}\, [NO_2] \tag{8.19}$$

8.3.8. Model M6-H (Salthammer et al., 2021; Kapalo et al., 2022) [98, 99]

The generation rate of carbon dioxide from burning candles can be estimated by stoichiometry. Equation 8.20 is the generic form of the reaction, which assumes complete combustion.

$$a_1\ C_xH_yO_z + a_2\ O_2 \rightarrow b_1\ CO_2 + b_2\ H_2O \tag{8.20}$$

If the candle fuel is palm stearin, Equation 8.14 becomes 8.21.

$$2\ C_{57}H_{110}O_6 + 163\ O_2 \rightarrow 114\ CO_2 + 110\ H_2O \tag{8.21}$$

If the candle burn rate, G_B, is known, the CO_2 generation rate, G_{CO2}, can be calculated from Equation 8.22.

$$G_{CO_2} = \frac{b_1\ m_{CO_2}}{a_1\ m_{fuel}}\ G_B \tag{8.22}$$

where coefficients a_1 and b_1 are from Equation 8.20.

For example, if the burn rate of palm stearin candles is 10 g/h, the theoretical CO_2 generation rate from Equations 8.21 and 8.22 is 28.1 g/h.

If the candle fuel is hydrocarbons, such as paraffin wax, Equation 8.23 applies.

$$C_nH_{2n+2} + (1.5\ n + 0.5)\ O_2 \rightarrow n\ CO_2 + (n+1)\ H_2O \tag{8.23}$$

8.3.9. Model M6-I (See and Balasubramanian, 2011) [100]

See and Balasubramanian (2011) tested fine particle emissions from six types of incense in a 1-m^3 chamber and developed a statistical model that links the emissions of particle-phase organic carbon to the carbon content in unburned incense sticks (Equation 8.24).

$$E_{OC} = 0.1\ C_{carbon} - 28.40 \quad (R^2 = 0.88) \tag{8.24}$$

where E_{OC} is emission factor for organic carbon in fine particles emitted from burning incense (mg/g), and C_{carbon} is carbon content in unburned incense sticks (mg/g).

Experimentally determined particle generate rate in (mg/h) and particle emission factor in (mg/g incense burned) were presented without statistical analyses. The correlation between the particle-phase elemental carbon and the carbon content in unburned incense was poor.

8.4. Additional comments

8.4.1. Database for $PM_{2.5}$ emissions from indoor combustion sources

Hu et al. (2012) developed a small database for $PM_{2.5}$ emission rates for cooking activities and burning candles and incense, including data from 522 cooking tests described in 13 papers and two reports on emissions from candles and incense.

8.4.2. Nitric oxide (NO) versus nitrogen dioxide (NO_2)

Most NO_x emitted from combustion sources are in the form of nitric oxide (NO), which can be oxidized in air by oxygen and other reactive species such as ozone and OH radicals. Thus, the ratio of NO:NO_2 depends on the residence time of NO in the room, room temperature, and the levels of oxidants in room air.

8.4.3. Scented versus unscented candles

In general, scented candles produce more combustion by-products—such as VOCs, including benzaldehyde and limonene—than unscented candles because the combustion of the fragrant components is more complex than the fuel.[98]

8.5. Summary

Genuine predictive models for combustion sources are almost nonexistent. Combustion processes are variable and are influenced by fuel type, appliance type, and conditions present (e.g., temperature, relative humidity, airflow) during combustion. Emissions are typically normalized by fuel usage, rather than mass or surface area. Most existing models rely on combustion experimental databases for key inputs, such as contaminant generation rate, fugitive emissions as a fraction of the total emissions, and typical combustion duration. Compilation and analysis of existing data that spread in many places would help reduce the uncertainties in predicting indoor air quality associated with combustion sources.

9. Models for emissions from indoor appliances and devices

9.1. Symbols and abbreviations

A = area of water in washing machine (m^2),
C_a = chemical concentration in room air (mg/m^3),
C_{am} = metal concentration in room air ($\mu g/m^3$),
C_{ap} = fine particle concentration in room air ($\mu g/m^3$),
C_H = chemical concentration in machine headspace (mg/m^3),
C_{in} = chemical concentration in indoor air (mg/m^3),
C_L = chemical concentration in water in washing machine (mg/m^3),
C_{L0} = initial chemical concentration in water in washing machine (mg/m^3),
$C_{L,in}$ = chemical concentration in water supply (mg/m^3),
C_{Lm} = metal concentration in fill water for humidifier (mg/L),
$C_{L,TDS}$ = concentration of total solved solids in fill water for humidifier (mg/L),
C_r = chemical concentration in room air at distance r from source ($\mu g/m^3$),
C_{SL} = concentration of dissolved solids in tap water (mg/L),
D_E = eddy diffusivity (m^2/min),
G = particle generation rate (µg/min),
E_x = specific particulate emission factor from 3D printer (µg/mg filament extruded),
H_S^{cc} = Henry's law solubility constant, $H_S^{cc} = C_L/C_a$ at equilibrium (dimensionless),
H_V^{cc} = Henry's law volatility constant, $H_V^{cc} = C_a/C_L$ at equilibrium (dimensionless),
K_{OL} = overall liquid-phase mass transfer coefficient (m/min),
L_c = characteristic length of the room (m) and $L_c = \sqrt[3]{V}$,
M_g = amount of contaminant in headspace (mg/m^3),
m_L = amount of contaminant in water (mg/m^3),
N = ventilation rate (min^{-1}),
Q = air exchange flow rate (m^3/min),
Q_H = headspace air exchange flow rate (m^3/min),
Q_L = water flow rate (m^3/min),
r = distance from source (m),
R_m = metal emission rate from ultrasonic humidifier (µg/min),
t = time (min),
T = temperature (°C),
V = room volume (m^3),
V_L = water volume (m^3),
V_H = headspace volume (m^3).

Abbreviations

ABS: acrylonitrile butadiene styrene,
VOC: volatile organic compound.

9.2. Overview

Home appliances include a wide range of machines and devices that serve certain household functions. In some cases, these appliances may become contaminant sources with different emission mechanisms. Models for predicting emission mechanisms for three types of appliances are discussed below.

Washing machines, dishwashers, and other water sources (kitchen sinks, showers, etc.): Volatilization of volatile chemicals from water-using appliances. The key transfer mechanism is best described by the two-film resistance theory. See Section 5.2.1 for details.

Humidifiers: Particle formation due to water evaporation from water droplets released from ultrasonic and natural evaporative humidifiers. Room and whole-house humidifiers are designed to release fine water droplets into room air, where water evaporates quickly, to increase indoor humidity. Tap water almost always contains soluble solids. Some tap water also contains insoluble particles. After water evaporates from the droplets, these soluble and insoluble solids become suspended fine particles, elevating the indoor particle concentration. The major concerns are fine particles and particle-borne heavy metals.

3D printers: Emissions of fine particles and volatile organic compounds (VOCs) from electronic devices, such as consumer-grade 3D printers, are caused by heating polymeric materials. The results of laboratory testing show that consumer-grade 3D printers can be significant sources of nano particles, organic compounds, and metals. Although several models have been published for emissions from 3D printing [101-105], they are used only for interpreting the test results (i.e., estimating the emission rates from concentration data) and, thus, not useful in predicting indoor air quality. Only one of these models is included in the list below.

Six models are discussed below, as shown in TABLE 9.1. Combustion appliances are discussed elsewhere (see Section 8).

TABLE 9.1 List of mass transfer and empirical models for contaminant emissions from home appliances.

Model ID	Appliance Type	Contaminants
M7-A [A]	Washing machine	VOCs and dissolved gases in tap water
M7-B [A]	Dishwasher	VOCs and dissolved gases in tap water
M7-C [A]	Kitchen sink	VOCs and dissolved gases in tap water
M7-D	Humidifier	Fine particles
M7-E	Humidifier	Metals in fine particles
M7-F	3D printer	Fine particles

[A] This model contains an error that can be easily corrected.

9.3. Model description

9.3.1. Model M7-A (Howard and Corsi, 1998) [106]

This model is for volatile component emissions from tap water in washing machines. It should also work for volatile chemicals in detergents such as fragrant chemicals. Typical operation of a residential washing machine consists of the following sequential steps: fill, wash, drain, spin, fill, rinse, drain, and spin. The

mass balances for the three key steps—fill, wash, and rinse—are given by Equations 9.1 through 9.4 and illustrated by Figure 9.1 and Figure 9.2.

For the fill cycle, the contaminant masses in water and headspace air are determined by Equations 9.1 and 9.2, respectively.

$$\frac{d(C_L V_L)}{dt} = Q_L C_{L,in} - A K_{OL}\left(C_L - \frac{C_H}{H_s^{cc}}\right) \tag{9.1}$$

$$\frac{d(C_H V_H)}{dt} = Q_H C_{H,in} - Q_H C_H + A K_{OL}\left(C_L - \frac{C_H}{H_s^{cc}}\right) \tag{9.2}$$

Note that, during the fill cycle, both the volumes of the headspace (V_H) and water (V_L) change over time and, thus, should be treated as variables.

For the wash/rinse cycle, both V_H and V_L become constant:

$$\frac{dm_L}{dt} = V_L \frac{dC_L}{dt} = - A K_{OL}\left(C_L - \frac{C_H}{H_s^{cc}}\right) \tag{9.3}$$

$$\frac{dm_g}{dt} = V_H \frac{dC_H}{dt} = Q_H C_{in} - Q_H C_H + A K_{OL}\left(C_L - \frac{C_H}{H_s^{cc}}\right) \tag{9.4}$$

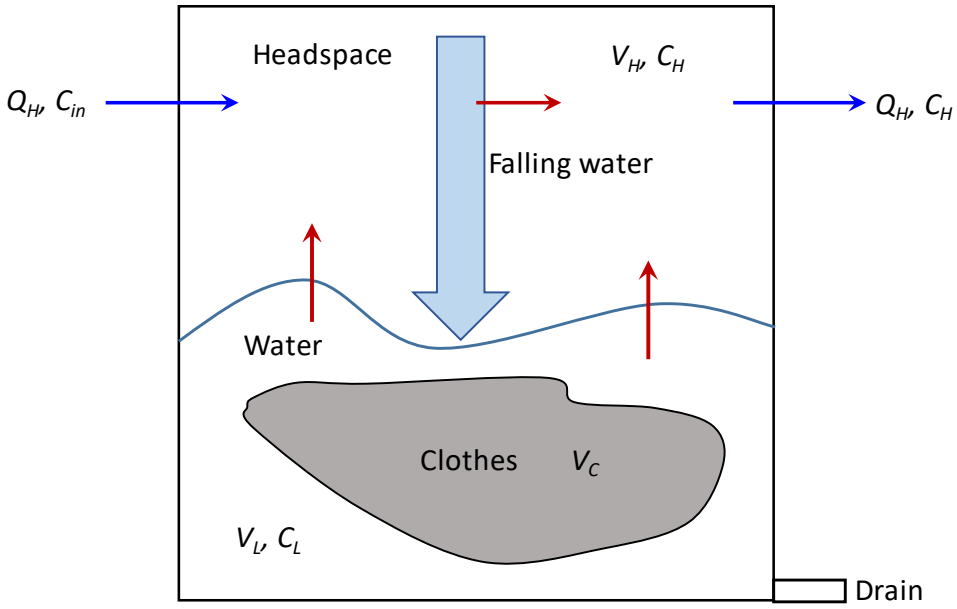

Figure 9.1 Schematic representation of the fill cycle during washing machine operation.

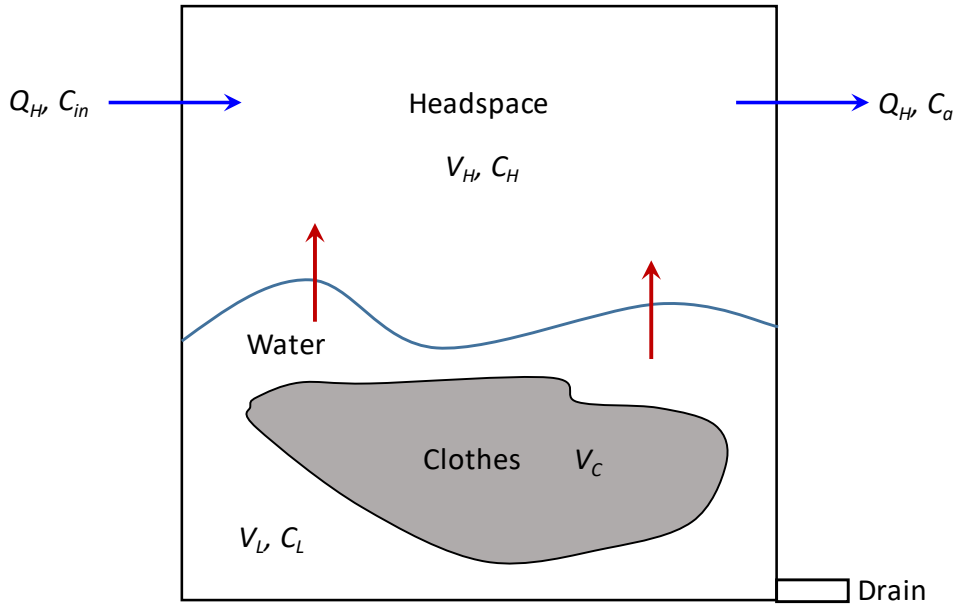

Figure 9.2 Schematic representation of the wash/rinse cycle during washing machine operation.

This model contains an error that can be easily corrected. The Henry's law constant shown in Equations 9.1 through 9.4 is the dimensionless Henry's law solubility constant (i.e., $H_s^{cc} = C_L/C_a$ at equilibrium). It should be the dimensionless Henry's law volatility constant (i.e., $H_v^{cc} = C_a/C_L$ at equilibrium) instead. See Section 5.2.1 for more information about their definitions.

There are two easy ways to correct this error: (1) replace H_s^{cc} with H_v^{cc}, or (2) replace $\frac{C_H}{H_v^{cc}}$ with $H_s^{cc}\ C_H$. For example, Equation 9.1 should be replaced by either Equation 9.5 or, equivalently, 9.6.

$$\frac{d(C_L V_L)}{dt} = Q_L\ C_{L,in} - A\ K_{OL}\left(C_L - \frac{C_H}{H_v^{cc}}\right) \tag{9.5}$$

$$\frac{d(C_L V_L)}{dt} = Q_L\ C_{L,in} - A\ K_{OL}(C_L - H_s^{cc}\ C_H) \tag{9.6}$$

The key input parameters of this model include the initial content of the volatile chemical substance in tap water (C_{L0}), the overall liquid-phase mass transfer coefficient (K_{OL}), surface area of water in washing machine (A), Henry's law constant (H_v^{cc}), and water temperature. The temperature dependence of Henry's law constant is well established.[107]

Because the surface area of water is difficult to accurately measure due to falling water during the fill cycle and agitation during the wash/rinse cycles, the authors of Ref. [106] lumped the water area (A) with the overall liquid-phase mass transfer coefficient (K_{OL}) and reported the combination as ($A\ K_{OL}$).

This model can be incorporated into a multi-zone indoor air quality model, as shown in Figure 9.3, by adding two mass balance equations (Equations 9.7 and 9.8), where subscripts 1 and 2 indicate zones 1 and 2, and subscript 0 denotes ambient air.

$$V_1 \frac{dC_{a1}}{dt} = Q_{H1}\, C_H - (Q_{1H} - Q_{10} - Q_{12})\, C_{a1} + Q_{21}\, C_{a2} \tag{9.7}$$

$$V_2 \frac{dC_{a2}}{dt} = -(Q_{20} + Q_{21})\, C_{a2} + Q_{12}\, C_{a1} \tag{9.8}$$

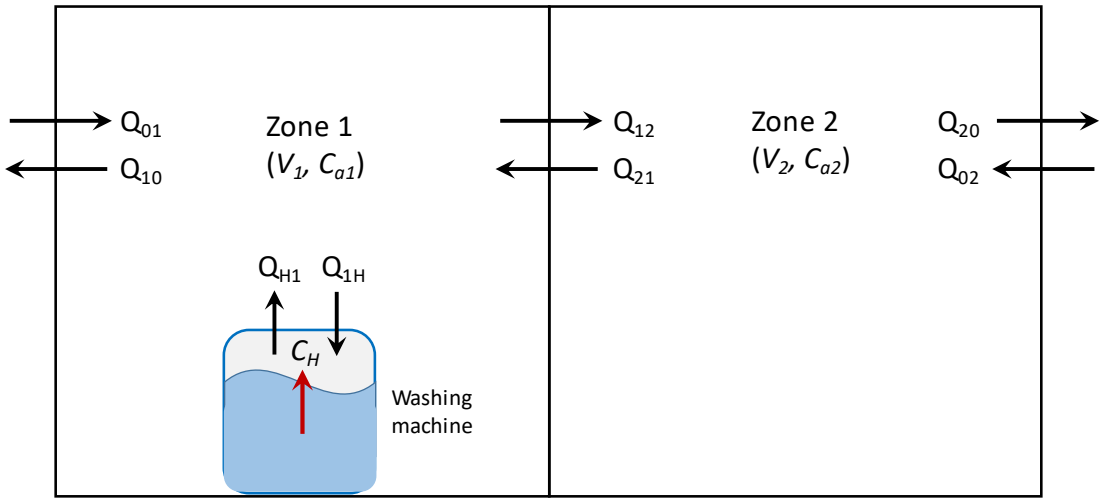

Figure 9.3 Illustration of incorporating the washing machine model into a multi-zone indoor air quality model.

Zone 1 is the laundry room; zone 2 is the rest of the indoor space.

9.3.2. Model M7-B (Howard-Reed, et al., 1999) [108]

This dishwasher model assumes that, during operation, the volumes of liquid (V_L) and headspace (V_H) are both constant (Figure 9.4). Thus, the mass balance equations for the water and headspace air are given by Equations 9.9 and 9.10.

$$V_L \frac{dC_L}{dt} = -A\, K_{OL} \left(C_L - \frac{C_a}{H_s^{cc}} \right) \tag{9.9}$$

$$V_H \frac{dC_H}{dt} = Q_H\, C_i - Q_H\, C_H + A\, K_{OL} \left(C_L - \frac{C_H}{H_s^{cc}} \right) \tag{9.10}$$

This model contains the same error as that in model M7-A. The Henry's law solubility constant H_s^{cc} in Equations 9.9 and 9.10 should be replaced with Henry's law volatility constant, H_v^{cc}.

To calculate the contaminant concentration in room air, mass balance Equations 9.7 and 9.8 can be used.

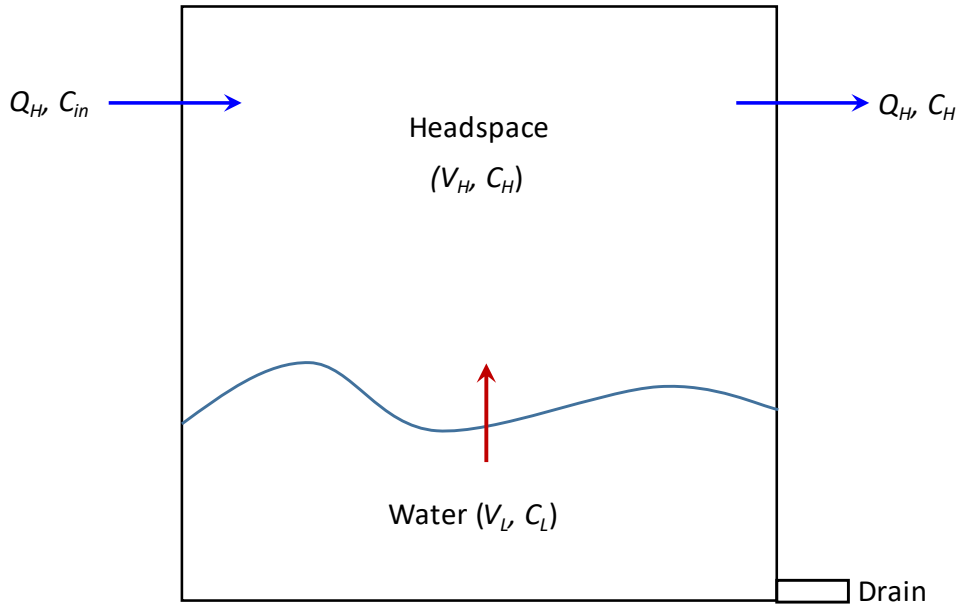

Figure 9.4 Schematic representation of the dishwasher operation.

9.3.3. Model M7-C (Corsi, 1996) [109]

This model is for emissions of volatile chemical substances from kitchen sinks during water use. The mass transfer equation used is given by Equation 9.11.

$$\frac{d(C_L V_L)}{dt} = -A K_{OL}\left(C_L - \frac{C_a}{H_s^{cc}}\right) \tag{9.11}$$

The contaminant concentration in the kitchen is given by Equation 9.12.

$$V \frac{dC_a}{dt} = A K_{OL}\left(C_L - \frac{C_a}{H_s^{cc}}\right) - Q C_a \tag{9.12}$$

Like the cases in models M7-A and M7-B, the Hanry's law constant in these equations is incorrect. For example, Equation 9.11 should be replaced by either Equation 9.13.

$$\frac{d(C_L V_L)}{dt} = -A K_{OL}\left(C_L - \frac{C_a}{H_v^{cc}}\right) \tag{9.13}$$

Because the water in the sink is in different states, including falling water from the faucet, underlying water, and splashes, it is difficult to determine the mass transfer coefficients for the individual transfer mechanisms. Therefore, the liquid-phase overall mass transfer coefficient, K_{OL}, in Equation 9.11 is a lumped or average value.

9.3.4. Model M7-D (Yao et al., 2020; Park et al., 2020) [110]

For fine particle emissions from ultrasonic humidifiers, a linear relationship exists between the content of the dissolved solids in water and the concentration of airborne particles (Equation 9.14)

$$C_{ap} = a_1 + b_1\, C_{SL} \tag{9.14}$$

Equation 9.15 is applicable to both the total suspended particles and the size-segregated particles. Some measured values of a_1 and b_1 are given by Yao et al. (2020) [110].

9.3.5. Model M7-E (Yao et al., 2021; Dietrich et al., 2023) [111, 112]

This statistical model is for fine particle formation due to the use of ultrasonic humidifiers with a focus on metals in airborne particles. The general form for the metal concentration in room air is given by Equation 9.15.

$$C_{am} = \frac{C_{Lm}}{C_{L,TDS}} \left(a_2\, C_{L,TDS} + b_2\right) \tag{9.15}$$

This model is difficult to use by others because coefficients a_2 and b_2 in Equation 9.15 are empirical coefficients dependent on water quality, room size, and air exchange rate. This model will be more useful if the test results are expressed as emission rates (Equation 9.16), which are dependent on the quality of the fill water but independent of room size and air exchange rate. Dietrich et al. (2023) presented three sets of coefficients a_2 and b_2 for different chamber sizes and ventilation rates. It is possible to combine the coefficients into a single set of coefficients (a_3 and b_3) by using Equation 9.16. The results would be much easier to use by others.

$$R_m \approx N\, V\, C_{am} = N\, V \frac{C_{Lm}}{C_{L,TDS}} \left(a_3\, C_{L,TDS} + b_3\right) \tag{9.16}$$

9.3.6. Model M7-F (Zontek et al., 2019) [103]

This model is for fine particle emissions from 3D printers. Equation 9.17 estimates the particle concentration at time *t* and a distance *r* from the printer.

$$C_r = \frac{G}{2\,\pi\, D_E\, r}\, erfc\left(\frac{r}{\sqrt{4\, D_E\, t}}\right) \tag{9.17}$$

where the continuous particle emission rate *G* is experimentally determined or from Equation 9.19 below; *erfc* is the complementary error function; and the eddy diffusivity D_E is estimated from Equation 9.18.

$$D_E = \frac{L_c^2\,(0.6\,N + 0.25)}{60} \tag{9.18}$$

The authors identified six factors that affect the particle emission rate: filament extrusion rate, eddy diffusivity, print time, distance from source, printer position, and extrusion temperature, among which the filament extrusion rate and eddy diffusivity are most important. Equation 9.19 links the particle generation rate to extrusion temperature. If the filament consumption rate is known, the particle generation rate *G* in Equation 9.17 can be calculated from the specific particle emission rate E_x. Note that Equation 9.19 is for a specific filament (1.75-mm diameter acrylonitrile butadiene styrene [ABS] filament). Its coefficients may not be applicable to other cases.

$$E_x = 0.3733\; e^{0.016\,T} \tag{9.19}$$

Existing standard test methods for 3D printers — ANSI/CAN/UL 2904 and ISO/DIS 27548 — contain several data analysis models. They are excluded from this report for the reason described in Section 9.4.3 below.

9.4. Additional comments

9.4.1. Fine and ultrafine particle emissions from laser printers

Laser printers are known to emit fine/ultrafine particles and VPCs. A study by Morawska et al. (2019) found reduced particle emissions for large commercial printers as compared to the emission levels before 2007. However, a similar emission reduction is not obvious for desktop printers. Predictive models are not available.

9.4.2. Air cleaning devices

Another class of indoor appliances that is worth mentioning is air cleaning devices. Many types of air cleaning devices are available on the market. They are designed to remove pollutants from the air based on many different technologies. It has been a topic of research for several decades to evaluate their cleaning efficiency, potential generation of unwanted byproducts, and potential contaminant re-emission over time. These are influenced by the technology type and physical form of pollutant (particulate, vapor, biological, etc.). The long-term effectiveness of air cleaning technologies is also an area of ongoing research. In general, there is a lack of models for this class of indoor appliances.

9.4.3. Exclusion of data analysis models

Many data analysis models are available for converting the chamber test results (typically concentrations in environmental media) to emission or transfer rates, such as those described in ASTM Standard Guide D5116.[113] Most papers and reports on product emission testing include similar equations. This report ignores them because they are not genuine source models. A key difference

between a predictive model and a data analysis model is whether the air concentration appears on the left or right-hand side of equation. In data analysis models, air concentration appears on the right-hand side of equation. In other words, air concentration is the output of the predictive model whereas it is an input for data analysis models.

9.5. Summary

Mass transfer models are available for volatile chemical emissions from water-use appliances, such as washing machines, dishwashers, and kitchen sinks. Some of the uncertainties in the input parameters include estimation of the average overall mass transfer coefficient and the area of the water-air interface. Existing models ignore the effects of surfactants on Henry's law constants. This is an area that needs more research. See Section 5.4.1 for more details.

There is a dearth of predictive models for other home appliances. Although sizable emissions data have accumulated, researchers have been unable to translate the laboratory observations into useful predictive models. This is partially because of the great variability of products even within the same type of appliance.

10. Mass transfer from solid articles/building materials to suspended and settled particulate matter

10.1. Symbols and abbreviations

A = area of SVOC source (m^2),
A_d = total surface area of settled dust (m^2),
A_{d_dep} = area of deposition of dust on floors (m^2),
A_p = total surface area of suspended particles (m^2),
A_s = total area of indoor surfaces (m^2),
A_{s_dep} = area of deposition of dust on non-floor surfaces (m^2),
A_{s_sus} = area of non-floor surfaces where deposited particles may resuspend (m^2),
C_a = SVOC concentration in air (gas phase) ($\mu g/m^3$),
C_{a_in} = SVOC concentration in air (gas phase) in inlet air ($\mu g/m^3$),
C_d = SVOC concentration in settled dust ($\mu g/m^3$ dust),
C_{d_in} = SVOC concentration in settled dust in inlet air ($\mu g/m^3$ dust),
C_m = SVOC concentration in the source ($\mu g/m^3$),
C_p = SVOC concentration in suspended particles ($\mu g/m^3$ air),
$C_{p,in}$ = SVOC concentration in suspended particles in inlet air ($\mu g/m^3$ air),
C_s = SVOC concentration in the organic films over interior surfaces ($\mu g/m^3$),
C_{TSP} = concentration of total suspended particles ($\mu g/m^3$),
D_a = gas-phase diffusion coefficient (m^2/s or m^2/h),
D_d = diffusion coefficient in dust phase (m^2/s),
D_g = diffusion coefficient in gas phase (m^2/s),
d_p = density of the particles ($\mu g/m^3$),
h_a = gas-phase mass transfer coefficient (m/h),
h_d = gas-phase mass transfer coefficient at the surfaces of dust particles (m/s),
h_p = gas-phase mass transfer coefficient for SVOC transfer from air to suspended particles (m/h),
h_s = gas-phase mass transfer coefficient for SVOC transfer from air to indoor surfaces (m/h),
k_d = dust removal rate constant (h^{-1}),
k_{1a_x} = reaction rate constant in the gas phase (h^{-1}),
k_{1a_x} = reaction rate constant in the settled particle (dust) phase (h^{-1}),
k_{1a_p} = reaction rate constant in the suspended particle phase (h^{-1}),
K_{da} = dust-air partition coefficient (dimensionless),
K_{ma} = solid material-air partition coefficient (dimensionless),
K_{oa} = octanol-air partition coefficient (dimensionless),
K_{pa} = particle-air partition coefficient (dimensionless),
K'_{pa} = particle-air partition coefficient ($m^3/\mu g$),
K_{sa} = partition coefficient between the organic film over indoor surfaces and air (dimensionless),
L = air boundary layer thickness (m),
L_a = height of the air layer above the dust (m),
Q = ventilation flow rate (m^3/h),

q_{d_in} = flow rate of dust entering the room (m^3/h),
q_d = flow rate of dust leaving the room (m^3/h),
R_{ad} = rate of mass transfer rate from air (gas phase) to settled dust (µg/h),
R_{ap} = rate of mass transfer rate from air (gas phase) to suspended particles (µg/h),
R_{as} = rate of mass transfer rate from air (gas phase) to interior surface films (µg/h),
R_{del} = removal rate for dust bound SVOC (µg/h/m^3 dust),
R_{dep} = rate of deposition of suspended particles (µg/h),
R_{d_io} = rate of mass change due to indoor-outdoor exchange (ventilation) (µg/h),
R_{ds} = rate of resuspension of settled (dust) particles (µg/h),
R_{ma} = rate of mass transfer rate from source material to indoor air (gas phase) (µg/h),
R_{sus} = rate of resuspension of deposited particles (h^{-1}),
R_{xa} = rate of removal due to homogeneous (gas phase) reactions (µg/h),
R_{xd} = rate of removal due to heterogeneous reactions with settled particles (dust) (µg/h),
R_{xp} = rate of removal due to heterogeneous reactions with suspended particles (µg/h),
t = time (h),
V = room volume (m^3),
V_d = total volume of settled dust (m^3),
V_{d_sus} = volume of settled dust that can be resuspended (m^3),
V_p = total volume of suspended particles (m^3),
V_s = total volume of organic films over interior surfaces (m^3),
X_d = average SVOC concentration in settled dust (µg/g dust),
X_p = SVOC concentration in suspended particles (µg/m^3 particles),
y_0 = gas-phase concentration at solid-air interface (µg/m^3),
y_a = average SVOC concentration in air above the source that the settled dust is exposed to (µg/m^3),
δ = thickness of the material (m),
δ_d = median diameter of dust particles (m),
δ_s = thickness of organic film on indoor surfaces (m),
θ = porosity of settled dust layer (fraction),
ρ = density of suspended particles or settled dust (µg/m^3),
υ_{dep} = deposition velocity (µg/hr).

Abbreviations

DEHP: di-(2-ethylhexyl)-phthalate,
ODE: ordinary differential equation,
PDE: partial differential equation,
PM: particulate matter,
QSAR: quantitative structure-activity relationship,
RIVM: Dutch National Institute for Public Health and the Environment,
SVOC: semi-volatile organic compound,
TVOC: total volatile organic compound.

10.2. Overview

10.2.1. Transfer Mechanisms

Chemical substances, especially semi-volatile organic compounds (SVOCs), can be transferred from solid consumer products and articles to suspended and settled particulate matter (PM) through different mechanisms:

- Air-mediated transfer. SVOCs in the source are emitted to indoor air (see Sections 3 and 4) and then interact with suspended and settled PM.
- Mass transfer from source to settled PM by direct contact.
- PM generated by abrasion of solid products becomes part of suspended or settled particulate matter.

10.2.2. Validity of the instantaneous equilibrium assumption for airborne particles

In modeling transfer from vapor-phase SVOCs to airborne particles, it is often assumed that there is an instantaneous equilibrium between the two phases.[20, 114, 115] While valid in many cases, this assumption tends to overestimate the particle-phase concentration if (1) the particle diameter is large; (2) the SVOC is less volatile, and (3) the particle-phase diffusion coefficient is small.[14, 116] Liu et al. (2013) estimated that, for the flame retardant di-(2-ethylhexyl)-phthalate (DEHP), which has a vapor pressure of 3.4×10^{-5} Pa at 20°C, the instantaneous equilibrium assumption could cause a factor-of-two error in the predicted particle-phase concentration and even greater error in the predicted gas-phase concentration.[116]

10.2.3. Definitions of particle-air partition coefficient for suspended particles

The particle-air partition coefficient determines the distribution of an SVOC between air and suspended particles at equilibrium. It has two definitions. One is dimensionless (Equation 10.1) and the other has units (Equation 10.2).

$$K_{pa} = \frac{C_p}{C_a} \tag{10.1}$$

$$K'_{pa} = \frac{C_p}{C_a\, C_{TSP}} \tag{10.2}$$

where

C_a is the SVOC concentration in the gas-phase (µg SVOC/m^3 air),
C_p is the chemical concentration in the particle phase (µg SVOC/m^3 particles),
C_{TSP} is the concentration of suspended particles (µg particles/m^3 air).
K_{pa} is the dimensionless particle-air partition coefficient,
K'_{pa} bears the unit of (m^3/µg particles),

Note that K'_{pa} can be converted to the dimensionless partition coefficient, K_{pa}, *w*ith equation. 10.3,

$$K_{pa} = K'_{pa}\, d_p \tag{10.3}$$

where d_p is the density of the particles (μg/m^3).

10.2.4. Models discussed

Five models are discussed in this section as shown in TABLE 10.1.

TABLE 10.1 List of models discussed in this section.

Model	Transfer Mechanisms Modeled	Model Form [A]
M8-A	Multi-media model for air-mediated transfer	ODEs
M8-B	Multi-media model for air-mediated transfer	ODEs
M8-C	Transfer from source to dust by direct contact	PDE
M8-D	Transfer from source to dust by direct contact	Exact solution
M8-E	Transfer from source to dust by direct contact	Exact solution

[A] ODEs = system of ordinary differential equations; PDE = partial differential equation.

10.3. Model description

10.3.1. Model M8-A (RIVM, undated) [117]

Developed by the Dutch National Institute for Public Health and the Environment (RIVM), *DustEx* is an on-line simulation tool for total volatile organic compound (TVOC) distribution in indoor media after emission from an indoor source. The mass transfer mechanisms considered by *DustEx* are summarized in TABLE 10.2.

TABLE 10.2 Transfer mechanisms and rate expressions incorporated in *DustEx* model.

Transfer Mechanism	Rate Expression
From source material to indoor air (gas phase)	$R_{ma} = A\, h_a \left(\frac{C_m}{K_{ma}} - C_a\right)$
From indoor air to suspended particles	$R_{ap} = A_p\, h_p \left(C_a - \frac{C_p}{K_{pa}}\right)$
From indoor air to settled dust	$R_{ad} = A_d\, h_a \left(C_a - \frac{C_d}{K_{da}}\right)$
From indoor air to interior surfaces (organic films) [A]	$R_{as} = \frac{h_a}{\delta_s}\left(C_a - \frac{C_s}{K_{Oa}}\right)$
Removal of indoor settled dust [B]	$R_{del} = k_d\, C_d$

[A] In this model, SVOC sorption by interior surfaces is represented by thin films of organic materials that cover the interior surfaces. The films have a thickness of δ_s and total volume of V_s.

[B] The activities for dust removal include vacuum cleaning and track-out. Replacement of clean dust keeps the dust loading constant.

The model consists of five ordinary differential equations. Equation 10.4 is for mass balance for SVOC concentration in the gas phase (C_a)

$$V\, \frac{dC_a}{dt} = R_{ma} - R_{ad} - R_{as} - R_{ap} - Q\, C_a \tag{10.4}$$

Equation 10.5 is for mass balance for SVOC concentration in suspended particles (C_p) in (µg/m^3 particles)

$$V_p \frac{dX_p}{dt} = R_{ap} \tag{10.5}$$

The online document gave the wrong equation for converting the particle-phase concentration C_p in (µg/m^3 particles) to the particle-phase concentration C_{p_a} in (µg/m^3 air). Equation 10.6 may have been the equation that the developer intended to use.

$$C_p = \frac{X_p \, C_{TSP}}{\rho_p} \tag{10.6}$$

Equation 10.7 is for mass balance for SVOC concentration in settled dust (C_d)

$$V_d \frac{dC_d}{dt} = R_{ad} - Q \, C_{del} \tag{10.7}$$

Equation 10.8 is for mass balance for SVOC concentration in surface films (C_s)

$$V_s \frac{dC_s}{dt} = R_{as} \tag{10.8}$$

This modeling tool lacks a complete technical document. The model requires many input parameters, but little discussion is provided on parameter estimation in the online document. Comparison of this model with a similar model (M8-B) is provided in Section 10.4.1.

The wrong equation (Equation 10 in the online document) was given for converting the chemical concentration in suspended particles from (µg SVOC per m^3 particles) to (µg SVOC per m^3 air).

It appears that the loss of suspended particles due to ventilation is missing from the mass balance equation (Equation 10.5 above and Equation 9 in the online document).

This model does not consider SVOC transfer from source to settled dust through direct contact.

10.3.2. Model M8-B (Wei et al., 2019) [118]

This model is similar to model M8-A but includes more transfer mechanisms, as summarized in TABLE 10.3.

TABLE 10.3 Transfer mechanisms and rate expressions incorporated in model M8-B.

Transfer Mechanism	Rate Expression
Mass transfer from source material to indoor air (gas phase) summed over *i* sources	$R_{ma} = \sum_i A_i\, h_{a\_i} \left(\frac{C_{m\_i}}{K_{ma\_i}} - C_a \right)$
Mass transfer from indoor air to suspended particles	$R_{ap} = A_p\, h_p \left(C_a - \frac{C_p}{K'_{pa}\, C_{TSP}} \right)$
Mass transfer from indoor air to settled dust	$R_{ad} = A_d\, h_d \left(C_a - \frac{C_d}{K_{da}} \right)$
Mass transfer from indoor air to interior surfaces summed over *j* interior surfaces	$R_{as} = \sum_j A_{s\_j}\, h_{s\_j} \left(C_a - \frac{C_{s\_j}}{K_{sa\_j}} \right)$
Removal due to gas-phase reactions of SVOCs summed over multiple oxidants (e.g., hydroxyl radicals, ozone)	$R_{xa} = V \sum_x k_{1a\_x}\, C_a$
Removal due to heterogeneous reactions of SVOCs in suspended particles summed over multiple oxidants (e.g., hydroxyl radicals, ozone)	$R_{xp} = V \sum_x k_{1p\_x}\, C_p$
Removal due to heterogeneous reactions of SVOC in settled dust summed over multiple oxidants (e.g., hydroxyl radicals, ozone)	$R_{xd} = C_d\, \rho_d\, V_d \sum_x k_{1d\_x}$
Deposition of suspended particles onto interior surfaces summed over *j* interior surfaces	$R_{dep} = C_p\, v_{dep} \left(A_{d\_dep} + \sum_j A_{s\_dep\_j} \right)$
Resuspension of settled dust from interior surfaces summed over *j* interior surfaces	$R_{ds} = R_{sus} \left(C_d\, \rho_d\, V_{d\_sus} + \sum_j C_{d\_j}\, A_{s\_sus\_j} \right)$
Gain of settled dust due to indoor-outdoor exchange [A]	$R_{d\_io} = q_{d\_in}\ \rho_{d\_in}\, C_{d\_in} - q_d\ \rho_d\, C_d$

[A] The validity of this expression is questionable because dust track-in and track-out have little to do with air flow. Besides, density ρ_{d_in} is not needed because this model treats settled dust as a whole with a density of ρ_d.

The model consists of three ordinary differential equations for, respectively, gas-phase concentration in indoor air, C_a (Equation 10.9), particle phase concentration in indoor air, C_p (Equation 10.10), and concentrations in settled dust, C_d (Equation 10.11).

$$V \frac{dC_a}{dt} = R_{ma} - R_{ap} - R_{ad} - R_{as} + Q\left(C_{a_{in}} - C_a\right) - R_{xa} \tag{10.9}$$

$$V \frac{dC_p}{dt} = R_{ap} - R_{dep} + R_{ds} + Q\left(C_{p_{in}} - C_p\right) - R_{xp} \tag{10.10}$$

$$V_d\, \rho_d \frac{dC_d}{dt} = R_{ad} + R_{dep} - R_{ds} - R_{xd} + R_{d\_io} \tag{10.11}$$

At least one equation is missing, which is for adsorption by interior surfaces. Without it, the transfer rate from indoor air to interior surfaces, R_{as}, cannot be calculated because $C_{s\text{-}j}$ is unknown. One additional equation is needed from each of the interior surface types. In addition, parameters A_{d_dep} and V_{d_sus} are

undefined. It is unclear whether the particles settled on interior surfaces other than the floor are tracked. If the deposition is irreversible, no additional equation is needed.

10.3.3. Model M8-C (Bi et al., 2021) [119]

This is a model for predicting the SVOC concentrations in settled dust in direct contact with the source. A graphic illustration of the modeling concept is shown in Figure 10.1.

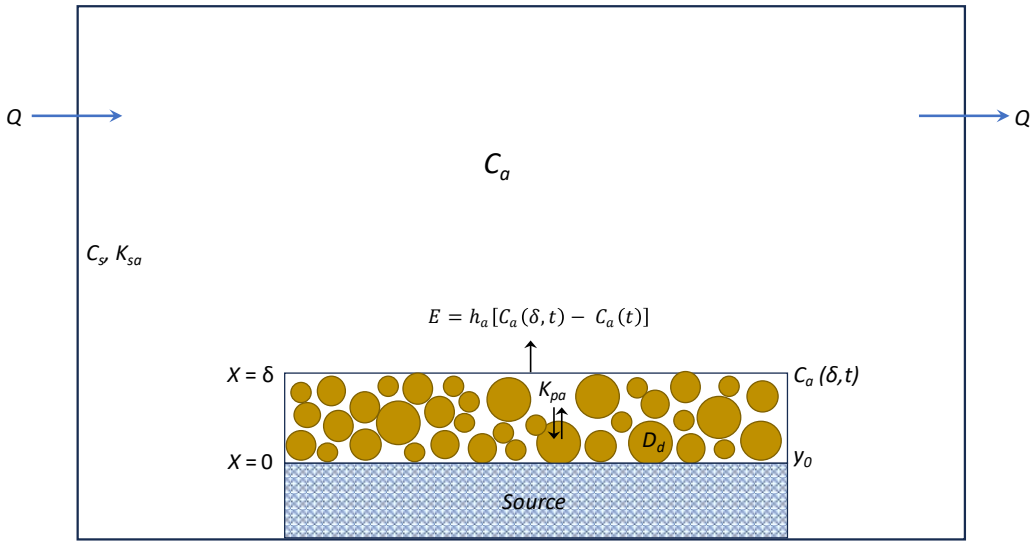

Figure 10.1 Illustration of mechanisms for direct source-to-dust transfer.

In this model, the SVOC emissions from the source are represented by y_0 (see model M2-A). It is assumed that, when the gas-phase molecules migrate through the dust layer, the major transfer mechanism is gas-phase diffusion through the voids. The governing equation for the diffusion and sorption in the dust layer is determined by Equation 10.12.

$$\theta \frac{\partial C_a(x,t)}{\partial t} + (1-\theta)\frac{\partial C_d(x,t)}{\partial t} = D_g \frac{\partial^2 C_a(x,t)}{\partial x^2} \tag{10.12}$$

It is further assumed that the internal diffusion inside the dust particles is relatively fast. Thus, Equation 10.13 holds.

$$C_d(x,t) = K_{da} C_a(x,t) \tag{10.13}$$

Then, the governing equation becomes Equation 10.14.

$$\frac{\partial C_a(x,t)}{\partial t} = D_{eff} \frac{\partial^2 C_a(x,t)}{\partial x^2} \tag{10.14}$$

Where D_{eff} is the effective gas-phase diffusion coefficient defined by Equation 10.15.

$$D_{eff} = \frac{D_g}{\theta + (1-\theta)\, K_{da}} \tag{10.15}$$

The boundary conditions for Equation 10.14 are given by Equation 10.16 (at $x = 0$) and Equation 10.17 (at $x = \delta$).

$$C_a(0,t) = y_0 \tag{10.16}$$

$$-D_e \frac{\partial C_a(x,t)}{\partial x} = h_a[C_a(\delta,t) - C_a(t)] \tag{10.17}$$

The initial condition for the gas and dust-phase SVOC concentrations in the dust layer are given by Equation 10.18.

$$C_a(0,t) = \frac{C_d}{K_{da}} \tag{10.18}$$

Equation 10.14 is solved numerically for $C_a(x,t)$, from which the dust-phase concentrations $C_d(x,t)$ can be calculated from Equation 10.13. The average SVOC concentration in the dust at any time t, $X_d(t)$, is calculated by dividing the average $C_d(x,t)$ between $x = 0$ and $x = \delta$ by the density of the dust:

$$X_d(t) = {}^{C_d}/_{\rho_d}$$

This model presents a useful tool for evaluating the mass transfer from the source to settled dust. The need to solve a partial differential equation may limit its use in routine exposure assessment.

As discussed in Section 10.4.2 below, the assumption that the internal diffusion inside the dust particles is relatively fast is not always valid. Additionally, the porosity and height of the dust layer appear challenging to determine.

A similar partial differential equation model was proposed by Kang et al. (2021) [120]

10.3.4. Model M8-D (Wang et al., 2022) [121]

This model predicts the SVOC concentration in settled dust due to direct contact with the source surfaces. The model treats the dust layer as a layer of porous solid material. Thus, the dust-laden source is equivalent to a two-layer solid material and Ficks' second law applies.

The average SVOC concentration in the settled dust is calculated from Equation 10.19.

$$X_d = \frac{2\, y_0\, K_{da}}{\rho_d} \sum_{n=1}^{\infty} \frac{F_n\,(1-\cos q_n)}{q_n^2\, G_n} \left[1 - exp\left(-\frac{D_d\, q_n^2\, t}{\delta_p}\right)\right] \tag{10.19}$$

where

$$F_n = Bi_m\, A_n \frac{\cos q_n}{K_{da}} - [A_n + \beta\, Bi_m(1 - B_s\, q_n^2)\,]\, q_n \sin q_n$$

$$G_n = \left[3\, A_n + 2B_s\, q_n^4 - 2\alpha + \beta\, Bi_m(1 - B_s\, q_n^2) + \frac{Bi_m}{K_{da} A_n}\right] \cos q_n - \left[A_n + \beta\, Bi_m(1 - B_s\, q_n^2) + \left(\frac{(2 + 2\alpha B_s + 2\xi - 4B_s\, q_n^2)}{K_{da}}\right) Bi_m\right]\, q_n \sin q_n$$

where

$$A_n = B_s\, q_n^4 - (1 + \alpha\, B_s + \xi\, q_n^2) + \alpha$$

$$Bi_m = \frac{h_a\, \delta}{D_d}$$

$$\alpha = \frac{Q\, \delta^2}{D_d\, V}$$

$$\beta = \frac{\delta\, A}{V}$$

$$\xi = \frac{A_s\, K_{sa}}{V}$$

$$B_s = \frac{K_{sa}\, D_d}{\delta^2\, h_s}$$

q_n is obtained by solving non-linear Equation 10.20.

$$q_n \cot q_n = -\frac{A_n\, Bi_m}{[A_n + \beta\, Bi_m\, (1 - B_s\, q_n^2)]\, K_{da}} \tag{10.20}$$

Although this model still requires basic numeric computation skills, it is much easier to use than the partial differential equation (PDE) models, which requires proprietary software to run.

Further clarification is needed regarding the validity of this model. Because the model treats the dust layer as a porous material, the effective diffusion coefficient, D_{eff}, should be used. However, the equations contain only the dust-air partition coefficient (K_{da}) and the dust-phase diffusion coefficient (D_d), which are for the solid dust particles, not for the porous dust layer.

10.3.5. Model M8-E (Cao et al., 2023) [122]

Cao et al. (2023) developed a model suitable for small dust loading (e.g., monolayer dust) that is close to realistic conditions in typical homes. It is well understood from experimental observations that dust loading affects the SVOC transfer rate due to direct contact.

The SVOC concentration in the dust phase, X_{dust}, in (µg/g dust) is given by Equation 10.21.

$$X_{dust}(t) = \frac{K_{da}\, y_0}{\rho_d}\left[1 - 2\sum_{n=1}^{\infty}\left(\frac{1-\cos p_n}{p_n^2 - p_n \cos p_n \sin p_n}\right)\exp\left(-\frac{D_d\, p_n^2\, t}{\delta_d^2}\right)\right] \tag{10.21}$$

where p_n (n = 1, 2, 3…) are the smallest positive roots of non-linear Equation 10.22.

$$p_n \cot p_n = \frac{D_g\, \delta_d}{K_{da}\, D_d\, L_a} \tag{10.22}$$

The authors also proposed a simplified model, Equation 10.23, by using only the first root of Equation 10.22, p_1. It works so long as the contact time is sufficiently long.

$$X_{dust}(t) = \frac{K_{da}\, y_0}{\rho_d}\left[1 - \frac{2\,(1-\cos p_1)}{p_1^2 - p_1\, \cos p_1\, sin\, p_1}\exp\left(-\frac{D_d\, p_n^2\, t}{\delta_d^2}\right)\right] \tag{10.23}$$

This model contains a parameter (L_a) for the height of the air layer above the dust. It is unclear whether L_a is the air boundary layer or a parameter specific to the chamber conditions that the authors used (i.e., a static chamber with sorbent located on the ceiling of the chamber). Clarification is needed about how to apply this model to realistic indoor environments.

Another issue that needs clarification is parameter δ_d, which is defined as the median diameter of monolayer dust particles. The authors did not elaborate on the type of size distribution the median diameter corresponds to; it could be the number, area, or volume (weight) distribution. The median diameters of these distributions differ significantly. For example, for the same number of 1 µm and 10 µm particles, the number ratio is 1:1 but the volume (weight) ratio is 1:1000. The number distribution gives more weight to small particles while the volume distribution gives more weight to large particles. Therefore, when using the median or mean diameter, the size distribution type must be indicated. It appears that this model should use the median diameter for the volume (weight) distribution.

In the same paper, the authors presented a similar analytical model for air-mediated transfer from source to dust.

10.4. Additional comments

10.4.1. Similarities and differences between models M8-A and M8-B

Models M8-A and M8-B use the same equations for the following mass transfer:

- Emissions from the source into indoor air,
- Transfer from indoor air (gas-phase) to suspended particles,
- Transfer from indoor air (gas-phase) to settled dust.

Other similarities include:

- Both models assume that the dust loading is constant,
- Both models assume that the concentration of suspended particles is constant,
- Neither model considers transfer from the source to settled dust by direct contact,
- Neither model considers particle sizes.

The differences between the two models are summarized in TABLE 10.4.

TABLE 10.4 The differences between models M8-A and M8-B.

Transfer mechanism	Model M8-A	Model M8-B
Emissions from sources	Allowing one source	Allowing multiples sources
Adsorption/absorption by indoor surface (sinks)	Absorption by organic film; allowing one sink	Surface adsorption; allowing multiples sinks
Dust removal	First-order decay	Incorrect equation
SVOC disappearance due to reactions with oxidants	Not included	Included
SVOC content in suspended particles in ambient air	Zero	Allowing non-zero values

10.4.2. The accuracy of the transfer rate from air to dust

Models M8-A and M8-B use the same equation to calculate the rate of mass transfer from air (gas phase) to settled dust (Equation 10.24),

$$R_{ad} = A_d\, h_d \left(C_a - \frac{C_d}{K_{da}} \right) \tag{10.24}$$

Equation 10.24 considers the gas-phase mass transfer resistance only. By ignoring the mass transfer resistance in the dust, Equation 10.24 is expected to overestimate the transfer rate. However, the magnitude of the predictive error or uncertainty of Equation 10.24 has never been evaluated. To estimate the magnitude of this potential error source, Equation 10.24 is compared with a state-space model that considers the mass transfer resistances in both phases.[14] Four cases were considered with different particle-air partition coefficients (K_{pa}) and dust-phase diffusion coefficients (D_p) as shown in TABLE 10.5. Other input parameters were V = 30 m^3, Q = 30 m^3/h, A = 10 m^2, y_0 = 7500 µg/m^3, d_p = 1 g/cm^3, h_p = 1 m/h, and dust diameter = 50 µm.

TABLE 10.5 Dust-air partition coefficients (K_{pa}) and dust-phase diffusion coefficients (D_d) used to compare models M8-A and M8-B with the state-space model.

Case	K_{pa} (dimensionless)	D_d (m^2/h)
1. Small K_{pa} and large D_d	1×10^4	1×10^{-9}
2. Large K_{pa} and large D_d	1×10^7	1×10^{-9}
3. Small K_{pa} and small D_d	1×10^4	1×10^{-12}
4. Large K_{pa} and small D_d	1×10^7	1×10^{-12}

As shown in Figure 10.2, the concentrations in the dust predicted by Equation 10.24 agree well with the state-space model when the dust-phase diffusion coefficient (D_d) is large. When D_d is small, however, Equation 10.24 overestimates the transfer rate significantly.

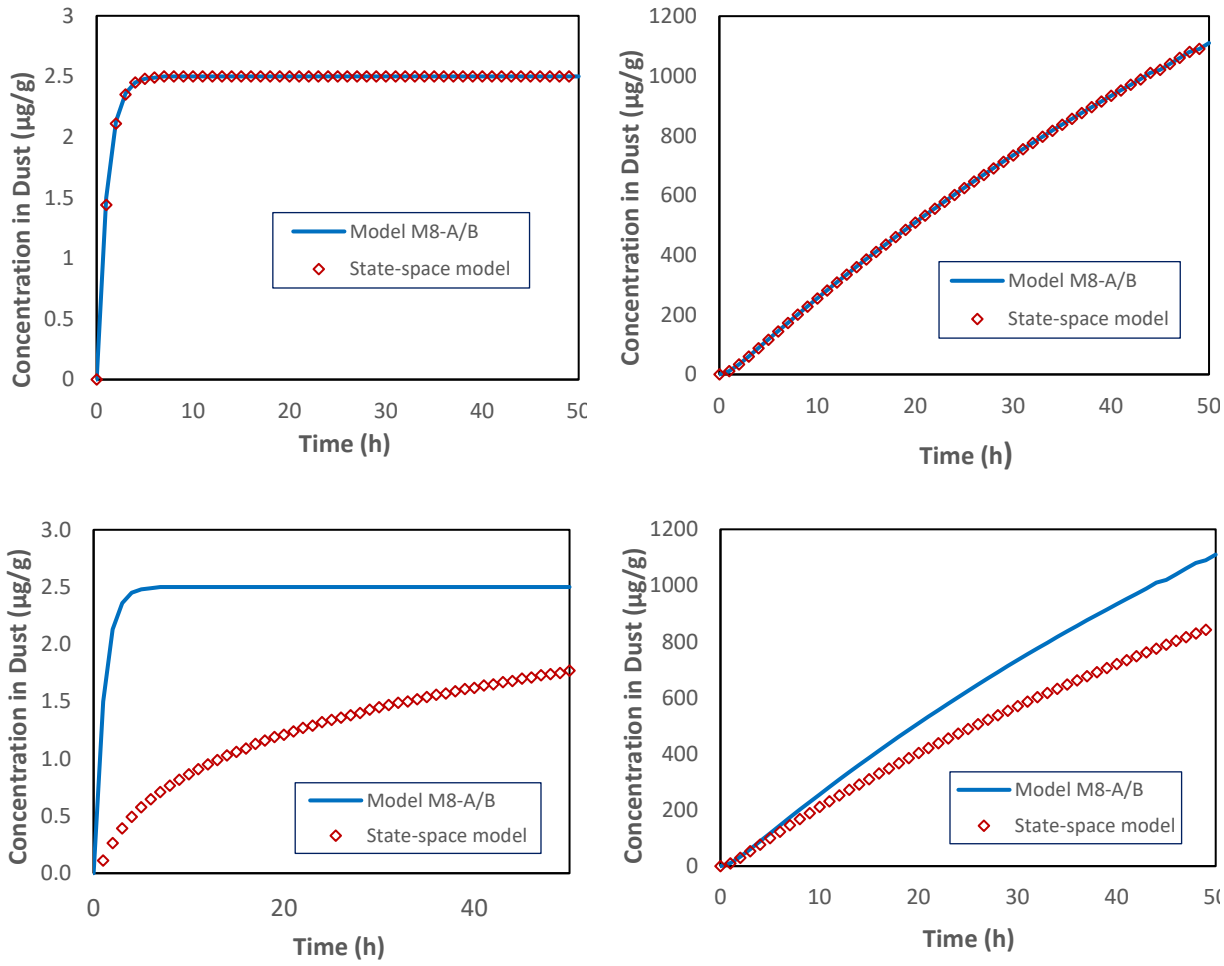

Figure 10.2 Comparison of the air-to-dust transfer model used in models M8-A and M8-B with a state-space model for SVOC interactions with particles.

CASE 1 (top-left): small K_{pa} and large D_d; CASE 2 (top-right): large K_{pa} and large D_d; CASE 3 (bottom-left): small K_{pa} and small D_d; CASE 4: (bottom-right): large K_{pa} and small D_d.

10.4.3. Estimation of the upper bound of the dust-phase concentration due to direct contact with the source

The upper bound of the mass transfer from source to dust by direct contact can be determined using the material-dust partition coefficient (K_{md}), which is defined by Equation 10.25 at equilibrium.

$$K_{mp} = \frac{C_m}{C_p} \tag{10.25}$$

Because $C_m = K_{ma}C_a$ and $C_p = K_{pa}C_a$ at equilibrium, Equation 10.26 becomes:

$$K_{mp} = \frac{K_{ma}\ C_a}{K_{pa}\ C_a} = \frac{K_{ma}}{K_{pa}} \tag{10.26}$$

where K_{ma} and K_{pa} can be either measured or estimated from quantitative structure-activity relationship (QSAR) models.

Then, the upper-bound concentration in dust particles in contact with the source can be determined by Equation 10.27.

$$C_p = \frac{C_m}{K_{pa}} \tag{10.27}$$

where C_m and C_p are both in (µg/m^3 dust).

10.4.4. An approach to developing a simplified model for direct source-to-dust transfer

The existing models for source-to-dust transfer by direct contact require user knowledge of numeric computation and is difficult, if not impossible, to incorporate into existing multi-media models for transfer from a source to suspended and settled dust. An approach to developing a simplified model is described below.

As shown in Figure 10.23, the dust particle sits inside the boundary layer above the source. The gas-phase SVOC concentration at the source-air interface is y_0. The concentration at the top of the boundary layer is C_a. Assuming that the concentration gradient inside the boundary layer is linear, and the diameter of the particle is d_p, the gas-phase concentration at $x = d_p$ (i.e., at the top of the particle) is determined by Equation 10.28.

$$C_x = y_0 - \frac{d_p\ (y_0 - C_a)}{L} \tag{10.28}$$

Then, the average concentration above the source that the dust particle is exposed to, y_d, can be calculated from Equation 10.29.

$$y_d = \frac{y_0 + C_x}{2} = y_0 - \frac{d_p\,(y_0 - C_a)}{2\,L} \tag{10.29}$$

Using the existing model for mass transfer from air to settled dust, the transfer rate can be calculated from Equation 10.30 (also see TABLE 10.2 and 10.3).

$$R_{ad} = A_d\,h_a\left(y_d - \frac{C_d}{K_{da}}\right) \tag{10.30}$$

Equation 10.30 is much simpler than the numeric and exact solution models and can be easily incorporated into existing air-mediated mass transfer models such as models M8-A and M-8B. More work is needed to evaluate the validity and usefulness of this approach.

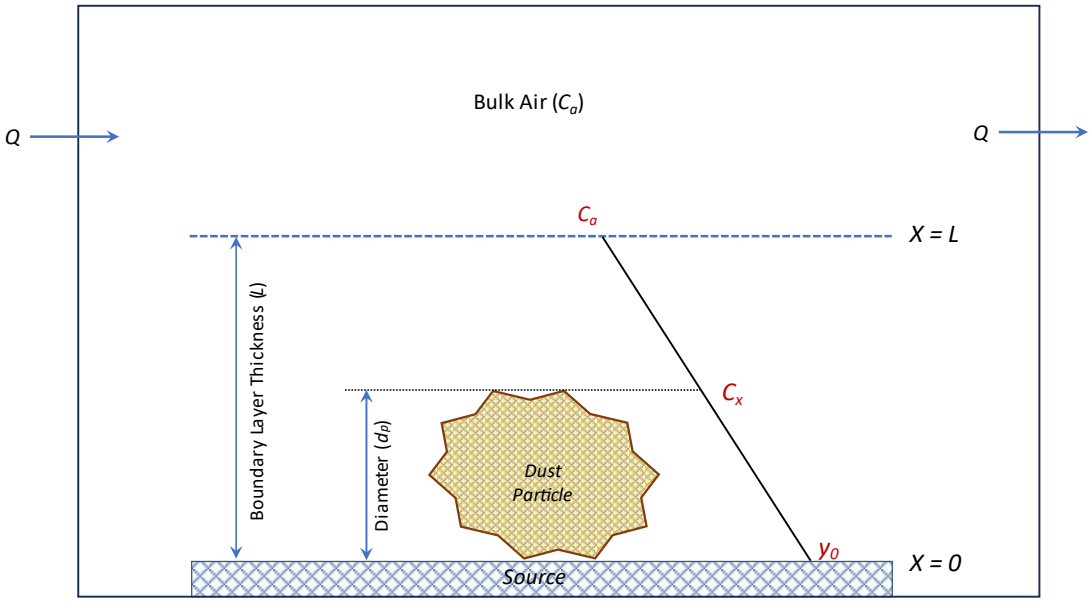

Figure 10.3 Graphical illustration of a simplified model for direct source-to-dust transfer

This approach does require knowledge of the thickness of the boundary layer above the dust (L) which is usually estimated with fluid dynamic models for laminar and turbulent air flows. The simplest model for laminar flow is $L = D_a/h_a$.

10.5. Summary

10.5.1. Air-mediated transfer models

Models M8-A and M8-B are multi-media models for SVOC transfer from the source to indoor air, suspended particles, settled dust, and interior surfaces. Neither model considers mass transfer from source to dust by direct contact.

The existing technical documents lack a few key details and contain errors that prevent them from being readily applied. These models require many input parameters but there is little discussion in the documents on how to estimate them, suggesting the need for additional research.

The equation for mass transfer from air to suspended particles (Equation 10.24) ignores the particle-phase resistance. The predicted transfer rates agree well with a state-space model that considers the transfer resistances in both gas and particle phases when the particle-phase diffusion coefficient (P_d) is large. The equation overestimates the transfer rate when D_d is small. Given the many uncertainties in modeling SVOC transfer from source to suspended and settled particles, this discrepancy should be considered acceptable.

10.5.2. Models for direct source-to-dust transfer

Significant progress has been made recently in developing models for direct source-to-dust transfer. The models are rather complex and inconvenient for routine exposure assessment. M8-C and M8-D require solving partial differential equations, while M8-E requires solving a non-linear equation. They cannot be easily incorporated into existing multi-media. For future research, the development of simplified mass transfer models is needed.

11. Models for leaching from solid consumer products to drinking water

11.1. Symbols and abbreviations

A = area of solid material (pipe) in contact with water (m^2),
C_L = concentration in liquid phase (mg/m^3),
C_{L0} = initial concentration in liquid phase (mg/m^3),
C_m = concentration in solid phase (mg/m^3),
C_{m0} = initial concentration in solid phase (mg/m^3),
C_{p0} = initial concentration of chemical substance in the polymeric pipe (mg/kg),
D_m = solid-phase diffusion coefficient (m^2/s),
h_L = liquid phase mass transfer coefficient (m/s),
K_{mL} = solid-water partition coefficient (dimensionless),
K_{Lm} = water-solid partition coefficient (dimensionless),
$m(t)$ = specific migration rate at time t ($mg/m^2/s$),
$M_{L,t}$ = mass of chemical substance migrated into water (mg),
M_τ = fraction of migrant leached out of the polymer at time τ (fraction),
t = time (s),
V_L = volume of water (m^3),
V_p = volume of the polymeric pipe (m^2/s),
W_τ = amount of migrant leached out of the polymer at dimensionless time τ (mg),
y_0 = liquid-phase concentration at the solid-liquid interface (mg/m^3),
δ = thickness of the polymeric material (m),
ρ_p = density of polymeric pipe (kg/m^3),
τ = time for integration (s),
τ' = dimensionless time.

Abbreviations

As: arsenic,
Ba: barium,
Cr: chromium,
HWT: hot water tank,
Na: sodium,
Mn: manganese,
PP: plumbing pipe,
PVC: polyvinyl chloride,
TOC: total organic carbon,
WDS: water distribution system,
Zn: zinc.

11.2. Overview

Leaching is the migration of a chemical substance, such as an additive or unwanted residual in polymeric materials, from a solid product to a liquid, typically water. Leaching may take place with different types

of consumer products, including indoor plumbing, plastic water bottles, coated cans, garden hoses, rain barrels, and pool products. The mass transfer involves three steps, similar to those for the diffusion models described in Section 3:

- Diffusion in the solid phase,
- Solid-air equilibrium at the solid-liquid interface, and
- Diffusion through the liquid boundary layer adjacent to the interface.

In the case of leaching in water pipes, the mobile phase is water, and the exposed surface of the solid material is the interior surface of the pipe (Figure 11.1).

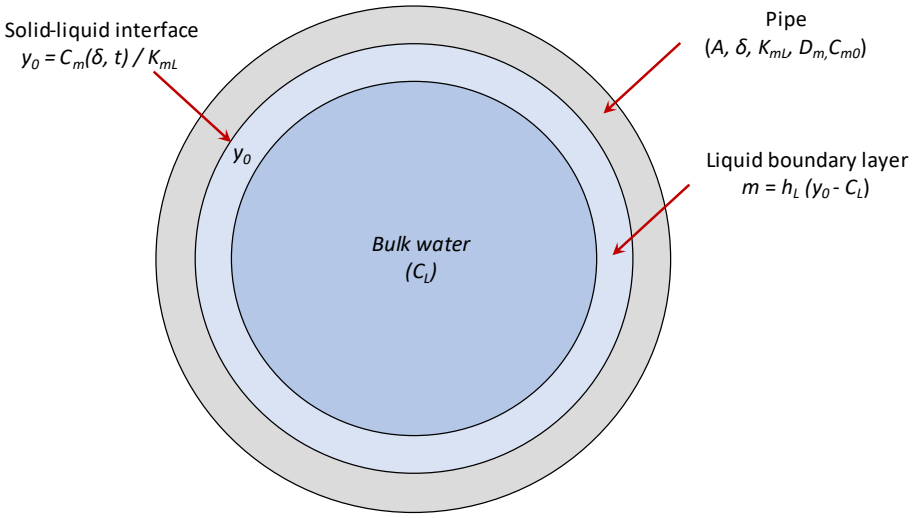

Figure 11.1 Graphic representation of chemical substance leaching from pipes into water.

Four models are discussed in this section. Their features and applicable conditions are shown in TABLE 11.1.

TABLE 11.1 List of mass transfer and empirical models for leaching of additives and residuals from solid products to water.

Model ID	Model Type	Conditions Modeled
M9-A	Exact solution model for leaching of additives from polymers	A fixed volume of water is recirculated and in contact with a pipe
M9-B	Exact solution model for leaching of additives from polymers	A fixed volume of water is recirculated and in contact with a pipe
M9-C	Dimensionless number relationship model for leaching of additives from polymers	A fixed volume of water in contact with a flat polymer surface or pipe
M9-D	Statistical model for leaching of heavy metals	Hot water heaters and household plumbing

11.3. Model description

11.3.1. Model M9-A (Adams et al, 2011) [123]

This model is based on Fick's second law (see Equation 3.1 in Section 3.2.1) and is for migration of additive chemicals from polyvinyl chloride (PVC) pipe into drinking water (Figure 11.1). The specific migration rate in (mg/m^2/s) is given by Equation 11.1.

$$m(t) = D_m \sum_{n=1}^{\infty} \left\{ sin^2(q_n\,\delta)\,\frac{2(q_n^2 + H^2)}{\delta\,(q_n^2 + H^2) + H} \cdot \left[(C_{m0} - K_{mL}\,C_L(0))\,e^{-D_m\,q_n^2\,t} + \int_0^t e^{-D_m\,q_n^2\,(t-\tau)}\,K_{mL}\,dC_L(\tau) \right] \right\} \quad (11.1)$$

where

$$H = \frac{h_L}{K_{mL}\,D_m}$$

q_n (n = 1, 2, 3…) are the positive roots of Equation 11.2.

$$q_n \tan(q_n\,\delta) = H \quad (11.2)$$

If the water is well mixed, the chemical substance concentration in water can be calculated from Equation 11.3.

$$V_L \frac{dC_L}{dt} = A\,m(t) \quad (11.3)$$

This model requires solving a non-linear equation (Equation 11.2) and numeric integration. It applies to conditions when no fresh water enters the system, a fixed volume of water is in contact with the pipe, and the water is well-mixed (i.e., water is recirculating). This condition rarely occurs in the real world, where the water in the pipe is either still or flowing. Therefore, this model is an approximate solution to cases where the water in the pipe is still. It is not suitable for cases where water flows through the pipe.

11.3.2. Model M9-B (Millet et al., 2016) [124]

This model applies to the same conditions as model M9-A, where a fixed volume of water recirculates through the pipe without fresh water coming in. The solution is much simpler than that of model M9-A. The amount of chemical substance migrated into water at time t is given by Equation 11.4. An example of predicted concentration in water as a function of time is shown in Figure 11.2.

$$M_{L,t} = A\, C_{p0}\, \rho_p\, \delta\, \alpha \left[1 - \exp\left(\frac{D_m\, t}{\delta^2\, \alpha^2}\right) \operatorname{erfc}\left(\frac{\sqrt{D_m\, t}}{\delta\, \alpha}\right)\right] \quad (11.4)$$

where $\alpha = \frac{V_L}{K_{mL}\, V_p}$

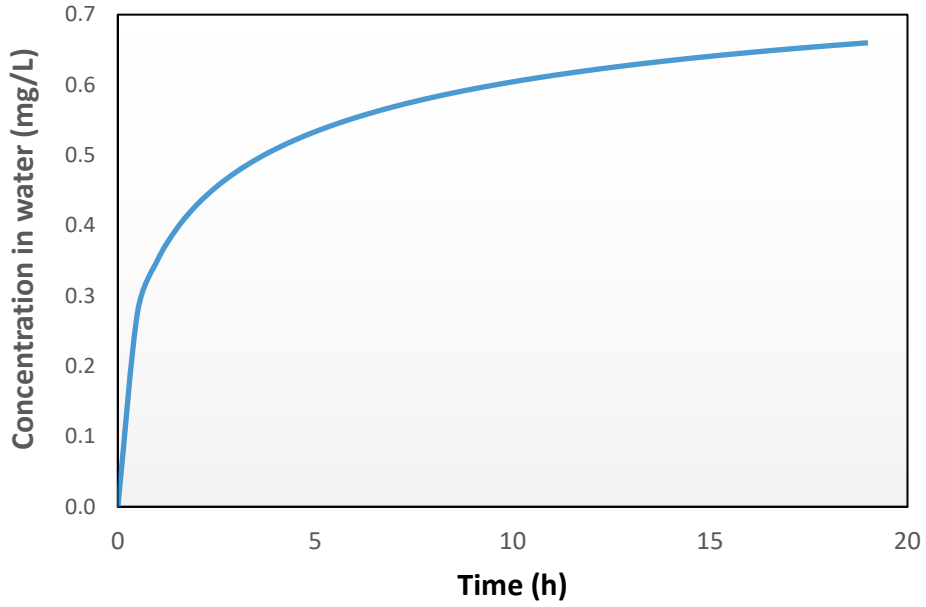

Figure 11.2 Predicted total organic carbon concentration in water as a function of time.

Input parameters were from Ref. [124] except pipe length and density: V_L = 5 L, K_{mL} = 1000, C_{p0} = 5000 mg/kg, D_m = 1 × 10^{-11} cm^2/s, pipe diameter = 15 mm, pipe length = 5 m, pipe thickness = 0.002 m, and pipe density = 1 g/cm^3.

Note that the definition of the solid-water partition coefficient in this model (K_{mL}) is slightly different from that in model M9-A. Although K_{mL} is dimensionless in both cases, the concentration units are different. The units are in mass per volume (e.g., µg/m^3) in model M9-A, as opposed to mass per mass (e.g., mg/kg) in model M9-B.

The experimentally determined solid-phase diffusion coefficient for total organic carbon (TOC) between 30 and 50°C ranged from 2.5 × 10^{-13} to 4.1 × 10^{-12} cm^2/s.

11.3.3. Model M9-C (Schwope and Goydan, 1990) [125]

This is a dimensionless number relationship model for leaching from polymeric materials. It uses three dimensionless numbers: τ', α, and Υ. The fraction of the original additive that is leached out at dimensionless time τ' is given by Equation 11.5.

$$M_\tau = \frac{W_\tau}{\delta\, C_{m0}} = \frac{\alpha}{1 + \alpha} + \sum_{n=1}^{\infty} \frac{\alpha^2}{Q_n}\, e^{-q_n^2\, \tau'} \quad (11.5)$$

where q_n is the positive root of non-linear Equation 11.6.

$$q_n \tan q_n = \frac{\alpha \gamma q_n^2}{\alpha q_n^2 - \gamma} \quad (11.6)$$

where

$$Q_n = \alpha + \frac{\gamma^2 (q_n \sin q_n \ \cos q_n)}{2 q_n (\gamma \cos q_n - q_n \sin q_n)^2}$$

$\tau' = \frac{D_m t}{\delta^2}$ is the dimensionless time.

$\alpha = \frac{K_{Lm} V_L}{A \delta}$ determines how much additive can eventually migrate into the liquid phase after equilibrium is approached between the two phases. If α = 1, 50% of the migrant will be in the liquid phase. If $\alpha >> 1$, the solid-phase concentration will be depleted completely. If $\alpha << 1$, the maximum value of M_τ is equal to α.

$\gamma = \frac{h_L K_{Lm} \delta}{D_m}$ indicates the importance of the liquid-phase resistance across the boundary layer. $\gamma > 100$ means the liquid-phase resistance is negligible.

Note that partition coefficient K_{Lm} is defined as $K_{Lm} = C_L/C_m$ at equilibrium and, thus, is the reciprocal of K_{mL}.

Ref. [125] provides methods for calculating the liquid-phase mass transfer coefficient under different conditions.

11.3.4. Model M9-D (Chowdhury, et al., 2021) [126]

This model consists of a group of statistical models for predicting the heavy metal concentrations in drinking water out of residential plumbing pipes (PPs) and hot water tanks (HWTs). The heavy metal contents may come from the water distribution system (WDS) and leach from PPs and HWTs (Figure 11.3).

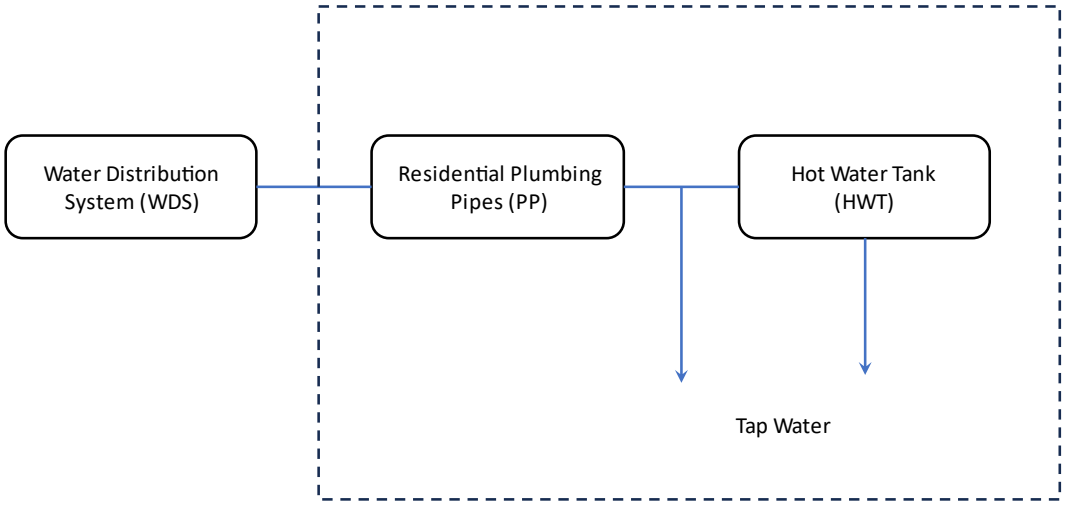

Figure 11.3 Model concept for predicting heavy metal concentrations in water out of residential plumbing pipes and hot water tanks.

The authors collected water samples from WDS, PPs, and HWTs, analyzed the heavy metal contents, and then used statistical tools to determine the heavy metal contents out of PPs and HWTs. Twenty-nine correlations were developed for different heavy metal concentrations. The heavy metal concentrations were associated with other common metal contents such as sodium (Na), zinc (Zn), and manganese (Mn). Two examples are shown below.

Arsenic (As) concentration in plumbing pipes is associated with Na in PPs, Zn in WDS, and Mn in WDS (Equation 11.7):

$$[As_{pp}] = 0.09 + 5.71 \times 10^{-6} [Na_{pp}] + 0.02 [Zn_{WDS}] - 0.12 [Mn_{WDS}] \quad (R^2 = 0.98) \quad (11.7)$$

As concentration in HWTs is associated with Na in HWTs, barium (Ba) in HWTs, and chromium (Cr) in HWTs (Equation 11.8):

$$[As_{HWT}] = -0.30 + 5.34 \times 10^{-6} [Na_{HWT}] + 0.0001 [Ba_{HWT}] + 0.44 [Cr_{HWT}] \quad (R^2 = 0.89) \quad (11.8)$$

Because the data used to develop the correlations were collected from a residential area in Saudi Arabia, the coefficients in the statistical models may not be applicable to other countries and regions. However, the method can be useful.

11.4. Summary

Exposure due to leaching of chemical substances from solid consumer products to drinking water has been an area of active research in recent years. The transfer mechanisms are similar to those for emissions from building materials, as described in Section 3.1. Models M9-A and M9-B were developed for recirculating water. They can be used to approximate the use conditions in homes, where water in

plumbing pipes is still when there is no water flow. Model M9-C is applicable to either flat polymer surfaces or pipes. The contact time is an important factor to consider when using these models. The three key parameters for using models M9-A, B, and C are the initial concentration of the additive compound in the pipe (C_{m0}), partition coefficient (K_{mL} or K_{Lm}), and solid-phase diffusion coefficient (D_m).

12. Models for non-dietary ingestion exposure to consumer products

12.1. Symbols and abbreviations

$A_{contact}$ = mouthing contact area (cm^2),
ADD = average daily potential dose (mg/kg/day),
AT = Averaging time (days),
C_{media} = contaminant concentration in the media (food, liquids, soil, or dust) (mg/g solid or mg/L liquid),
C_{pack} = concentration of chemical substance in food packaging material (kg/m^3),
$C_{residue}$ = concentration of contaminant on the surface of hands or objects that are mouthed (mg/cm^2),
CR = contact rate with contaminated surface (cm^2/event),
D_{app} = applied dose for oral exposure (µg/event),
D_{ext} = external dose for oral exposure (kg chemical substance/kg body weight),
D_i = potential ingestion dose for individual exposure events (mg/kg body weight),
D_{int} = internal dose for oral exposure (kg chemical substance),
D_{ptn} = potential dose for oral exposure for a single event (µg/event),
ED = exposure duration (years),
EF = exposure frequency (days/year),
ET = Exposure time (hours/day),
EV = Event frequency (events/hour),
f_{abs} = fraction of ingested chemical residue available for absorption by the gastrointestinal tract,
f_b = fraction of chemical substance absorbed from the intestinal lumen into blood (fraction),
F_{ho} = proportion of the hand or object involved in contact (fraction),
f_m = frequency of object-to-mouth contact during a mouthing event (events/hr)
F_{OF} = object-to-surface concentration ratio (dimensionless),
$IngR$ = ingestion rate (g/day for solids and L/day for liquids),
L_d = loading of substance on hand or object (mg/cm^2),
L_{obj} = loading of chemical substance on object surface ($\mu g/m^2$),
L_w = loading of substance on hand or object (mg),
m_0 = initial chemical mass in the product (µg),
M_{bf} = mass migrated into biological fluids (e.g., saliva, stomach acid, intestinal fluid) during experiment (kg),
N = number of hand or object-to-mouth contacts,
R_m = specific migration rate of chemical substance from product to saliva ($kg/m^2/s$),
R_{mgr} = mouth-to-saliva migration rate (µg/10 cm^2/min)),
$R_{i,p}$ = rate of product ingestion (kg/s),
S = surface area of the product that is mouthed (m^2),
S_A = surface area of hand or object that is in contact with the mouth (cm^2),
S_{pack} = contact area between food and packaging material (m^2),
t = duration over which the product is ingested or in contact with mouth (s or min),
t_e = duration of the mouthing event (h),
TE_{HM} = transfer efficiency of substance from hands to mouth (fraction),
TE_{OM} = transfer efficiency of substance from object surface to mouth (fraction),

TE_{hp} = transfer efficiency from hand or object to the perioral area (fraction),
TE_{po} = transfer efficiency from the perioral area to the oral cavity (fraction);
w_f = weight fraction of the chemical substance in the products,
W_{body} = body weight of the exposed person (kg),
W_{cons} = amount of food consumed (kg),
W_{food} = amount of food packed in the packaging material (kg),
$W_{i,p}$ = amount of product swallowed (kg),
$W_{i,pe}$ = amount of product tested in swallowing experiment (kg),
$W_{i,x}$ = amount of chemical substance ingested (kg),
W_m = amount of product in mouth (kg),
W_{pack} = amount of chemical substance that can migrate from packaging material to food (kg),
δ = thickness of food packaging material (m).

Note that kilogram was chosen as a common unit in some models to avoid use of conversion factors. The mass of ingested chemical substances from equations described is more likely to be at the ng, µg, or mg level and appropriate conversion factors can be used to convert to commonly used dose metrics µg/mg/day or mg/kg/day.

Abbreviations

ADD: average daily potential dose,
ATSDR: Agency for Toxic Substances and Disease Registry,
CDC: Centers for Disease Control and Prevention,
GI: gastrointestinal,
SHEDS: Stochastic Human Exposure and Dose Simulation,
U.S. EPA: United States Environmental Protection Agency.

12.2. Overview

12.2.1. Terminology

Contaminant intake by non-dietary ingestion can be expressed as exposure (in mass unit), dose (in mass per body weight), or daily dose (in mass per body weight per day). It is important to know that there are different definitions for ingestion doses (TABLE 12.1) and that different organizations and research groups often use different terms. Unless otherwise indicated, the models discussed in this section are for potential doses.

TABLE 12.1 Definitions of ingestion doses used by different agencies.

Agency	Terminology	Definition
U.S. EPA [127]	Potential dose	The amount of contaminant ingested (i.e., amount that gets in the mouth), not all of which is actually absorbed.
	Applied dose	The amount of contaminant at the absorption barrier (e.g., gastrointestinal [GI] tract) that can be absorbed by the body. The applied dose might be smaller than the potential dose if the contaminant is only partially bioavailable.
	Internal dose	The amount of contaminant that gets past the exchange boundary (GI tract) and into the blood, or the amount of contaminant that can interact with organs and tissues to cause biological effects.
	Biologically effective dose	The amount of contaminant that interacts with the internal target tissue or organ.
CDC/ATSDR [128]	Exposure dose	Equivalent to U.S. EPA's potential dose.
RIVM [76]	External dose	The dose that can be absorbed orally per kg body weight on the day exposure occurs. Equivalent to U.S. EPA's potential dose.
	Internal dose	The amount of chemical substance that gets past the intestinal lumen into blood. Equivalent to U.S. EPA's internal dose.

Furthermore, for inadvertent ingestion, there is a difference between direct and indirect exposures [129], as defined below.

Inadvertent ingestion exposure: Ingestion that arises from contact between the mouth or the perioral region (the area surrounding the mouth) and contaminated hands or objects, which results in ingestion of which the individual may be oblivious.

Direct (inadvertent ingestion) exposure: Inadvertent ingestion arising from hands/objects directly into the mouth.

Indirect (inadvertent ingestion) exposure: Hands/objects to the perioral area and subsequent transfer to the oral cavity during lip licking.

12.2.2. General equations for calculating dietary and non-dietary ingestion doses

The United States Environmental Protection Agency (U.S. EPA) recommends using Equation 12.1 to estimate the average daily potential dose (ADD) from ingestion of food, water, or soil and dust, and Equation 12.2 for ingestion of surface residues from hand-to-mouth or object–to-mouth contact.[127]

$$ADD = \frac{C_{media} \times IngR \times EF \times ED}{W_{body} \times AT} \quad (12.1)$$

$$ADD = \frac{C_{residue} \times CR \times EV \times ET \times EF \times ED}{W_{body} \times AT} \quad (12.2)$$

It is worth noting that, particularly in the case of exposure to residues, there is an assumption of complete transfer of the residue from the object or hands to the mouth, which provides an upper bound to the ADD for this pathway. These equations are for repeated exposures over a long period. For individual exposure events, which are relevant to ingestion of consumer products, Equations 12.1 and 12.2 are reduced to Equations 12.3 and 12.4, respectively. Most models described below are based on either of these two equations.

$$D_i = \frac{C_{media} \times IngR}{W_{body}} \quad (12.3)$$

$$D_i = \frac{C_{residue} \times CR}{W_{body}} \quad (12.4)$$

Note that C_{media} in Equation 12.3 is the contaminant concentration in bulk product in (mg/g) for solids or (mg/L) for liquids, whereas $C_{residue}$ in Equation 12.4 is the surface concentration in (mg/cm^2).

12.2.3. List of models

Nine models are discussed below (TABLE 12.2). Most models are for potential doses except model M10-E and M10-F (applied dose) and model M10-I (internal dose). Models for ingestion of soil and dust are not considered.

TABLE 12.2 List of models for inadvertent ingestion of consumer products.

Model ID	Model Type
M10-A	Direct intake (e.g., swallowing an object containing a chemical substance)
M10-B	Hand-to-mouth transfer
M10-C	Hand-to-mouth transfer
M10-D	Direct intake from product to saliva (e.g., product in mouth)
M10-E	Direct intake from product to saliva (e.g., product in mouth)
M10-F	Object-to-mouth transfer
M10-G	Object-to-mouth transfer
M10-H	Inadvertent ingestion by indirect exposure
M10-I	Generic internal dose model
M10-J	Migration to all biological matrices during ingestion and internal dose

12.3. Model description

12.3.1. Model M10-A (RIVM, 2017) [76]

This is a screening-level, direct-intake model for exposure to a chemical substance contained in a product that is swallowed as a single event. Note that ($W_{i,p}$ w_f) in Equation 12.5 is equivalent to C_{media} in Equation 12.3 and that the external dose (D_{ext}) is equivalent to the potential dose in TABLE 12.1. In other words, not all the chemical substances that are swallowed are actually absorbed by the human body.

$$D_{ext} = \frac{W_{i,p}\, w_f}{W_{body}} \tag{12.5}$$

12.3.2. Model M10-B (RIVM, 2017) [76]

This model is for oral exposure, via hand to mouth contact, that occurs over a period of time (*t*). This model can be used to estimate exposure both due to dermal contact with hands and subsequent hand-to-mouth contact. It is assumed that the hand to mouth transfer rate is constant.

$$D_{ext} = \frac{R_{i,p}\, w_f\, t}{W_{body}} \tag{12.6}$$

12.3.3. Model M10-C (Zartarian et al., 2000) [130]

U.S. EPA's Stochastic Human Exposure and Dose Simulation (SHEDS)-Residential model uses Equation 12.7 to calculate the dose from hand-to-mouth contact.

$$D_{app} = L_d \times S_A \times TE_{HM} \times f_{abs} \tag{12.7}$$

The result from Equation 12.7 is the applied dose because f_{abs} is the fraction of chemical residue available for absorption by the gastrointestinal tract.

12.3.4. Model M10-D (RIVM, 2017) [76]

This model is for inadvertent ingestion through mouthing, a process during which the chemical substance migrates from a mouthed product into saliva (Equation 12.8).

$$D_{ext} = \frac{W_m\, w_f}{W_{body}} \left[1 - exp\left(-\frac{R_m\, S}{W_m\, w_f}\, t\right)\right] \tag{12.8}$$

The model predicts that, as object-to-saliva transfer occurs, the migration rate decreases over time due to the depletion of the chemical substance in the object. After a certain time, the dose no longer increases with time (Figure 12.1). This model assumes that the depletion of the chemical substance in the object through exponential decay, and that the decay rate constant is determined by the chemical substance mass ingested ($R_m\, S\, t$) as a fraction of the total mass of chemical substance in the object ($R_m\, w_f$).

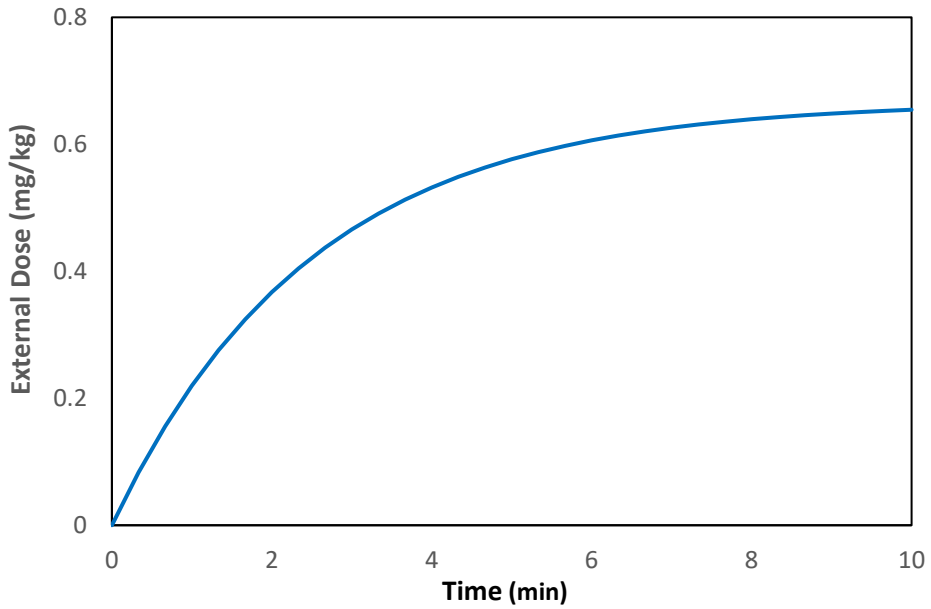

Figure 12.1 External dose predicted by Equation 12.7 due to product mouthing as a function of time.

Input parameters: W_m = 0.01 kg, w_f = 0.001, R_m = 1 × 10^{-4} kg/m^2/s, S = 0.002 m^2, and BW = 15 kg.

12.3.5. Model M10-E (Aurisano et al., 2022) [131]

Developed by Aurisano et al. (2022), this model predicts the migration rate of chemical substances from consumer products in children's mouth into saliva (Equation 12.9).

$$R_{mgr} = \frac{f_{mgr}\, m_0}{A_{contact}\, t} \tag{12.9}$$

Note that there is an inconsistency in the units of the migration rate (R_{mgr}) in the original paper. The right-hand side of Equation 12.9 gives the migration rate in (µg/cm^2/min) but R_{mgr} is in (µg/10 cm^2/min). Thus, the result from Equation 12.9 should be multiplied by 10.

A key parameter in this model is f_{mrg}, which is defined as the fraction of the product of the chemical originally in the children's product that is migrated to the saliva after a certain duration. Estimation of f_{mrg} is based on a quantitative property-property relationship model developed by Huang et al. (2019). This is a somewhat complex model initially developed for migration from food-packaging to food. For more details, refer to the original paper. The key input parameters include the thickness and volume of the product, solid-phase diffusion coefficient of the chemical substance, and material-saliva partition coefficient.

12.3.6. Model M10-F (Zartarian et al., 2000) [130]

Equation 12.10 is used by the SHEDS-Residential model to calculate the applied dose from object-to-mouth contact.

$$D_{app} = L_{obj} \times S_A \times TE_{OM} \times f_{abs} \quad (12.10)$$

Note that parameter L_{obj} has the same dimensions (mass/area) as $C_{residue}$ in Equation 12.4 and L_d in Equation 12.7.

This model is for ingestion of contaminants on the surface of the object, such as pesticide residue and, thus, is not suitable for consumer products if the chemical substance is present in the bulk material.

12.3.7. Model M10-G (Glen et al., 2012) [132]

This is another object-to-mouth model used by U.S. EPA's SHEDS-Residential model. The modeled scenario is as follows: children leave their toys on contaminated floors or other places with surface contamination; the contaminants on the surfaces transfer to toys; children then play with or chew the toys. The ingestion dose for a mouthing event, which may include multiple object-to-mouth contacts, is given by Equation 12.11.

$$D_{ptn} = C_{obj} F_{OF} S_A \left[1 - \left(1 - TE_{om}{}^{f_m t_e}\right)\right] \quad (12.11)$$

As shown in Figure 12.2, the potential dose is a function of the duration of the mouthing event when the duration of the mouthing event is short. After a certain point, the dose no longer increases.

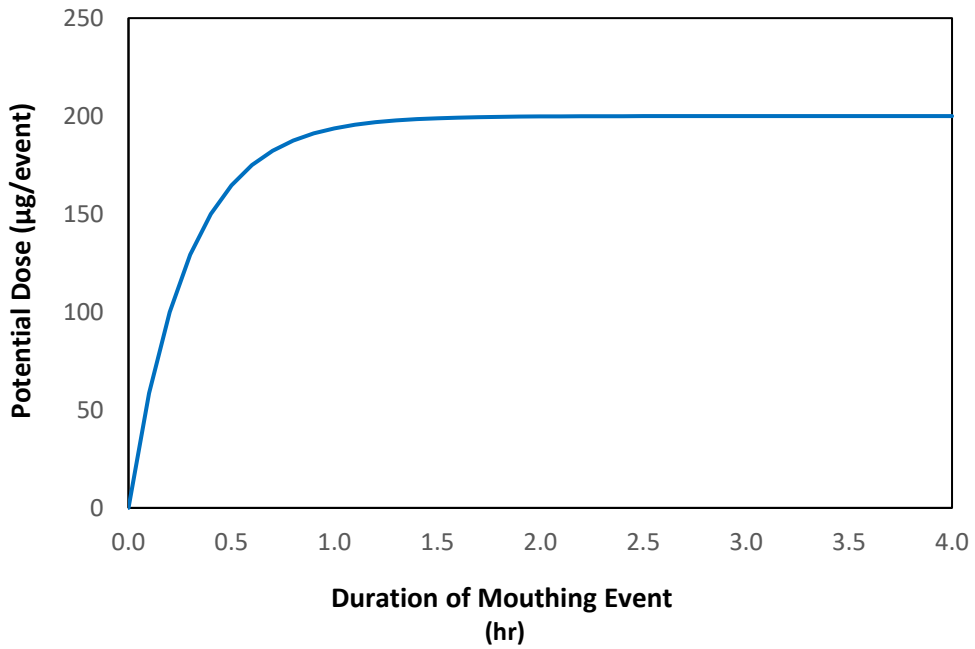

Figure 12.2 Predicted potential ingestion dose by Equation 12.11 due to product mouthing as a function of event duration (t_e).

Input parameters: C_{obj} = 1000 µg/cm^2, f_{OF} = 0.01, S_O = 20 cm^2, TE_{OM} = 0.5, and f_m = 5 events/hr.

The technical document[132] did not show how this model was derived.

12.3.8. Model M10-H (Christopher, 2008) [133]

This model is for indirect inadvertent ingestion exposure, involving contaminant transfer from hands/objects to the perioral area and subsequent transfer to the oral cavity during lip licking (Equation 12.12).

$$E_{ii,i} = L_w \, TE_{hp} \, TE_{op} \, F_{ho} \, N \tag{12.12}$$

12.3.9. Model M10-I (RIVM, 2017) [76]

Unlike models M10-A through H, which calculate the potential exposure or dose, or applied dose, this model is the generic formula for calculating the internal dose (i.e., the amount of chemical substance that gets past the intestinal lumen) as a fraction of the chemical substance ingested (Equation 12.13). For the worst-case scenario, set f_b = 1. More discussion on bioavailability is given in Section 12.4 below.

$$D_{int} = f_b \, W_{i,x} \tag{12.13}$$

12.4. Additional comments

12.4.1. Bioavailability

Most models described above are for potential doses. To convert potential dose to internal dose or biologically effective dose, an additional parameter — bioavailability — is needed.

There are three interrelated terms for bioavailability. Their definitions shown below are from EPA (2007) [134]

Bioavailability is the fraction of an ingested dose that crosses the gastrointestinal epithelium and becomes available for distribution to internal target tissues and organs.

Absolute bioavailability is expressed in either fraction or percentage of an ingested dose.

Relative bioavailability is the ratio of the bioavailability of a chemical substance in one exposure context (i.e., physical chemical matrix or physical chemical form of the metal) to that in another exposure context.

Bioavailability is an important factor in assessing exposure due to incidental ingestion. A recent study on human soil ingestion indicates that use of 100% bioavailability as a default value may dramatically overestimate the chronic exposure.[135]

Chen et al. (2023) reviewed the advances in this field over the last five decades.[136] Bioavailability data is mainly obtained by *in vitro* laboratory tests. Bioavailability studies on environmental samples have focused on ingestion of heavy metals in soil. Data for consumer products is scarce. Development of predictive models for bioavailability of consumer products is, in general, still in the early stage.

When directly measuring bioavailability is challenging, it may be preferable to directly measure and/or estimate migration of chemical substance from an ingested product into biological matrices and then scale the mass migrated in the experiment to the expected mass ingested from a swallowing event.

12.4.2. Migration into biological fluids related to ingestion/digestion

Additional progress is being made in quantifying and estimating absorption of substances during ingestion. For example, NTP hosted a workshop in October 2023 entitled *Trust Your Gut: Establishing Confidence in Gastrointestinal Models.* This workshop discussed approaches to measure and/or model absorption of chemical substances after ingestion. While it is possible to measure the amount of a chemical substance that is likely absorbed after migration from consumer product matrix into simulated biological fluids (e.g., saliva, stomach acid, intestinal fluid), these measurement approaches and modeling approaches are not yes standardized and not widely published.

The proposed model (Equation 12.14) assumes that 100% of mass that migrates into saliva, stomach acid, and intestinal fluid is absorbed by the body during digestion processes. Experimental design should be sufficiently robust to approximate a digestion event occurring over hours with appropriate simulated fluids at relevant biological temperatures. Units for the amount of product swallowed may need to be adjusted based on expected mass, density, and volume depending on whether the physical form of the ingested product (e.g., solid, liquid, semi-solid, powder, expandable water bead, gummy, etc.,)

$$D_{int} = \frac{M_{bf}}{W_{i,pe}} \times W_{i,p} \quad (12.14)$$

12.5. Summary

Non-dietary ingestion exposures may occur during incidental or accidental events such as swallowing solids or liquids and during inadvertent events arising from object-to-hand contaminant transfer, hand-to mouth transfer, and hand/object to the perioral area and subsequent transfer to the oral cavity during lip licking. A general guide on model selection is provided in TABLE 12.3.

Intentional ingestion exposure is more easily quantified than inadvertent exposure that is dependent on both the environment itself (e.g., chemical loading on surfaces, transfer efficiencies from surfaces to hands or objects that are mouthed) and the interaction of the human with the environment (e.g., frequency and duration of hand and object-to-mouth events).

TABLE 12.3 suggestions on selecting non-dietary ingestion models.

Exposure Scenario	Applicable Models	Concentration Unit
Swallowing of solids	Equation 12.3, M10-A	(mass/mass)
Swallowing of liquids	Equation 12.3, M10-A	(mass/volume)
Mouthing/Chewing of solids	M10-D	(mass/area)
Hand to mouth	M10-B, M10-C	(mass/area)
Object to mouth	M10-E, M10-F	(mass/area)

Most existing models contain at least one empirical parameter (such as migration rate, transfer rate, or transfer efficiency) whose value is mainly obtained from existing databases.

13. Models for dermal exposures associated with consumer products

13.1. Symbols and abbreviations

C_i = concentration in the i^{th} compartment of the skin or vehicle in a multi-compartment model (m^3),
C_{skin} = concentration in skin ($\mu g/cm^3$),
$\bar{C}_{skin}$ = average concentration in skin ($\mu g/cm^3$),
C_{surf} = pesticide residue concentration on surface material ($\mu g/cm^2$),
$\bar{C}_{ss}$ = steady state concentration in skin ($\mu g/cm^3$),
C_v = concentration in vehicle ($\mu g/cm^3$),
D_{ext} = external dose (kg/kg body weight),
D_{ptn} (τ) = potential dose on day τ after the surface is treated (mg/day),
D_{skin} = effective diffusion coefficient of skin (cm^2/s),
E_T = exposure time per day (h/day),
f_{ai} = fraction of active ingredient on surface (fraction),
$f_{contact}$ = fraction of total skin surface of body part (e.g., hand) of interest that contacts a treated surface,
f_d = fraction of residue that dissipates daily (fraction),
$f_{dislodge}$ = amount product dislodged from the surface (kg/m^2),
f_{leach} = leachable fraction of the amount of chemical substance in unit amount of product (fraction),
f_w = weight fraction of chemical substance in the product (fraction),
k_{v2} = first-order rate constant for transfer of liquid chemical substance from vehicle to skin (h^{-1}),
k_{va} = first-order rate constant for evaporation of liquid chemical substance from vehicle (h^{-1}),
K_{ow} = octanol-water partition coefficient (dimensionless),
K_{sv} = skin-vehicle partition coefficient and $K_{sv} = C_{skin}/C_v$ at equilibrium (dimensionless),
K_{sc} = partition coefficient for stratum corneum membrane (dimensionless),
K_{ved} = partition coefficient for viable epidermis/dermis membrane (dimensionless),
L = thickness of skin (cm),
L_{sc} = thickness of the stratum corneum membrane (cm)
L_{ved} = thickness of the viable epidermis/dermis membrane (cm),
m = molecular weight (g/mol),
m_1 = amount of chemical substance remaining in the vehicle (i.e., compartment 1) (µg or kg),
P_{sc} = permeability of stratum corneum (cm/h),
P_{skin} = permeability of the skin (m/s or cm/h),
P_{tot} = overall permeability of stratum corneum and viable epidermis/dermis (cm/h),
P_{ved} = permeability of viable epidermis/dermis (cm/h),
R_{ai} = application rate of active ingredient (mg/cm^2),
R_{app} = rate at which the product is applied to skin (kg/s),
S = exposed skin area (cm^2 or m^2),
S_{tot} = total surface area of a body part (e.g., hand) (cm^2),
S_{rub} = area of the surface rubbed by a person (m^2),
t = elapsed time (s),
t_A = duration of product application on skin (s),
T_e = surface-to-skin residue transfer efficiency (dimensionless),

V_i = volume of the i^{th} compartment of the skin in a multi-compartment model (m^3),
V_{sub} = volume of the substance on the skin (m^3),
W_{abs} = amount of chemical substance absorbed by skin (kg),
W_{app} = amount of product app to skin (kg),
W_{body} = body weight (kg),
W_{derm} = amount of chemical substance absorbed by skin (μg),
W_{prod} = amount of chemical substance on a product in contact with skin (kg),
W_{skin} = amount of chemical substance on the skin (kg),
x = depth of skin (cm),
τ = post-application time (day).

Abbreviations

ATSDR: Agency for Toxic Substances and Disease Registry,
CDC: Centers for Disease Control and Prevention,
CSTR: continuous stirred-tank reactor,
NIOSH: National Institute for Occupational Safety and Health,
QSAR: quantitative structure-activity relationship,
RIVM: National Institute for Public Health and the Environment, The Netherlands,
SHEDS: Stochastic Human Exposure and Dose Simulation,
U.S. EPA: United States Environmental Protection Agency.

13.2. Overview

13.2.1. Types of dermal absorption models

A large number of models are available for dermal absorption of chemical substances, and they can be categorized into three groups:

- Empirical models,
- Compartmental models, and
- Diffusion-based models.

The existing dermal models vary greatly in their complexity. Advanced models, such as multi-layer, multi-dimension models, are typically used in research on drug delivery through topical and transdermal applications and safety of personal care products. There have been discussions on the level of detail that is needed for exposure assessment. This section attempts to give examples for each group with a focus on relatively simple models that are more suitable for routine exposure assessment.

13.2.2. Terminology

It is important to know that there are different definitions for dermal doses, which are yet to be harmonized (TABLE 13.1).

TABLE 13.1 Definitions of dermal absorption doses used by different agencies.

Agency	Terminology	Definition
U.S. EPA [137]	Potential dose	The amount of contaminant applied to skin, not all of which is actually absorbed
	Applied dose	The amount of contaminant at the absorption barrier (e.g., skin) that can be absorbed by the body
	Internal dose	The amount of contaminant absorbed and available for interaction with biological receptors (e.g., organs, tissues)
	Biologically effective dose	The amount of contaminant that interacts with the internal target tissue or organ
CDC/ATSDR [138]	Dermal absorbed dose	The amount of chemical absorbed through the skin. Equivalent to U.S. EPA's internal dose
RIVM [76]	External dose	The dose that can be absorbed orally per kg body weight on the day exposure occurs. Equivalent to U.S. EPA's potential dose
	Internal dose	Equivalent to U.S. EPA's internal dose

13.2.3. Models discussed

Eleven dermal models are discussed, including seven empirical models, two compartmental models, and two diffusion-based models (TABLE 13.2).

TABLE 13.2 List of models for dermal exposures to chemical substances in consumer products.

Model ID	Model Type	Contact Scenario
M11-A	Empirical model	Skin in direct contact with product; instant application
M11-B	Empirical model	Skin in direct contact with product; constant application rate
M11-C	Empirical model	Skin in direct contact with product; finite source (e.g., instant application of an aqueous solution)
M11-D	Empirical model	Skin in direct contact with product (e.g., leaching from clothing)
M11-E	Empirical model	Skin in contact with a treated surface (e.g., floor and tabletop)
M11-F	Empirical model	Skin in contact with a treated surface (e.g., floor, hard surface)
M11-G	Empirical model	Skin in contact with a treated surface (e.g., floor, hard surface)
M11-H	Two-compartment model	Typically for topical applications of liquid products
M11-I	Three-compartment model	Typically for topical applications of liquid products
M11-J	One-layer diffusion-based model	Skin in direct contact with liquids or solvent-deposited solids
M11-K	Two-layer diffusion-based model	Skin in direct contact with liquids or solvent-deposited solids

13.3. Model description

13.3.1. Model M11-A (RIVM, 2017) [76]

This simple model provides a rough estimate of the external dose following instant application of a chemical substance in the absence of more details about the skin application. It simply assumes that the entirety of the chemical substance applied to the skin is available for skin absorption. As shown in Equation 13.1, the only information needed regarding the product is the amount of product applied (W_{app}) to the skin and the fraction of the chemical substance in the product (f_w).

$$D_{ext} = \frac{W_{app}\, f_w}{W_{body}} \tag{13.1}$$

This is a screening-level model for estimating the maximum potential dermal absorption dose because it assumes that all of the chemical substance applied to the skin is absorbed by the skin.

13.3.2. Model M11-B (RIVM, 2017) [76]

Like model M11-A, this is a screening-level model for dermal absorption. It assumes that the product is applied to the skin at a constant rate, R_{app}, and over a period of time, t_A. This model is equivalent to model M11-A because $R_{app}\, t_A$ in Equation 13.2 is equal to W_{app} in Equation 13.1. Thus, Equation 13.2 estimates the maximum potential dermal absorption dose.

$$D_{ext} = \frac{R_{app}\, t_A\, f_w}{W_{body}} \tag{13.2}$$

13.3.3. Model M11-C (RIVM, 2017) [76]

Unlike models M11-A and B, which ignore the properties of the skin, this model takes into consideration the skin permeability (also known as the skin permeability coefficient), which is a measure of the conductance of skin to a particular chemical from a particular vehicle.[139] It also considers the exposure duration (t). This model treats dermal absorption as a first-order decay process at the exposed skin surface, where the decay rate constant is determined by the skin permeability (P_{skin}), the exposed skin area (S) and the volume of the finite source V_{sub} (Equation 13.3).

$$W_{abs} = W_{skin}\left[1 - exp\left(-\frac{P_{skin}\, S}{V_{sub}}\, t\right)\right] \tag{13.3}$$

This model inexplicitly assumes that the source is finite, and that the evaporation loss of the chemical substance can be ignored. Parameter V_{sub} in Equation 10.3 is defined as the volume of the substance on the skin. Therefore, V_{sub} can be calculated only if the chemical substance of interest is a liquid at room temperature. V_{sub} is difficult to estimate if the chemical is a dissolved solid.

Methods for estimating skin permeability are briefly discussed in Section 13.4.1.

13.3.4. Model M11-D (RIVM, 2017) [76]

This model is for migration of a chemical substance to skin when a material is in contact with skin, such as dyes in clothing leaching to skin. Empirical parameter f_{leach} is the leachable fraction of the chemical substance in the unit amount of the product.

$$D_{ext} = \frac{W_{prod}\, f_{contact}\, f_{leach}}{W_{body}} \tag{13.4}$$

13.3.5. Model M11-E (RIVM, 2017) [76]

This model is for skin contact with a surface, such as a floor or tabletop treated with a product. A key parameter is the dislodgeable amount per unit area ($f_{dislodge}$).

$$D_{ext} = \frac{S_{rub}\, f_{dislodge}\, f_w}{W_{body}} \tag{13.5}$$

13.3.6. Model M11-F (U.S. EPA, 2007) [140]

This model is also for skin contact with a treated surface but differs from model M11-E in that the dislodgeable residue decreases over time (Equation 13.6).

$$D_{ptn}(\tau) = R_{ai}\, f_{ai}\, (1 - f_d)^{\tau}\, E_T \tag{13.6}$$

The result is the potential dermal dose on day τ after the surface is treated. It is not the cumulative dose from day 1 to day τ.

13.3.7. Model M11-G (Zartarian et al., 2000) [130]

This model is used by U.S. EPA's Stochastic Human Exposure and Dose Simulation (SHEDS)-Residential model for transfer of pesticide residue on treated surfaces (e.g., carpet and hard floor) to skin for a single event (Equation 13.7).

$$W_{derm} = C_{surf}\, S_{tot}\, f_{contact}\, T_e \tag{13.7}$$

This model contains two empirical constants: $f_{contact}$ is the fraction of the total skin surface of the body part (e.g., hand) of interest that contacts a treated surface, and T_e is the surface-to-skin residue transfer efficiency.

13.3.8. Model M11-H (Mitragotri et al., 2011) [141]

Compartmental models are used in many scientific branches to describe the movement of chemical substances from one compartment to another. A key assumption of all compartmental models is that the chemical substance is well mixed in the compartment. Because each compartment acts like a

continuous stirred-tank reactor (CSTR), compartmental models are also known as tank models. Two and three-compartment models are most commonly used to describe the dermal absorption of chemical substances. In the two-compartment model, different layers of skin are lumped into a single compartment while, in three-compartment models, the skin is represented by two compartments, one for the stratum corneum and the other for the viable epidermis (Figure 13.1).

The general mass balance equation for the concentration in the skin (C_2) is given by Equation 13.8.

$$V_2 \frac{dC_2}{dt} = k_{12}\, C_1 - k_{21}\, C_2 - k_{2b}\, C_2 + k_{b2}\, C_b \qquad (13.8)$$

Coefficient k_{ij} in Equation 13.8 is the first-order rate constant for transfer from compartment *i* to compartment *j* and bears the unit of (cm^3/h). It can be regarded as a lumped parameter for the skin area and skin permeability. For example, k_{12} in Equation 13.7 is equal to or proportional to S (cm^2) × P_{skin} (cm/h).

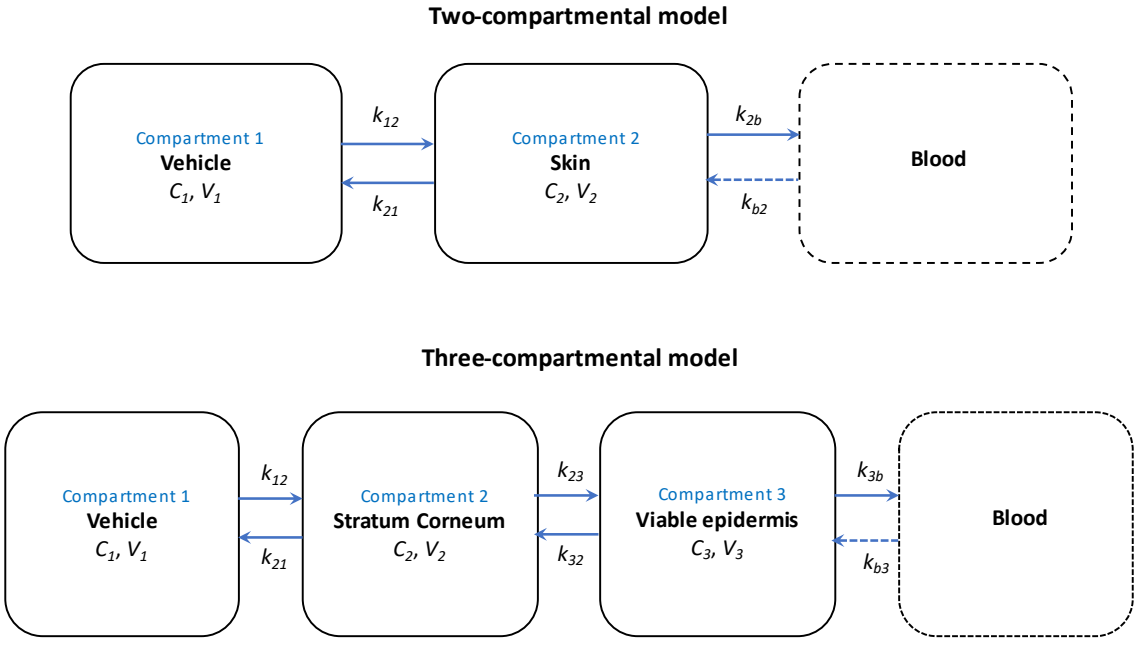

Figure 13.1 Schematic representations of two and three-compartment models for dermal absorption.

Parameter k_{ij} is the first-order rate constant for mass flow from compartment *i* to compartment *j* ($time^{-1}$).

Note that the concentration of the chemical substance of interest in the vehicle (compartment 1), C_1, is a constant. If C_1 changes over time, an additional equation or compartment can be added. For example, Equation 13.9 treats the vehicle as a first-order decay source.[142]

$$\frac{dm_1}{dt} = -k_{va}\, m_1 - k_{v2}\; m_1 \qquad (13.9)$$

13.3.9. Model M11-I (Mitragotri et al., 2011) [141]

In a three-compartment model, the skin is represented by two compartments: stratum corneum and viable epidermis. The general mass balance equation for the chemical substance in the two zones (C_2 and C_3) are given by Equations 13.10 and 13.11, respectively.

$$V_2 \frac{dC_2}{dt} = k_{12} C_1 - k_{21} C_2 - k_{23} C_2 + k_{32} C_3 \tag{13.10}$$

$$V_3 \frac{dC_3}{dt} = k_{23} C_2 - k_{32} C_3 - k_{3b} C_3 + k_{b3} C_b \tag{13.11}$$

The definitions of the rate constants ($k_{i,j}$) are the same as in model M11-H.

13.3.10. Model M10-J (Todo et al., 2013) [143]

The diffusion-based models for skin permeation are similar to the diffusion-based models for solid building materials (described in Section 3) except that dermal models deal with soft tissues. In a one-layer model, the skin is represented by a single membrane. Under the assumption that the permeation is one-dimensional, the classical solution to diffusion through a uniform membrane is applicable. The concentration in the skin at depth *x* and time *t*, $C_{skin}(x,t)$, is determined by Equation 13.12; the average concentration in the skin, $\bar{C}_{skin}(t)$, is determined by Equation 13.13; and the steady-state concentration, $\bar{C}_{ss}$, is determined by Equation 13.14.

$$C_{skin}(x,t) = K_{sv} C_v \left\{ \left(1 - \frac{x}{L}\right) - \frac{2}{\pi^2} \sum_{n=1}^{\infty} \left[sin \frac{n x \pi}{L} exp\left(- \frac{D_{skin} n^2 \pi^2}{L^2} t \right) \right] \right\} \tag{13.12}$$

$$\bar{C}_{skin}(t) = \frac{K_{sv} C_v}{2} \left\{ 1 - \frac{8}{\pi^2} \sum_{n=1}^{\infty} \left[\frac{1}{(2n-1)^2} exp\left(- \frac{D_{skin} (2n-1)^2 \pi^2}{L^2} t \right) \right] \right\} \tag{13.13}$$

$$\bar{C}_{ss} = \frac{K_{sv} C_v}{2} \tag{13.14}$$

The key parameters of this model are the skin-vehicle partition coefficient (K_{sv}), diffusion coefficient of the skin (D_{skin}), and the concentration of the chemical substance in the vehicle (C_v).

13.3.11. Model M10-K (Todo et al., 2013) [143]

In a two-layered diffusion model, the skin is represented by two membranes, one for the stratum corneum and the other for the viable epidermis/dermis. The exact solutions of the two-layered diffusion models are rather long and complex.[144, 145] Todo and his co-workers (2013) showed the steady-state concentration in the skin can be calculated from Equation 13.15.

$$\overline{C_{ss}} = \frac{C_v}{2\,L}\left[K_{sc}\,L_{sc}\left(1+\frac{P_{tot}}{P_{ved}}\right)+\,K_{ved}\,L_{ved}\,\frac{P_{tot}}{P_{ved}}\right] \tag{13.15}$$

where the total skin permeability P_{tot} is calculated from the permeability of the stratum corneum P_{sc} and the permeability of the viable epidermis/dermis (Equation 13.16).

$$\frac{1}{P_{tot}} = \frac{1}{P_{sc}} + \frac{1}{P_{ved}} \tag{13.16}$$

Limited data are available for the partition and diffusion coefficients for skin.[146]

13.4. Additional comments

13.4.1. Estimation of skin permeability

Skin permeability is a key input parameter for estimating the internal dose, which is the amount of contaminant absorbed and available for interaction with biological receptors (e.g., organs, tissues). This parameter is applicable for skin as a single layer (P_{skin}) and for different layers, such as the stratum corneum (P_{sc}) and viable epidermis/dermis (P_{ved}). This parameter can be either obtained from existing databases—a sizable amount of data is available—or estimated with quantitative structure–activity relationship (QSAR) models. The most commonly used QSAR models correlate skin permeability with the octanol-water partition coefficient (K_{ow}) and molecular weight of the chemical substance (m) as shown in Equation 13.17.

$$\log P_{skin} = a + b\log K_{ow} - c\,m \tag{13.17}$$

where coefficients a, b, and c are obtained from statistical analysis of measured skin permeability.

The octanol-water partition coefficient K_{ow} can be estimated by using U.S. EPA's *EPI Suite*^{TM} [28] or free chemical structure database *ChemSpider* (http://www.chemspider.com/). Be aware that the K_p values in Equation 13.16 may bear different units. For example,

In Ref. [140]: P_{skin} is in (cm/h) with a = −2.72, b = 0.71, and c = 0.0061.

In Ref. [141]: P_{skin} is in (cm/s) with a = −6.3, b = 0.71, and c = 0.0061.

The National Institute for Occupational Safety and Health (NIOSH) has developed a skin permeability calculator that is available to the public.[139] The program includes the Flynn database of experimentally determined skin permeability.

13.4.2. Estimation of the rate constants in compartment models

There are many methods for estimating the first-order rate constants in compartmental models (see model M11-K above). McCarley and Bunge (2001) [145] reviewed 11 compartmental models and found that models developed by Kubota and Maibach (1994)[147] and McCarley and Bunge (1998)[148]

perform better than other models. However, the overall performance of compartmental models is inferior to that of diffusion-based models.

13.5. Summary

Many dermal absorption models have been developed. Sophisticated models are mainly used in pharmaceutical research and development of personal care products. Exposure assessment mainly uses empirical dermal models. A general guide on model selection is provided in TABLE 13.3.

TABLE 13.3 Suggestions on selecting dermal absorption models.

Exposure Scenario	Dose Type	Models	Key Parameters
Liquids/semi-liquid applied to skin	Potential dose	M11-A, B	Amount applied
	Internal dose	M11-C	Skin permeability
	Internal dose	M11-H, I	First-order rate constants
	Internal dose	M11-J, K	Partition and diffusion coefficients
Skin in contact with solid products	Potential dose	M11-D	Leachable fraction
Skin in contact with treated surfaces	Potential dose	M11-E	Dislodgeable fraction
	Potential dose	M11-F	Residue dissipation rate
	Internal dose	M11-G	Surface-to-skin residue transfer efficiency

14. Crosswalk tables of consumer products with chemical substances and models

Eight crosswalk tables that link consumer product types and chemical substance classes to example models are presented below. TABLES 14.1, 14.3, 14.5, and 14.7 are sorted by product type or exposure scenario while TABLES 14.2, 14.4, 14.6, and 14.8 by model.

These tables are mainly for readers who are unfamiliar with indoor exposure modeling. Experienced readers are encouraged to read through the relevant sections to better understand the features and limitations of the available models and, more importantly, consult the original papers.

TABLE 14.1 Crosswalk table of modeled product categories and chemical substances associated with inhalation exposure — (1) Sorted by product types.

Product category	Example Product	Example Chemical Substances	Example Model	References	Notes
Solid building materials	Carpet	Formaldehyde, styrene, etc.	M1-A	[4]	A
	Particle board	TVOC, hexanal, α-pinene,	M1-B	[5]	B
	Aged caulking	PCBs	M1-K	[16]	C
Liquids applied on indoor surfaces	Hard-surface cleaners	solvents	M3-D	[52]	
	Hard-surface cleaners	ammonia, acetone	M3-G, M3-E	[58]	
	Solvent-based coatings	Alkanes, xylenes, etc.	M4-A, M4-B	[63]	
	Water-based coatings	glycols	M4-F	[70]	
Liquids for spray applications	Air fresheners	volatile solvents	M5-A, M5-B	[76]	
	Air fresheners, personal care products	Non-volatiles	M5-C	[76, 77]	D
Combustion appliances	Cooking stoves	CO, NO_2, PM	M6-B	[91]	E
	Unvented kerosene heaters	CO, NO, SO_2, PM	M6-D	[94]	
	Gas cooking ranges	CO, NOx, PM	M6-E, M6-F	[95, 96]	
	Candles	CO, CO_2, NO_x, HCHO	M6-G, M6-H	[97-99]	
	Incense	Organic carbon	M6-I	[100]	
Water-use appliances	Washing machine, dishwasher, kitchen sink	Aromatic hydrocarbons, acetone, etc.	M7-A, M7-B, M7-C	[106, 108, 109]	
	Humidifiers	PM, metals	M7-D, M7-E	[110, 149]	
Printers	3D printers	PM	M7-F	[102]	

[A] Model M1-A is implemented in simulation program IAQX.[41]
[B] M1-B performs better than M1-A but requires basic programming skills.
[C] This model is implemented in simulation programs i-SVOC and IECCU.[25, 33]
[D] This model is implemented in simulation program *ConsExpo Web*.[76]
[E] This model is implemented in simulation program HOMES.[91]

TABLE 14.2 Crosswalk table of modeled product categories and chemical substances associated with inhalation exposure — (2) Sorted by model ID.

Model	Product Modeled	Chemicals Modeled	References
M1-A	Carpet	styrene, ethylbenzene, xylenes, formaldehyde, etc.	[4]
M1-B	Particle boards	TVOC, hexanal, α-pinene	[5]
M1-K	Aged caulking	PCBs	[16]
M3-D	Hard surface cleaners	solvents	[52]
M3-G, H	Hard surface cleaners	ammonia, acetone	[58]
M4-A, M4-B	Solvent-based paints	alkanes, xylenes	[63]
M4-F	Water-based paint	glycols	[70]
M5-A, M5-B	Spray air fresheners	solvents	[76]
M5-C	Spray air fresheners	non-volatiles	[76, 77]
M6-B	Cooking stoves	CO, NO_2, PM	[91]
M6-D	Unvented kerosene heaters	CO, NO, SO_2, PM	[94]
M6-E, M6-F	Gas cooking ranges	CO, NOx, PM	[95, 96]
M6-G, M6-H	Candles	CO, CO_2, NO_x, HCHO	[97-99]
M6-I	Incense	Organic carbon	[100]
M7-A, M7-B, M7-C	Washing machine, dishwasher, kitchen sink	Aromatic hydrocarbons, acetone	[106, 108, 109]
M7-D, M7-E	Humidifiers	PM, metals	[111, 149]
M7-F	3D printers	PM	[102]

TABLE 14.3 Crosswalk table of consumer product type containing chemical substances associated with migration from sources to indoor media — (1) Sorted by migration mechanism.

Transfer Scenario	Transfer to	Example Chemical Substances	Example Models	References	Notes
Air-mediated transfer from solid materials	Indoor air (vapor and PM), settled dust, interior surfaces	Broad range of SVOCs	M8-A	[117]	A
Air-mediated transfer from solid materials (vinyl flooring)	Indoor air (vapor and PM), settled dust, interior surfaces	Flame retardants	M8-B	[118]	B
Direct contact with the source (painted surface)	Settled dust	Phthalates	M8-E	[122]	B
Leaching from consumer products (polyethylene pipe)	Drinking water	Total organic carbon	M9-B	[124]	

[A] Model M8-A is implemented in simulation program *DustEx*.
[B] This model requires basic programming skills.

TABLE 14.4 Crosswalk table of consumer product type containing chemical substances associated with migration from sources to indoor media — (2) Sorted by model ID.

Model	Migration Scenario	Product Modeled	Chemicals Modeled	References
M8-A	Source to dust (air-mediated)	Solid materials	broad range of SVOCs	[117]
M8-B	Source to dust (air-mediated)	Vinyl flooring	flame retardants	[118]
M8-E	Source- to dust (direct contact)	Painted surface	phthalates	[122]
M9-B	Leaching to tap water)	Cross-linked polyethylene pipe	total organic carbon	[124]

TABLE 14.5 Crosswalk table of consumer product type containing chemical substances associated with non-dietary ingestion exposure — (1) Sorted by exposure scenario.

Exposure Scenario	Example Chemical Substances	Example Model	References	Notes
Swallowing of solids	Components or additives	Equation 12.3, M10-A	[76]	A, B
Swallowing of liquids	Components of liquid	Equation 12.3, M10-A	[76]	A, B
Mouthing/Chewing of solids	Components or additives	M10-D	[76]	
Hand to mouth	Surface contaminants	M10-B, M10-C	[76, 130]	B
Object to mouth	Children's products	M10-F, M10-G	[130, 132]	

[A] This is a screening-level model for estimating the upper bound of the potential dose.
[B] Models M10-A, M10-B, M10-C, and M10-D are implemented in simulation program *ConsExpo* Web.[76]

TABLE 14.6 Crosswalk table of consumer product type containing chemical substances associated with non-dietary ingestion exposure — (2) Sorted by model ID.

Model	Exposure Scenario	Product Modeled	Chemicals Modeled	References
M10-A	Swallow	Solids or liquids	components or additives	[76]
M10-D	Chewing	Solid objects	components or additives	[76]
M10-B	Hand-to-mouth	contaminated surfaces	components or additives	[76]
M10-C	Hand-to-mouth	contaminated surfaces	pesticides	[130]
M10-F	Object-to-mouth	Children's products	plasticizers, flame retardants, pesticides, etc.	[130]
M10-G	Object-to-mouth	Surface-contaminated solid objects	pesticide residue	[132]

TABLE 14.7 Crosswalk table of consumer product type containing chemical substances associated with dermal exposure — (1) Sorted by Exposure scenario.

Exposure Scenario	Example Chemical Substances	Example Models	References	Notes
Liquids/semi-liquid applied to skin	Solvents or other components	M11-A, M11-B, M11-C, M11-J	[76, 143]	A, B
Skin in contact with solid products	Components or additives	M11-D	[76]	A
Skin in contact with treated surfaces	Surface contaminants (e.g., pesticides)	M11-E, M11-F, M11-G	[76, 140]	C

[A] Models M11-A, B, and C are simple models and implemented in simulation tool *ConsExpo Web*.[76]
[B] Model M11-J requires basic programming skills.
[C] Model M11-G is implemented in simulation tool SHEDS-Residential.[132]

TABLE 14.8 Crosswalk table of consumer product type containing chemical substances associated with dermal exposure — (2) Sorted by model ID.

Model	Product/use scenario	Chemicals Modeled	References
M11-A, M11-B, M11-C	Direct contact with liquid product	solvents	[76]
M11-D	Direct contact with solid product (e.g., clothing)	dyes	[76]
M11-E, M11-F, M11-G	Direct contact with contaminated surfaces	surface contaminants (e.g., pesticides)	[76, 140]

References

1. Haghighat, F. and H. Huang, *Integrated IAQ model for prediction of VOC emissions from building material.* Building and Environment, 2003. **18**(8): p. 1007-1017.
2. Li, F. and J. Niu, *Control of volatile organic compounds indoors—Development of an integrated mass-transfer-based model and its application.* Atmospheric Environment, 2007. **41**(11): p. 2344-2354.
3. ASTM, *Standard Terminology Relating to Sampling and Analysis of Atmospheres*. 2020, ASTM International.
4. Little, J.C., A.T. Hodgson, and A.J. Gadgil, *Modeling emissions of volatile organic compounds from new carpets.* Atmospheric Environment, 1994. **28**(2): p. 227-234.
5. Deng, B. and C.N. Kim, *An analytical model for VOCs emission from dry building materials.* Atmospheric Environment, 2004. **38**(8): p. 1173-1180.
6. Zhang, X., et al., *Predicting the emissions of VOCs/SVOCs in source and sink materials: Development of analytical model and determination of the key parameters.* Environment International, 2022. **160**.
7. Huang, H. and F. Haghighat, *Modelling of volatile organic compounds emission from dry building materials.* Building and Environment, 2002. **37**(11): p. 1127-1138.
8. Deng, B., et al., *Numerical modeling of volatile organic compound emissions from multi-layer dry building materials.* Korean Journal of Chemical Engineering, 2010. **27**(4): p. 1049–1055.
9. Guo, M., et al., *A numerical model predicting indoor volatile organic compound Volatile Organic Compounds emissions from multiple building materials.* Environmental science and pollution research international, 2020. **27**(1): p. 587–596.
10. Yang, X., Q. Chen, and P.M. Bluyssen, *Prediction of short-term and long-term VOC emissions from SBR bitumen-backed carpet under different temperatures.* ASHRAE Transactions, 1998. **104**.
11. Xu, Y. and Y. Zhang, *An improved mass transfer based model for analyzing VOC emissions from building materials.* Atmospheric Environment, 2003. **37**: p. 2497-2505.
12. Qian, K., et al., *Dimensionless correlations to predict VOC emissions from dry building materials,.* Atmospheric Environment, 2007. **41**(2): p. 352-359.
13. Yan, W., Y. Zhang, and X. Wan, *Simulation of VOC emissions from building materials by using the state-space method.* Building and Environment, 2009. **44**(3): p. 471-478.
14. Guo, Z., *A framework for modelling non-steady-state concentrations of semivolatile organic compounds indoors – II. Interactions with particulate matter.* Indoor and Built Environment, 2013. **23**(1): p. 26-43.
15. Huang, L., et al., *Modeling chemical releases from building materials: The search for extended validity domain and parsimony.* Building Simulation, 2021. **14**(4): p. 1277-1293.
16. Guo, Z., *A Framework for Modelling Non-Steady-State Concentrations of Semivolatile Organic Compounds Indoors – I: Emissions from Diffusional Sources and Sorption by Interior Surfaces.* Indoor and Built Environment, 2013. **22**(4): p. 685-700.
17. Wang, X. and Y. Zhang, *General analytical mass transfer model for VOC emissions from multi-layer dry building materials with internal chemical reactions.* Chinese Science Bulletin, 2011. **56**: p. 222–228.
18. Little, J.C., et al., *Barrier materials to reduce contaminant emissions from structural insulated panels*. Advances in Building Technology, ed. M. Anson, J.M. Ko, and E.S.S. Lam. Vol. 1. 2002, Oxford, UK: Elsevier.
19. Kumar, D. and J.C. Little, *Characterizing the source/sink behavior of double-layer building materials.* Atmospheric Environment, 2003. **17**(39-40): p. 5529-5537.

20. Xu, Y. and J.C. Little, *Predicting Emissions of SVOCs from Polymeric Materials and Their Interaction with Airborne Particles.* Environmental Science & Technology, 2006. **40**(2): p. 456-461.
21. Hu, H.P., et al., *An analytical mass transfer model for predicting VOC emissions from multi-layered building materials with convective surfaces on both sides.* International Journal of Heat and Mass Transfer, 2007. **50**: p. 2069-2077.
22. Xiong, J., C. Liu, and Y. Zhang, *A general analytical model for formaldehyde and VOC emission/sorption in single-layer building materials and its application in determining the characteristic parameters.* Atmospheric Environment, 2012. **47**: p. 288-294.
23. Treyball, R.E., *Mass transfer operations*. 1968, New York, NY: McGraw-Hill.
24. EPA. *User's Guide and Download for IECCU- Indoor Environmental Concentrations in Buildings with Conditioned and Unconditioned Zones*. 2019; Available from: https://www.epa.gov/tsca-screening-tools/users-guide-and-download-ieccu-indoor-environmental-concentrations-buildings.
25. Guo, Z., *Simulation Program i-SVOC User's Guide*. 2013, US Environmental Protection Agency.
26. Huang, L., et al., *A quantitative property-property relationship for the internal diffusion coefficients of organic compounds in solid materials.* Indoor Air, 2017. **27**(6): p. 1128-1140.
27. Huang, L. and O. Jolliet, *A quantitative structure-property relationship (QSPR) for estimating solid material-air partition coefficients of organic compounds.* Indoor Air, 2018. **29**(1): p. 79-88.
28. EPA, *Estimation Programs Interface Suite™ for Microsoft® Windows, v 4.11*. 2012, US EPA: Washington, DC.
29. Begley, T., et al., *Evaluation of migration models that might be used in support of regulations for food-contact plastics.* Food Additives & Contaminants, 2005. **22**(1): p. 73-90.
30. Wang, X., Y. Zhang, and J. Xiong, *Correlation between the solid/air partition coefficient and liquid molar volume for VOCs in building materials.* Atmospheric Environment, 2008. **42**(33): p. 7768-7774.
31. Cox, S.S., J.C. Little, and A.T. Hodgson, *Measuring concentrations of volatile organic compounds in vinyl flooring.* J Air Waste Manag Assoc, 2001. **51**(8): p. 1195-201.
32. Guo, Z., *Review of indoor emission source models. Part 2. Parameter estimation.* Environ Pollut, 2002. **120**(3): p. 551-64.
33. EPA, *IECCU User's Guide*. 2019, US Environmental Protection Agency.
34. Lee, C.S., F. Haghighat, and W.S. Ghaly, *A study on VOC source and sink behavior in porous building materials - analytical model development and assessment.* Indoor Air, 2005. **15**(3): p. 183-96.
35. Liu, Y., et al., *A diffusivity model for predicting VOC diffusion in porous building materials based on fractal theory.* J Hazard Mater, 2015. **299**: p. 685-95.
36. Liu, Y., et al., *A prediction model of VOC partition coefficient in porous building materials based on adsorption potential theory.* Building and Environment, 2015. **92**(Part 2): p. 221-233.
37. Liu, Z., et al., *How to predict emissions of volatile organic compounds from solid building materials? A critical review on mass transfer models.* J Environ Manage, 2022. **302**(Pt A): p. 114054.
38. Guo, Z. and H.F. Hubbard, *Chemical reactions in indoor sources.* Indoor and Built Environment, 2015. **24**(6): p. 725-728.
39. Tian, S., S. Ecoff, and J. Sebroski. *Predicting TCPP Emissions and Airborne Concentrations from Spray Polyurethane Foam Using USEPA i-SVOC Software: Parameter Estimation and Result Interpretation*. in *Developing Consensus Standards for Measuring Chemical Emissions from Spray Polyurethane Foam (SPF) Insulation*. 2017. ASTM International.

40. Liu, X., M.R. Allen, and N.F. Roache, *Characterization of organophosphorus flame retardants' sorption on building materials and consumer products.* Atmospheric Environment, 2016. **140**: p. 333-341.
41. Guo, Z., *Simulation tool kit for indoor air quality and inhalation exposure (IAQX) version 1.0 user's guide.* 2000, US Environmental Protection Agency.
42. Guo, Z., *Simulation Program i-SVOC User's Guide*. 2013, US Environmental Protection Agency.
43. Little, J.C., et al., *Rapid Methods to Estimate Potential Exposure to Semivolatile Organic Compounds in the Indoor Environment.* Environmental Science & Technology, 2012. **46**(20): p. 11171-11178.
44. Liang, Y., X. Liu, and M.R. Allen, *Measurements of Parameters Controlling the Emissions of Organophosphate Flame Retardants in Indoor Environments.* Environ Sci Technol, 2018. **52**(10): p. 5821-5829.
45. Huang, L. and O. Jolliet, *A parsimonious model for the release of volatile organic compounds (VOCs) encapsulated in products.* Atmospheric Environment, 2016. **127**: p. 223-235.
46. Christiansson, J., T.W. Yu, and I. Neretnieks. *Emission of VOCs from PVC-floorings - models for predicting the time dependent emission rates and resulting concentrations*. in *Proceedings of the 6th International Conference on Indoor Air*

Quality and Climate. 1993. Helsinki, Finland.
47. Chang, J.C.S. and K.A. Krebs, *Evaluation of para-dichlorobenzene emissions from solid moth repellant as a source of indoor air pollution.* 1992. **42**: p. 1214-1217.
48. Liu, X., et al., *Chamber study of PCB emissions from caulking materials and light ballasts.* Chemosphere, 2015. **137**: p. 115-21.
49. Lyman, W.J., W.F. Reehl, and D.H. Rosenblatt, *Handbook of chemical property estimation methods: Environmental behavior of organic compounds*. 1990, United States: Washington, DC (United States); American Chemical Society. Medium: X; Size: Pages: (530 p) 2008-02-08 American Chemical Society, 1155 16th Street, NW, Washington, DC 20036 (United States).
50. Little, J.C., *Applying the two-resistance theory to contaminant volatilization in showers.* Environmental Science & Technology, 1992. **26**(7): p. 1341-1349.
51. Sander, R., et al., *Henry's law constants (IUPAC Recommendations 2021).* Pure and Applied Chemistry, 2022. **94**(1): p. 71-85.
52. Delmaar, J.E. and A.G. Schuur, *ConsExpo Web 1.0.2 model documentation*. 2017.
53. Yoo, G., et al., *Development of a New Evaporation Exposure Model: Chemical Product Evaporation Model (CPEM).* Applied Sciences, 2022. **12**(6).
54. Braun, K.O. and K.J. Caplan, *Evaporation rate of volatile liquids*. 1989, US EPA: Washington, DC.
55. Wei, W., et al., *Modeling Primary Emissions of Chemicals from Liquid Products Applied on Indoor Surfaces.* International journal of environmental research and public health, 2022. **19**(6).
56. Arnold, S., et al., *Estimating the time-varying generation rate of acetic acid from an all-purpose floor cleaner.* Journal of Exposure Science & Environmental Epidemiology, 2020. **30**(2): p. 374-382.
57. Guo, Z. and N.F. Roache, *Overall mass transfer coefficient for pollutant emissions from small water pools under simulated indoor environmental conditions.* The Annals of occupational hygiene, 2003. **47 4**: p. 279-86.
58. Guo, Z., L.E. Sparks, and N.F. Roache, *Modeling small-scale spills of aqueous solutions in the indoor environment.* Journal of Hazardous Materials, 2008. **153**(1-2): p. 444-453.
59. Yang, T., et al., *Predicting Indoor Emissions of Cyclic Volatile Methylsiloxanes from the Use of Personal Care Products by University Students.* Environmental Science & Technology, 2018. **52**(24): p. 14208-14215.

60. Evans, W.C., *Development of continuous-application source terms and analytical solutions for one- and two-compartment systems*, in *Characterizing Sources of Indoor Air Pollution and Related Sink Effects (ASTM STP 1287)*, B.A. Tichenor, Editor. 1996, American Society for Testing and Materials. p. 279-293.
61. EPA, *Wall Paint Exposure Model (WPEM) Version 3.2 User's Guide*. 2001: Washington, DC.
62. Zeh, H., K. Kohlhammer, and M. Krell, *VOC-emission from latex paints and plasters during application.* Surface Coatings International, 1994. **77**(4): p. 142-151.
63. Guo, Z., et al., *Estimation of the rate of VOC emissions from solvent-based indoor coating materials based on product formulation.* Atmospheric Environment, 1999. **33**(8): p. 1205-1215.
64. Clausen, P.A., *Emission of volatile and semivolatile organic compounds from water-borne paints -- the effect of the*

film thickness. Indoor Air, 1993. **3**: p. 269-275.
65. Tichenor, B.A., Z. Guo, and L.E. Sparks, *Fundamental Mass Transfer Model for Indoor Air Emissions from Surface Coatings.* Indoor Air, 1993. **3**(4): p. 263-268.
66. Guo, Z., et al., *Predicting the emissions of individual VOCs from petroleum-based indoor coatings.* Atmospheric Environment, 1998. **32**: p. 231-237.
67. Zhang, Y., et al., *Exponential Decay Model of TVOC Emission from Indoor Building Materials*, in *IOP Conf. Series: Earth and Environmental Science*. 2020. p. 6.
68. Chang, Y.M., et al., *A study on dynamic volatile organic compound emission characterization of water-based paints.* J Air Waste Manag Assoc, 2011. **61**(1): p. 35-45.
69. Wilkes, C., et al., *Estimation of emission profiles for interior latex paints.* Indoor air, 1996. **96**: p. 55-60.
70. Sparks, L.E., et al., *Volatile organic compound emissions from latex paint--Part 1. Chamber experiments and source model development.* Indoor Air, 1999. **9**(1): p. 10-7.
71. Guo, Z., et al. *Modeling the VOC emissions from interior latex paint applied to gypsum board*. in *Proceedings of Indoor Air '96*. 1996.
72. Corsi, R.L. and C.-C. Lin, *Emissions of 2,2,4-Trimethyl-1,3-Pentanediol Monoisobutyrate (TMPD-MIB) from Latex Paint: A Critical Review.* Critical Reviews in Environmental Science and Technology, 2009. **39**(12): p. 1052-1080.
73. Zhou, X., et al., *Mathematical model for characterizing the full process of volatile organic compound emissions from paint film coating on porous substrates.* Building and Environment, 2020. **182**: p. 107062.
74. He, J., M. Lv, and X. Yang, *A one-dimensional VOC emission model of moisture-dominated cure adhesives.* Building and Environment, 2019. **156**: p. 171-177.
75. Chang, J.C.S., et al., *Evaluation of Sink Effects on VOCs from a Latex Paint.* Journal of the Air & Waste Management Association, 1998. **48 10**: p. 953-958.
76. RIVM, *ConsExpo Web -- Consumer Exposure models model documentation*. 2017, National Institute for Public Health and the Environment, The Netherlands. p. 67.
77. Delmaar, J.E. and H.J. Bremmer, *The ConsExpo spray model -- Modelling and experimental validation of the inhalation exposure of*

consumers to aerosols from spray cans and trigger sprays. 2009, National Institute for Public Health and the Environment, The Netherlands. p. 69.
78. Tischer, M. and J. Meyer, *A New Model Algorithm for Estimating the Inhalation Exposure Resulting from the Spraying of (Semi)-Volatile Binary Liquid Mixtures (SprayEva).* Int J Environ Res Public Health, 2022. **19**(20).
79. EPA, *Consumer Exposure Model (CEM) Version 2.1 User's Guide*. 2019, EPA Office of Pollution Prevention and Toxics.

80. ESIG, *User Manual for Consumer GES/CSA Tool, EGRET Version 2.1*. 2023, The European Solvents Industry Group.
81. RIVM. *User Manual ConsExpo Nano Tool*. 2019; Available from: https://www.consexponano.nl/.
82. Koch, W., et al., *Validation of an EDP assisted model for assessing inhalation exposure and dermal exposure during spraying processes*. 2012, Federal Institute for Occupational Safety and Health, Germany: Dortmund, Germany.
83. BAUA. *SprayExpo: modelling exposure during spray applications*. undated; Available from: https://www.baua.de/EN/Topics/Work-design/Hazardous-substances/Assessment-unit-biocides/Sprayexpo.html.
84. Dols, W.S., A.K. Persily, and B.J. Polidoro, *Development of Airborne Nanoparticle Exposure Modeling Tools*. 2018, National Institute of Standards and Technology.
85. Abattan, S.F., et al., *Modeling occupational exposure to solvent vapors using the Two-Zone (near-field/far-field) model: a literature review.* Journal of Occupational and Environmental Hygiene, 2021. **18**(2): p. 51-64.
86. LeBlanc, M., et al., *Comparison of the near field/far field model and the advanced reach tool (ART) model V1.5: exposure estimates to benzene during parts washing with mineral spirits.* International Journal of Hygiene and Environmental Health, 2018. **221**(2): p. 231-238.
87. Hofstetter, E., et al., *Evaluation of recommended REACH exposure modeling tools and near-field, far-field model in assessing occupational exposure to toluene from spray paint.* Ann Occup Hyg, 2013. **57**(2): p. 210-20.
88. Huang, L., et al., *A review of models for near-field exposure pathways of chemicals in consumer products.* Science of The Total Environment, 2017. **574**: p. 1182-1208.
89. Jayjock, M.A., *Estimating overspray exposure potential from aerosol sprayed products onto surfaces.* J Occup Environ Hyg, 2012. **9**(9): p. D155-60.
90. Traynor, G.W., et al., *Macromodel for assessing residential concentrations of combustion-generated pollutants: model development and preliminary predictions for CO, N02, and respirable suspended particles*. 1989, Lawrence Berkeley Laboratory,.
91. WHO, *Model documentation: WHO Household Multiple Emission Sources (HOMES) Model*. Undated. p. 18.
92. WHO, *Database of input variables for the WHO Household Multiple Emission Sources (HOMES) and Performance Targets (PT) Models*. Undated.
93. Johnson, M., et al., *Modeling indoor air pollution from cookstove emissions in developing countries using a Monte Carlo single-box model.* Atmospheric Environment, 2011. **45**(19): p. 3237-3243.
94. Zhou, Y. and Y.-S. Cheng, *Characterization of Emissions from Kerosene Heaters in an Unvented Tent.* Aerosol Science and Technology, 2000. **33**(6): p. 510-524.
95. Chan, W.R., et al., *Simulations of short-term exposure to NO2 and PM2.5 to inform capture efficiency standards*. 2020, Lawrence Berkeley National Laboratory.
96. Singer, B.C., et al., *Pollutant concentrations and emission rates from natural gas cooking burners without and with range hood exhaust in nine California homes.* Building and Environment, 2017. **122**: p. 215-229.
97. Klosterköther, A., et al., *Determination of the emission indices for NO, NO2, HONO, HCHO, CO, and particles emitted from candles.* Indoor Air, 2021. **31**(1): p. 116-127.
98. Salthammer, T., et al., *Measurement and evaluation of gaseous and particulate emissions from burning scented and unscented candles.* Environment International, 2021. **155**: p. 106590.
99. Kapalo, P., A. Eštoková, and O. Voznyak, *The carbon dioxide generation rate from burning of candle and its effect on room ventilation*, in *IOP Conference Series: Materials Science and Engineering*. 2022.

100. See, S.W. and R. Balasubramanian, *Characterization of fine particle emissions from incense burning.* Building and Environment, 2011. **46**(5): p. 1074-1080.
101. Zhang, Q., et al., *Metal compositions of particle emissions from material extrusion 3D printing: Emission sources and indoor exposure modeling.* Science of The Total Environment, 2023. **860**: p. 160512.
102. Zontek, T.L., et al., *Modeling Particle Emissions from Three-Dimensional Printing with Acrylonitrile–Butadiene–Styrene Polymer Filament.* Environmental Science & Technology, 2019. **53**(16): p. 9656-9663.
103. Gu, J., et al., *Characterization of particulate and gaseous pollutants emitted during operation of a desktop 3D printer.* Environment International, 2019. **123**: p. 476-485.
104. Davis, A.Y., et al., *Characterization of volatile organic compound emissions from consumer level material extrusion 3D printers.* Building and Environment, 2019. **160**: p. 106209.
105. Mendes, L., et al., *Characterization of Emissions from a Desktop 3D Printer.* Journal of Industrial Ecology, 2017. **21**(S1): p. S94-S106.
106. Howard, C. and R.L. Corsi, *Volatilization of chemicals from drinking water to indoor air: the role of residential washing machines.* J Air Waste Manag Assoc, 1998. **48**(10): p. 907-14.
107. Sander, R., *Compilation of Henry's law constants (version 4.0) for water as solvent.* Atmos. Chem. Phys., 2015. **15**(8): p. 4399-4981.
108. Howard-Reed, C., R.L. Corsi, and J. Moya, *Mass Transfer of Volatile Organic Compounds from Drinking Water to Indoor Air: The Role of Residential Dishwashers.* Environmental Science & Technology, 1999. **33**(13): p. 2266-2272.
109. Corsi, C., *Volatilization of Chemicals from Drinking Water to Indoor Air: Role of the Kitchen Sink.* Journal of the Air & Waste Management Association, 1996. **46 9**: p. 830-837.
110. Yao, W., et al., *Human exposure to particles at the air-water interface: Influence of water quality on indoor air quality from use of ultrasonic humidifiers.* Environment International, 2020. **143**: p. 105902.
111. Yao, W., et al., *Children and adults are exposed to dual risks from ingestion of water and inhalation of ultrasonic humidifier particles from Pb-containing water.* Sci Total Environ, 2021. **791**: p. 148248.
112. Dietrich, A.M., et al., *Environmental risks from consumer products: Acceptable drinking water quality can produce unacceptable indoor air quality with ultrasonic humidifier use.* Science of The Total Environment, 2023. **856**: p. 158787.
113. ASTM, *ASTM D5116-17 Standard Guide for Small-Scale Environmental Chamber Determinations of Organic Emissions from Indoor Materials/Products*. 2017, ASTM International.
114. Weschler, C.J. and W.W. Nazaroff, *Semivolatile organic compounds in indoor environments.* Atmospheric Environment, 2008. **42**(40): p. 9018-9040.
115. Liu, C., B. Zhao, and Y. Zhang, *The influence of aerosol dynamics on indoor exposure to airborne DEHP.* Atmospheric Environment, 2010. **44**(16): p. 1952-1959.
116. Liu, C., et al., *Analysis of the Dynamic Interaction Between SVOCs and Airborne Particles.* Aerosol Science and Technology, 2013. **47**(2): p. 125-136.
117. RIVM. *The DustEx modelling tool*. undated [cited 2023 August 6]; Available from: https://www.rivm.nl/en/consumer-exposure-to-chemical-substances/exposure-models/dustex.
118. Wei, W., O. Ramalho, and C. Mandin, *A long-term dynamic model for predicting the concentration of semivolatile organic compounds in indoor environments: Application to phthalates.* Building and Environment, 2019. **148**: p. 11-19.
119. Bi, C., et al., *Direct Transfer of Phthalate and Alternative Plasticizers from Indoor Source Products to Dust: Laboratory Measurements and Predictive Modeling.* Environmental Science & Technology, 2021. **55**(1): p. 341-351.

120. Kang, L., et al., *Direct and non-direct transfer of phthalate esters from indoor sources to settled dust: Model analysis.* Building and Environment, 2021. **202**: p. 108012.
121. Wang, H., et al., *Investigation on the Direct Transfer of SVOCs from Source to Settled Dust: Analytical Model and Key Parameter Determination.* Environmental Science & Technology, 2022. **56**(9): p. 5489-5496.
122. Cao, J., et al., *Role of dust loading in dynamic transport of semi-volatile organic compounds (SVOCs) into house dust: From multilayer to monolayer.* Building and Environment, 2023. **233**: p. 110084.
123. Adams, W.A., et al., *Predicting the Migration Rate of Dialkyl Organotins from PVC Pipe into Water.* Environmental Science & Technology, 2011. **45**(16): p. 6902-6907.
124. Millet, P., et al., *Diffusion of chemicals from the surface of pipe materials to water in hydrodynamic conditions: applications to domestic drinking water installations.* WIT Transactions on Ecology and The Environment, 2016. **209**: p. 161-172.
125. Schwope, A.D. and R. Goydan, *Methodology for Estimating the Migr4tion of Additives and Impurities from Polymeric Material*, in *Methods For Assessing Exposure to Chemical Substances*. 1990, US EPA.
126. Chowdhury, S., et al., *Models for predicting heavy metal concentrations in residential plumbing pipes and hot water tanks.* AQUA - Water Infrastructure, Ecosystems and Society, 2021. **70**(7): p. 1038-1052.
127. EPA. *Exposure Assessment Tools by Routes - Ingestion*. 2023 [cited 2023 Sept. 13, 2023]; Available from: https://www.epa.gov/expobox/exposure-assessment-tools-routes-ingestion#methods.
128. ATSDR. *Estimating Site-Specific Ingestion and Dermal Exposure Doses*. 2022 [cited 2023 Sept. 16]; Available from: https://www.atsdr.cdc.gov/pha-guidance/conducting_scientific_evaluations/epcs_and_exposure_calculations/estimating-site-specific-ingestion-and-dermal-exposure-doses.html#SoilSedimentIngestion.
129. Gorman Ng, M., et al., *The relationship between inadvertent ingestion and dermal exposure pathways: a new integrated conceptual model and a database of dermal and oral transfer efficiencies.* Ann Occup Hyg, 2012. **56**(9): p. 1000-12.
130. Zartarian, V.G., et al., *A modeling framework for estimating children's residential exposure and dose to chlorpyrifos via dermal residue contact and nondietary ingestion.* Environ Health Perspect, 2000. **108**(6): p. 505-14.
131. Aurisano, N., et al., *Estimating mouthing exposure to chemicals in children's products.* Journal of Exposure Science & Environmental Epidemiology, 2022. **32**(1): p. 94-102.
132. Glen, G., et al., *SHEDS-Residential version 4 Technical Manual*. 2012, US EPA.
133. Christopher, Y., *Inadvertent ingestion exposure to hazardous substances in the workplace*. 2008, University of Aberdeen: Aberdeen, UK. p. 284.
134. EPA, *Guidance for Evaluating the Oral Bioavailability of Metals in Soils for Use in Human Health Risk Assessment*. 2007, US Environmental Protection Agency.
135. Fernández-Landero, S., I. Giráldez, and J.C. Fernández-Caliani, *Predicting the relative oral bioavailability of naturally occurring As, Cd and Pb from in vitro bioaccessibility measurement: implications for human soil ingestion exposure assessment.* Environmental Geochemistry and Health, 2021. **43**(10): p. 4251-4264.
136. Chen, H.Y., et al., *A 50-year systemic review of bioavailability application in Soil environmental criteria and risk assessment.* Environmental Pollution, 2023. **335**: p. 122272.
137. EPA. *Exposure Assessment Tools by Routes - Dermal*. 2023 May 24, 2023 [cited 2023 Sept. 19]; Available from: https://www.epa.gov/expobox/exposure-assessment-tools-routes-dermal.

138. ATSDR, *Exposure Dose Guidance for Dermal and Ingestion Exposure to Surface Water*. 2018, CDC Agency for Toxic Substances and Disease Registry: Atlanta, GA.
139. NIOSH. *Skin Permeation Calculator*. 2022 [cited 2023 October 1]; Available from: https://www.cdc.gov/niosh/topics/skin/skinpermcalc.html.
140. EPA, *Dermal Exposure Assessment:A Summary of EPA Approaches*. 2007.
141. Mitragotri, S., et al., *Mathematical models of skin permeability: An overview.* International Journal of Pharmaceutics, 2011. **418**(1): p. 115-129.
142. Ernstoff, A.S., et al., *Multi-pathway exposure modeling of chemicals in cosmetics with application to shampoo.* Environment International, 2016. **92-03**: p. 87-96.
143. Todo, H., et al., *Mathematical model to predict skin concentration after topical application of drugs.* Pharmaceutics, 2013. **5**(4): p. 634-51.
144. Cleek, R.L., *Application of dermal absorption models to risk assessment*. 1998, Colorado School of Mines.
145. McCarley, K.D. and A.L. Bunge, *Pharmacokinetic models of dermal absorption.* J Pharm Sci, 2001. **90**(11): p. 1699-719.
146. Ellison, C.A., et al., *Partition coefficient and diffusion coefficient determinations of 50 compounds in human intact skin, isolated skin layers and isolated stratum corneum lipids.* Toxicology in Vitro, 2020. **69**: p. 104990.
147. Kubota, K. and H.I. Maibach, *Significance of viable skin layers in percutaneous permeation and its implication in mathematical models: theoretical consideration based on parameters for betamethasone 17-valerate.* J Pharm Sci, 1994. **83**(9): p. 1300-6.
148. McCarley, K.D. and A.L. Bunge, *Physiologically relevant one-compartment pharmacokinetic models for skin. 1. Development of models.* J Pharm Sci, 1998. **87**(4): p. 470-81.
149. Dietrich, A.M., et al., *Environmental risks from consumer products: Acceptable drinking water quality can produce unacceptable indoor air quality with ultrasonic humidifier use.* Sci Total Environ, 2023. **856**(Pt 1): p. 158787.